ATMOSPHERIC BOUNDARY LAYER SIMILARITY THEORY FOR APPLICATIONS IN WIND ENERGY FIELDS

A THESIS

Presented to

The Faculty of the Division of Graduate

Studies and Research

By

Amir Samaan Mikhail

In Partial Fulfillment

of the Requirements for the Degree

Doctor of Philosophy

In the School of Aerospace Engineering

Georgia Institute of Technology

September, 1977

ATMOSPHERIC BOUNDARY LAYER SIMILARITY THEORY FOR

APPLICATIONS IN WIND ENERGY FIELDS

Approved:

Chairman

Date approved by Chairman: 8/8/77

ACKNOWLEDGMENTS

I take great pleasure in expressing my deep gratitude to Dr. Carl G. Justus for suggesting this thesis topic, his guidance throughout the course of this research and more important, for his continued support and encouragement during my whole graduate career.

My appreciation goes also to the members of my committee; Dr. R. G. Roper for his understanding and willingness to discuss various aspects of the endeavor; Dr. D. P. Giddens for his helpful discussion and patient examination of the thesis.

The financial assistance of the Energy Research and Development Administration is gratefully acknowledged.

My sincere thanks go to Mrs. Peggy Weldon for her patience and skillful typing.

I am also grateful to my parents for their many years of guidance, encouragement and unselfish sacrifice.

Lastly, I am grateful to all my friends who made a long journey seem shorter especially Aunt Franscis and Mr. N. L. Sankar. I cannot rightfully close without giving thanks to God who ultimately gives purpose and meaning to all endeavors.

TABLE OF CONTENTS

Page

LIST OF TABLES

LIST OF TABLES (Continued)

LIST OF ILLUSTRATIONS

LIST OF ILLUSTRATIONS (Continued)

LIST OF ILLUSTRATIONS (Continued)

LIST OF ILLUSTRATIONS (Continued)

NOMENCLATURE

f	Coriolis parameter
g	Acceleration due to gravity
H	$C_p \rho \overline{w'T'}$, turbulent heat flux
k	Von-Karman constant (= 0.4)
K_m	$(u_*^2/\frac{\partial U}{\partial Z})$, turbulent transfer coefficient for momentum
K_H	$-H/[\rho C_p (\frac{\partial \theta}{\partial Z})]$, turbulent transfer coefficient for Heat
L	Monin-Obukov Length $-u_*^3 \frac{C_p \rho T}{kg}$
L'	Pr. L
Pr	K_H/K_m reciprocal of the turbulent Prandtl number
RI	$(\frac{g}{\bar{T}}) [\frac{\partial \theta/\partial Z}{(\partial U/\partial Z)^2}]$, gradient Richardson number
R_f	Flux Richardson number = $RI \cdot \frac{K_H}{K_m}$
R_{Zo}	Richardson number based on roughness length
T	mean temperature
T_*	$(-1/ku_*)(H/\rho C_p)$, a scaling temperature
T'	Temperature perturbation around the mean
U,V	mean wind speed
u_*	$(\tau/\rho)^{1/2}$, friction velocity
u_g	Geostrophic wind
w'	vertical velocity perturbation around the mean
y_+	non-dimensional height = $y(\nu/u_*)$ or y/Z_o for rough surfaces
Z	vertical space coordinate
Z_o	Roughness length

NOMENCLATURE (Continued)

α	First power coefficient in Taylor's series expansion of ϕ_1
Γ	g/C_p, adiabatic lapse rate
δ	thickness of the planetary boundary layer
θ	$T + \Gamma Z$, potential temperature
ϕ_1	$\frac{kZ}{u_*}\frac{\partial U}{\partial Z}$ non-dimensional wind speed gradient
ϕ_2	$\frac{Z}{T_*}\frac{\partial \theta}{\partial Z}$ non-dimensional potential-temperature gradient
ν	kinematic viscosity
τ	tangential stress
ρ	air density

SUMMARY

Two sets of tower data, taken at Kennedy Space Flight Center and Argonne National Laboratories, were used to investigate the possibility of establishing a theoretical model for projection of wind speed with height within the atmospheric boundary layer using wind speed at a prefixed level and net radiation for boundary conditions. The required value of net radiation can either be measured directly or estimated. The latest work that has been done for relating cloud cover, time of day, latitude and net radiation is discussed and referenced.

Different methods were suggested for isolation of the set of neutrally stable profiles during five years of hourly data, both for Kennedy and Argonne. Neutral Stability is necessary for estimating the roughness of the terrain as a function of direction. The logarithmic law was used for the neutral profiles to check on the values of roughness lengths estimated.

A comparison was made between the empirical representation of the non-dimensional wind speed and temperature gradients and the theoretical representation referred to as KEYPS function. It was found that they both represent the profiles within the accuracy of measurement.

The value of the critical Richardson number was computed for both towers and it was found to be much higher than it is usually assumed to be, which in turn introduced changes in Webb's formula for extremely stable stratification.

Since the Monin-Obukov length is a function of net radiation, wind shear and roughness length, an attempt was made to describe the nature of this dependence.

The hourly wind speed and temperature profiles were used to calculate the Monin-Obukov Length that would minimize the error between the theoretical model and the measured data for different net radiation classes, speed classes and roughness lengths.

The results obtained show the right physically plausible trend for variation of the Monin-Obukov length with net radiation and wind speed at a given level. Also it shows that within the surface layer the wind speed profile can be predicted within measurement errors.

Since the range of variation of roughness lengths of the two towers is limited, the functional dependence of the Monin-Obulov length on roughness length had to be investigated, otherwise the values obtained for the Monin-Obukov length will be true only locally and it could not be guaranteed for all types of terrain.

The rate of change of the Monin-Obukov length L with respect to roughness length was deduced. In some stability regions the functional dependence of L on roughness length was found in a closed form. The theoretical form of the functional dependence of L on roughness length was checked by comparing values of L calculated theoretically with averaged values of L at specific direction intervals for the Argonne and Kennedy towers at the same roughness length.

The values of L predicted theoretically agreed fairly well with the values of L averaged from the profiles.

The relation between L and roughness length was solved for a wide range of roughness lengths given L at the average roughness length at

the Argonne tower as initial conditions. Hence the complete dependence of L on wind speed at a given level, net radiation and roughness length was established.

The methodology for the projection of wind speed with height given wind speed at a predetermined level, net radiation and roughness length was suggested. The final check on the methodology suggested was carried out for both Kennedy and Argonne tower data by calculating the root mean square error between measured and predicted profiles. The projected profiles were based on the values of Monin-Obukov lengths determined for each profile from given tables.

The results obtained indicate the soundness of the methodology for levels of practical importance to wind energy applications.

Finally the Monin-Obukov length determined atmospheric stability was related to Pasquill-Gifford stability classes.

CHAPTER I

INTRODUCTION

1.1 Background

The main purpose of this thesis is seen as a contribution to wind energy studies. The choice of a suitable site for optimum power production depends to a great extent on the theoretical power available in the wind. The only nationwide available data is National Weather Service data where wind speed is recorded at one anemometer height.

The problem of projecting wind speed with height is very important for preliminary analysis of site power outputs and economics studies. Also the atmospheric boundary layer analysis involved in this problem will contribute to Agro-meteorological studies and Geophysical studies, since dynamic interaction of the atmosphere and the substrate, the feeding of energy into the atmosphere by moisture and heat is realized through the ground layer. Also the analysis of the Monin-Obukov length involved in the atmospheric boundary layer similarity theory and relating it to Pasquill-Gifford stability classes would contribute to giving a quantitative description of atmospheric stability that would reflect on air pollution and diffusion studies.

A first approach to the problem can be made by using empirical laws to describe the profile, given one wind speed measurement at one level. A power law is then assumed, with an exponent that is a function of terrain roughness (Davenport 1965) or wind speed at reference height

(Reed 1974) or atmospheric stability (Smith 1968). The power law has been used in predicting diffusion characteristics (Calder 1949) or wind tunnel modeling of wind forces (Davenport 1965). Also the logarithmic law has been used (Simiu 1973) where the profile could be expressed in terms of one speed measurement at a fixed height and terrain roughness length.

Different studies have been made on the effects of terrain roughness on the profiles, Calder (1949), Chamberlain (1966), and Ciono (1965).

Some efforts were made to replace the terrain roughness length by an aerodynamic roughness length to get a better fit for the profile.

The second approach to the problem is statistical; Justus and Mikhail (1976) suggested a methodology for the height projection of Weibull velocity probability distribution parameters. Reed (1975) proposed a power law profile with an exponent that is a function of wind speed at a reference height. Justus and Mikhail related the exponent to projected Weibull wind speed probability distribution parameters.

A more rigorous approach treats the problem as a turbulent flow near a heated or cooled horizontal rough surface, which is a notoriously difficult problem.

The first step for the analysis of the problem is estimating the roughness length of the surrounding terrain. Panofsky and Peterson (1972) analyzed the Riso tower data and Peterson (1975) added some modifications to the methods suggested before by Peterson and Panofsky. The Kennedy tower data were analyzed by Fichtl (1970).

The most outstanding contribution to the problem was made by Monin and Obukov (1954) where the similarity parameter for stratified boundary layers was introduced by combining buoyancy, turbulent shear stress and heat flux. The non-dimensional wind speed and temperature gradients (ϕ_1, ϕ_2) were expressed in terms of the similarity parameter (Z/L), where Z is the height from the ground (more accurately from roughness level) and L is known as the Monin-Obukov length.

The functional dependence of ϕ_1 and ϕ_2 on the similarity parameter (Z/L) was not suggested by Monin and Obukov, whereas an attempt was made to expand the function around the neutral stratification point for very small values of the similarity parameter (i.e. slightly stratified).

Ellison (1957) suggested a form for this function by interpolating between free and forced convection. The same relation was later obtained independently by Yamamato (1959) and Panofsky (1961). This relationship was called the KEYPS function and it was supposed to predict the profiles both for stable and unstable conditions. Unfortunately the agreement is good for unstable profiles only.

Panofsky (1961) arrived at the same relationship using an alternative derivation which explains the reason why the KEYPS function is restricted to unstable conditions.

Bussinger (1966) and Dyer (unpublished) have independently suggested a profile representation for unstable conditions which assumes an empirical relationship between Richardson number (RI) and similarity parameter (Z/L). It also assumes an increasing Prandtl number with decreasing stability.

Paulson (1970) successfully integrated the non-dimensional velocity and temperature gradients for the KEYPS function and for the Bussinger-Dyer representation. Swinbank's (1964) observations were used to compare the two approaches.

For the slightly stable case the Taylor expansion around the neutral stratification ($Z/L \neq 0$) can be used since (Z/L) is small. The expansion coefficients were estimated by Bussinger et al. (1971) and by Webb (1970) who extended the analysis to extremely stable stratification based on pure empirical observation.

A critical Richardson number was estimated both by Bussinger et al. and Webb.

Swinbank (1964) suggested the exponential profile which is expected to be applicable for all heights and stratifications by introducing a transformation that would express both energy supplies from buoyancy and shear in one pseudo shearing stress term.

Some work has also been done in higher closure modeling by Wyngaard et al. (1974) for the steady state structure of neutral and convective cases, for baroclinic cases by Arya and Wyngaard (1975), and also for the evolution of the convective planetary boundary layer (Wyngaard and Cote', 1974). But this work is beyond the scope of interest of this thesis since we are only interested in heights that are approximately within the surface layer ($\leq$ 100 m.).

Hanna (1969) compared five different approaches for the estimation of the total thickness of the planetary boundary layer.

Golder (1972) related the Pasquill-Gifford stability classes to Monin-Obukov length based stability classes, for different roughness

lengths by analyzing different tower data.

In estimating the total insolation by the time of day and year, latitude and longitude and relating it to net incident radiation through given estimates of cloud cover and turbidity and possibly other factors, extensive research is currently being done. The most outstanding being the NOAA solar radiation model in which data from 52 stations are utilized. Also Kimura and Stephenson (1969) have derived a relationship between theoretical insolation and net solar intensity based on a cloud cover factor for Ottawa, Ontario.

Another empirical relation has been published in a Boeing Company report (1964). It also relates insolation to net radiation by a factor that depends on the type and amount of cloud cover.

This thesis endeavors to utilize and extend the present knowledge about the surface layer to propose a methodology for projection of wind speed with height using the minimum possible parameters. Data from two meteorological towers will be used.

The first section in Chapter II gives a dimensional argument that primarily shows that the surface layer is in the region of interest of the wind energy applications. It also describes the Monin-Obukov similarity principle and gives a summary of different profile representations obtained using the Monin-Obukov similarity principle.

Section 2.2 discusses the basic quantities affecting the similarity layer. The parameters describing these quantities are suggested to be the 10 m. level wind speed, net radiation, and roughness length. This in turn implies that the Monin-Obukov length L is a function of the above three quantities. The dependence of (1/L) on wind speed and

net radiation is extracted from the data. The dependence of (1/L) on roughness length is derived in section 2.3.

If the net radiation measurements are not available, then different methods for net radiation estimation are given in section 2.4. Roughness length estimation based on topography and surface cover is given in section 2.5. In Chapter III the roughness lengths around the two towers are calculated and the universal values of Monin-Obukov length are given as a function of wind speed at 10 m., net radiation, and roughness length. Also a methodology for projection of wind speed with height is suggested and checked. Also the Monin-Obukov Length based atmospheric stability is related to Pasquill-Gifford Stability and used as a part of the methodology (for cases when measured net solar radiation is not available).

1.2 Research Goals

(1) Isolation of neutral profiles and accurate estimation of roughness lengths as a function of direction for the two sets of tower data used.

(2) Most of the data used for verifying the above mentioned approaches for modeling the surface layer extend only up to 16 m. at most, which is below the level needed for wind energy applications. Hence the height up to which the laws of the similarity layer apply within a certain permissible error need to be estimated using Kennedy and Argonne data.

(3) Comparing Bussinger-Dyer and KEYPS function for best fit of the unstable profile and optimizing the arbitrary constants in the

two formulae. Also comparing the Webb and Bussinger profile representation in the stable stratification and optimizing the first order coefficient in the Taylor expansion of ϕ_1 and ϕ_2.

(4) Using the tower data to estimate the critical Richardson number.

(5) Using the given net radiation, wind speed at ten m. level and estimated roughness length to establish the dependence of the Monin-Obukov universal length on the above mentioned parameters.

(6) Since we have a very limited variation of the estimated roughness length for the two towers, the theoretical functions dependence of L on roughness length has to be established.

(7) In case net radiation measurements are not available, a relationship between the theoretical insolation based on time of day, longitude, latitude and time of year, and net insolation needs to be suggested. The factor of proportionality is expected to be a function of many factors such as cloud cover, turbidity and moisture content.

Hence the outline of the methodology suggested for wind speed projection with height is:

(i) Estimate the roughness of the proposed site based on the type of terrain and surface cover (Plate, 1971).

(ii) Use net radiation and wind speed at ten m. level to evaluate L from tables given at a wide range of roughness lengths.

If net radiation measurements are not available then the theoretical insolation can be estimated from given formulae and modified according to cloud cover, and turbidity to estimate the net radiation.

If the anemometer height for the wind speed measurement is slightly different from the ten m. level then the statistical model developed by Justus and Mikhail could be used to adapt the wind speed to ten m. level.

(iii) Apply the suitable profile representation according to the stability region determined by the value of L.

(8) Relate the Pasquill-Gifford stability classes to the corresponding Monin-Obukov length interval which gives a quantitative description of the stability of the atmosphere.

CHAPTER II

PROCEDURE

2.1 Profile Representation

2.1-1 Dimensional Argument

The boundary layers of meteorology differ from those in aerodynamics in that high Reynold's numbers prevail, which implies greater thickness and larger extent for the surface layer. If we consider an average geostrophic wind speed of three m/s and use Hanna's (1969) formula for the estimation of the total thickness of the planetary boundary layer

$$\delta(U_g/f) = .006 \frac{U_g}{f} \approx 1 \text{ Km.}$$

$$R_e(\delta) = \frac{.006\ U_g^2}{f \cdot \nu} \approx 10^7$$

The actual thickness of the surface layer is a function of Reynold's number, stability and roughness length. Kennedy and Argonne data will be used to estimate the thickness of the inertial sublayer or rather the thickness of the layer where similarity laws apply within a permissible error. This layer will be referred to as the similarity layer. The variation of the thickness of the similarity layer with stability will be investigated from an analysis of the tower data.

Different estimates have been given for the total thickness of the depth at the inertial sublayer, Panofsky (1964) suggested that it

varies between 20 - 200 m. based on a dimensional argument. Hanna (1969) used different methods for estimates of the thickness of the planetary boundary layer which was then related to the thickness of the inertial sublayer. The average thickness of the planetary boundary layer for all the methods used was 1000 m. Using the most conservative method for neutral condition estimates, the boundary layer thickness is given as

$$\delta(u_*) = .2\ u_*^2/f$$

for Kennedy

$$\delta = 2.9 \times 10^3 u_*$$

for Argonne

$$\delta = 2.1 \times 10^3 u_*$$

For Argonne tower data u_* in neutral conditions could be estimated as 0.5 m/s, (see Figure 23) which still gives δ in the neighborhood of 10^3 m.

Tennekes and Lumley (1972) also gives an estimate of δ to be around 1000 m. Plate (1971) expects that a larger portion than the lowest 15% of the atmospheric boundary layer is possibly inertial.

Tennekes and Lumley (1972) define a surface to be rough if $R_{Z_o} = \frac{u_* Z_o}{\nu} > 5$. If u_* is given the conservative estimate of 0.1 m/s, Z_o to be 0.001, then $R_{Z_o} >> 5$, which implies that the dominant length scale in the viscous sublayer is Z_o instead of (ν/u_*).

The edge of the viscous sublayer is estimated to be for values of $(Z/Z_o) < 5$. Hence all values of $Z < 5Z_o$ don't belong to the inertial sublayer.

2.1-2 Similarity Solution

It is customary to treat the atmospheric boundary layer as if the properties near the surface are independent of the state of the flow at great heights. The turbulent shear stress and heat flux are considered to be independent of height. A steady state is assumed which may not be always the case. The fluid is considered incompressible, moreover the fractional changes in density are sufficiently small that their effect on the inertia of the fluid is negligible, so they need to be taken into account only in the vertical (gravitational field) direction.

Two different methods were used to estimate the roughness of the terrain surrounding the towers. In the first method the Richardson number and static temperature slope were calculated and all profiles with very small Richardson number ($|RI| < .03$) and with static temperature profile that is close to the adiabatic lapse rate were isolated and least square fit with a logarithmic profile. In the second method all the profiles are fit with a logarithmic profile and roughness lengths are calculated and averaged for different speed classes and then extrapolated to infinite velocity where very high mixing should ensure neutral conditions.

If the deviation of density from the reference state locally may be denoted by ρ', pressure p', and temperature T' so that

$$\begin{aligned} \rho &= \rho_R + \rho' = \rho_m + \Delta\rho + \rho' \\ p &= p_R + p' = p_m + \Delta p + p' \\ T &= T_R + T = T_m + \Delta T + T' \end{aligned} \qquad (1)$$

where the subscript m denotes mean values for the whole layer except for temperature where it denotes the mean value of temperature locally in the layer, T_R is temperature condition for constant potential temperature. Hence the Navier-Stokes equations and energy equation reduce to

$$\frac{D}{Dt}(\vec{V}) = 1\ \frac{1}{\rho}\nabla p' - \frac{g}{\rho}\rho'\ \underline{k} + \nu[\nabla^2\vec{V} + \frac{1}{3}\nabla(\nabla\cdot\vec{V})] + F_c \tag{2}$$

$$\rho C_v \frac{D}{Dt}(T) = -p\nabla\cdot\vec{V} + K\nabla^2 T' + \rho\phi + \rho C_p R \tag{3}$$

where ϕ is energy dissipation, R is energy radiation, F_c is Coriolis force.

If we neglect the changes in density due to pressure changes we can combine the first two terms on the right hand side of (2) in the form $\frac{gT'}{T_m}\underline{k}$. Also Coriolis force can be neglected since we are interested in smaller length scales. Due to the high turbulent intensity in the atmospheric boundary layer all molecular transfer of heat and momentum can be neglected compared to turbulent transfer of heat and momentum. Hence the equations reduce to

$$\begin{aligned}
\frac{Du}{DT} &= -\frac{1}{\rho}\frac{\partial p'}{\partial x} \\
\frac{Dv}{Dt} &= -\frac{1}{\rho}\frac{\partial p'}{\partial y} \\
\frac{Dw}{Dt} &= -\frac{1}{\rho}\frac{\partial p'}{\partial z} + \frac{g}{T_m}T'
\end{aligned} \tag{4}$$

$$\frac{\partial u}{\partial x} + \frac{\partial v}{\partial y} + \frac{\partial w}{\partial z} = 0 \tag{5}$$

$$\frac{DT'}{Dt} = 0 \tag{6}$$

The above equations contain one dimensional constant $(\frac{g}{T_m})T'$ and if the Reynold's decomposition is performed on them the boundary conditions will be

$$\overline{w'T'} = \frac{H}{\rho C_p} = \text{constant}$$

$$-\rho\overline{u'w'} = \tau = -u_*^2 = \text{constant}$$

The above three quantities can form two non-dimensional parameters (Z/L) and (T/T_*) where

$$L = -u_*^3/(k\,\frac{g}{T}\,\frac{H}{\rho C_p}) \tag{7}$$

$$T_* = -(1/ku_*)(H/\rho C_p) \tag{8}$$

Since L contains all the quantities that affect the turbulent energy transfer to the surface layer, namely buoyancy, turbulent momentum and heat transfer, the non-dimensional velocity and temperature gradient functions, $\phi_1 = \frac{kZ}{u_*}\frac{\partial U}{\partial Z}$, $\phi_2 = \frac{Z}{T_*}\frac{\partial \theta}{\partial Z}$ could be expressed in terms of the similarity parameter (Z/L).

The quantity $(-Z/L)$ can be written as the ratio of the production rate of convective energy $gH/C_p\rho T$, and u_*^3/kZ. Since the latter measures the rate of mechanical energy production in neutral air, we can say that $-Z/L$ expresses the ratio of convective to mechanical energy production in near neutral air. In this, it therefore plays the same role as the Richardson number $RI = (g/T)(\partial\theta/\partial Z)/(\partial U/\partial Z)^2$, which is the ratio of buoyancy to inertia forces, which indeed becomes equal to Z/L when Z/L is small, that is, when the buoyancy effect is small. The advantage of

Z/L over RI is that the vertical variation of the former is known. Also various assumptions concerning the turbulent Prandtl number, which is the ratio between turbulent momentum and heat transfer coefficients, i.e. $Pr = K_H/K_m$, will be stated.

A. Unstable Stratification. A general form of ϕ_1 and ϕ_2 was suggested by Ellison (1957) where he interpolated between free convection ($RI << 0$, $K_m \rightarrow y_* Z R_f^{1/4}$) and forced convection ($RI >> 0$, $K_m \rightarrow 0$) and neutral stratification ($RI \rightarrow 0$, $K_m \rightarrow \frac{u_* Z}{k}$). After some manipulations and relating K_m to ϕ_1, we get

$$\phi_1^4 - \gamma(\frac{Z}{L})\phi_1^3 = 1 \qquad (9)$$

The above relation does not work for stable stratification (Panofsky 1960) because in an alternative derivation Panofsky showed that Ellison's interpolation formula implies assuming a turbulence length scale that is proportional to Z which is not the case for stable stratification when smaller size eddies prevail.

Another representation for the profile is from Bussinger (1966) and Dyer (unpublished), who have independently suggested that the relation between gradient Richardson number and similarity parameter obeys the empirical law, RI = Z/L, which was based on Kerang's observation (Swinbank, 1964) and consequently Prandtl number is equal to the inverse of the non-dimensional velocity gradient.

Later on Paulson (1970) integrated the non-dimensional gradient in the following forms

$$u = \frac{u_*}{k}\,[\ln(Z/Z_o) - \psi_1] \tag{10}$$

$$T - T_o = T_*[\ln(Z/Z_o) - \psi_2] \tag{11}$$

$$\psi_1 = \int_o^{\xi} \frac{1 - \phi_1(\xi')}{\xi'}\, d\xi' \tag{12}$$

$$\psi_2 = \int_o^{\xi} \frac{1 - \phi_2(\xi')}{\xi'}\, d\xi' \tag{13}$$

(i) KEYPS Function

ϕ_1 is related to the similarity parameter through (9) and

$$\psi_1 = 1 - \phi_1 - 3 \ln \phi_1 + 2 \ln\left[\frac{(1+\phi_1)}{2}\right] + 2\tan^{-1}\phi_1 - \frac{\pi}{2} + \ln\left[\frac{1+\phi_1^2}{2}\right] \tag{14}$$

$$\frac{Z}{L} = \frac{RI}{(1 - \gamma \cdot RI)^{1/4}} \tag{15}$$

$$Pr = 1 \tag{16}$$

If one knows RI, the corresponding 1/L could be calculated from (15). With L determined, by this or other means, (1/L) is substituted in (9) which in turn is numerically solved for ϕ_1, which is substituted in (14) for ψ_1. The profile can then be predicted using (10).

(ii) Bussinger-Dyer

$$Pr = 1/\phi_1 \tag{17}$$

$$RI = Z/L \tag{18}$$

$$\phi_1 = \left(1 - \frac{\gamma Z}{L}\right)^{-1/4} \tag{19}$$

$$\phi_2 = (1 - \frac{\gamma Z}{L})^{-1/2} \tag{20}$$

$$\psi_1 = 2\ \ln[(\frac{1+x}{2})] + \ln[\frac{1+x^2}{2}] - 2\tan^{-1}x + \pi/2 \tag{21}$$

$$\psi_2 = 2\ \ln[\frac{1+x^2}{2}] \tag{22}$$

$$x = (1 - \frac{\gamma Z}{L})^{1/4} \tag{23}$$

B. Near Neutral Conditions. In this region the logarithmic law; $u = \frac{u_*}{k}\ [\ln(Z/Z_o)]$, applies and the value of the similarity parameter (Z/L) approaches zero.

C. Stable Stratification. The non-dimensional velocity and temperature gradients are expanded around neutral conditions (Z/L = 0), which results, after integration, in the log-linear profile.

Bussinger et al. (1971) suggested 4.7 for the value of the first power coefficient in the expansion which implies a critical Richardson number of 0.21

$$\phi_1 = 1 + 4.7(Z/L) \tag{24}$$

$$\phi_2 = 0.74 + 4.7(Z/L) \tag{25}$$

$$RI = (Z/L)\frac{(.74 + 4.7(Z/L))}{(1 + 4.7(Z/L)^2)} \tag{26}$$

$$\psi_1 = 4.7(Z/L) = \psi_2 \tag{27}$$

$$Pr = 1\ . \tag{28}$$

Webb (1970) suggested the value of 4.5 for the first power coefficient in the expansion for lapse conditions and a value of 5.2 for inversion conditions which results in a critical Richardson number of 0.20. Also taking Pr = 1 he arrived at the relationship between RI and (Z/L)

$$RI = \left(\frac{Z}{L}\right)\left(1 + \alpha\frac{Z}{L}\right)^{-1} \tag{29}$$

D. Strongly Stable Stratification. In the limit as $L \to 0$ and (Z/L) tends to infinity, Richardson number tends to $(1/\alpha)$ which is the critical value for the Richardson number after which turbulence ceases to be self sustaining. For very high values of the Richardson number every layer in the boundary layer will act independently and all forms of energy transport will cease.

Hence the value of α determines the critical Richardson number which was evaluated by Bussinger et al. and Webb to be around 0.2.

Some other investigators like Proudman (1953) and Sir Geoffry Taylor noticed that turbulence can be maintained at large values of Richardson number, they even found appreciable turbulent transport of momentum associated with Richardson numbers up to ten.

Webb (1970) noticed that for highly stable profiles a transition from log-linear profiles to simple logarithmic profiles occur and suggested the following form, which is mainly based on empirical observation.

$$RI = (Z/L)/(1+\alpha) \tag{30}$$

$$Pr = 1 \tag{31}$$

$$\phi_1 = \phi_2 = 1+\alpha \tag{32}$$

2.2 Analysis of the Monin-Obukov Length

There are three quantities that are sufficient to describe the turbulent atmospheric boundary layer according to similarity theory.

1) Buoyancy - Directly related to temperature gradients and the heating of the surface layer.

2) Shear Stress - Assumed constant with height and it is the turbulent transfer of momentum (neglecting molecular viscosity). In mixing length theory and in the inertial sublayer it is directly related to the velocity gradient.

3) Heat Flux - Assumed to be constant with height and it is the turbulent transfer of heat (neglecting molecular heat exchange). In the mixing length theory and in the inertial sublayer it can be related to temperature gradient.

The above three quantities could fairly well be expressed by the following three parameters.

1) Wind Speed at a fixed level (e.g. anemometer measured wind).

2) Net radiation (either measured by pyranometer or estimated by cloud cover, location, time of day, and time of year).

3) Roughness length (based on type of terrain and ground cover).

For every hourly profile given in the Kennedy and Argonne data the corresponding net radiation and wind speed class (wind speed measured at ten m. level) will be recorded and the dependence of the Monin-Obukov

length on net radiation and wind speed at ten m. level will be given in tabular form or in regression form; this analysis will apply only locally since L also depends on the roughness of the surrounding terrain which is a local feature. Hence the functional dependence of L on roughness length should be established.

2.3 Variation of Monin-Obukov Length with Roughness Length

$$L = - \frac{u_*^3}{H} \frac{C_p \rho T}{kg}$$

Assuming that the only two quantities that will vary considerably with roughness length Z_o are u_* and H, then

$$\frac{1}{L} \frac{\partial L}{\partial Z_o} = \frac{3}{u_*} \frac{\partial u_*}{\partial Z_o} - \frac{1}{H} \frac{\partial H}{\partial Z_o} \tag{33}$$

from equation (8)

$$\frac{1}{L} \frac{\partial L}{\partial Z_o} = \frac{2}{u_*} \frac{\partial u_*}{\partial Z_o} - \frac{1}{T_*} \frac{\partial T_*}{\partial Z_o} \tag{34}$$

But from (10)

$$u_{10} = \frac{u_*}{k} \left[\ln \frac{10}{Z_o} - \psi_1 \left(\frac{10}{L}\right) \right] \tag{35}$$

Differentiating partially w.r.t. Z_o

$$\frac{1}{u_*} \frac{\partial u_*}{\partial Z_o} = \frac{u_*}{u_{10} k} \left[\frac{1}{Z_o} - \frac{10}{L^2} \frac{\partial L}{\partial Z_o} \cdot \psi_1' \left(\frac{10}{L}\right) \right] \tag{36}$$

From (11)

$$T_{10} = T_o + T_*[\ln(10/Z_o - \psi_2] \tag{37}$$

Differentiating (37) with ZO

$$\frac{1}{T_*}\frac{\partial T_*}{\partial Z_o} = \frac{T_*}{T_{10}-T_o}\left[\frac{1}{Z_o} - \psi_2'\left(\frac{10}{L}\right)\left(\frac{10}{L^2}\right)\frac{\partial L}{\partial Z_o}\right] \tag{38}$$

Hence from (34), (36), (38)

$$\frac{1}{L}\frac{\partial L}{\partial Z_o} = \frac{2u_*}{u_{10}k}\left[\frac{1}{Z_o} - \frac{10}{L^2}\frac{\partial L}{\partial Z_o}\psi_1'\left(\frac{10}{L}\right)\right] + \frac{T_*}{T_{10}-T_o}\left[-\frac{1}{Z_o} + \frac{10}{L^2}\frac{\partial L}{\partial Z_o}\psi_2'\left(\frac{10}{L}\right)\right] \tag{39}$$

$$\frac{1}{L}\frac{\partial L}{\partial Z_o} = \left[\ln\frac{10}{Z_o} - \psi_1\left(\frac{10}{2}\right)\right]^{-1}\left(\frac{2}{Z_o} - \frac{20}{L^2}\frac{\partial L}{\partial Z_o}\psi_1'\left(\frac{10}{L}\right)\right) +$$

$$\left(\ln\frac{10}{Z_o} - \psi_2\left(\frac{10}{L}\right)\right)\left(-\frac{1}{Z_o} + \frac{10}{L^2}\frac{\partial L}{\partial Z_o}\psi_2'\left(\frac{10}{L}\right)\right) \tag{40}$$

Hence

$$\frac{\partial L}{\partial Z_o} =$$

$$\frac{\left(\frac{L}{Z_o}\right)\left\{\ln\frac{10}{Z_o} + \psi_1\left(\frac{10}{L}\right) - 2\psi_2\left(\frac{10}{L}\right)\right\}}{\left(\ln\frac{10}{Z_o} - \psi_1\left(\frac{10}{L}\right)\right)\left(\ln\frac{10}{Z_o} - \psi_2\left(\frac{10}{L}\right)\right) + \frac{10}{L}\left(2\ln\frac{10}{Z_o}\psi_1'\left(\frac{10}{L}\right) - 2\psi_1'\left(\frac{10}{L}\right)\psi_2\left(\frac{10}{L}\right) - \psi_2'\left(\frac{10}{L}\right)\ln\frac{10}{Z_o} + \psi_2'\left(\frac{10}{L}\right)\psi_1\left(\frac{10}{L}\right)\right)} \tag{41}$$

a) Unstable Conditions

i) Bussinger-Dyer

From (21), (22), (23)

$$\frac{\partial\psi_1}{\partial L}\left(\frac{10}{L}\right) = \left(\frac{2x}{1+x^2} + \frac{2}{1+x} - \frac{2}{1+x^2}\right)\left(\frac{40}{L^2}\right)\left(1 - \frac{160}{L}\right)^{-3/4} \tag{42}$$

$$\frac{\partial \psi_2}{\partial L}\left(\frac{10}{L}\right) = \left(\frac{4x}{1+x^2}\right)\left(\frac{40}{L^2}\right)\left(1 - \frac{160}{L}\right)^{-3/4} \tag{43}$$

Substituting (21), (22), (42), (43) in (41) we obtain $\frac{\partial L}{\partial Z_o}$ for Bussinger Dyer formula.

ii) KEYPS Function

$$\psi_1 = \psi_2 = \psi$$

$$\phi_1 = \phi_2 = \phi$$

Substituting in (41)

$$\frac{\partial L}{\partial Z_o} = \frac{\frac{L}{Z_o}}{\left(\ln \frac{10}{Z_o} - \psi\left(\frac{10}{L}\right)\right) + \left(\frac{10}{L}\right)\left(\psi_1'\left(\frac{10}{L}\right)\right)} \tag{44}$$

From (9)

$$L = \frac{10\gamma\phi^3}{\phi^4 - 1} \qquad \begin{array}{l} 0 < \phi < 1 \\ -.003 < 1/L < -\infty \end{array} \tag{45}$$

$$\frac{\partial L}{\partial \phi} = \frac{-10\gamma(\phi^2)(\phi^4-3)}{(\phi^4 - 1)^2}$$

From (14)

$$\frac{\partial \psi}{\partial \phi} = 1 - \frac{3}{\phi} + \frac{2}{1+\phi} + \frac{2}{1+\phi^2} + \frac{2\phi}{1+\phi^2} \tag{46}$$

Hence

$$\frac{\partial \psi}{\partial L} = \left\{-1 - \frac{3}{\phi} + \frac{2}{1+\phi} + \frac{2}{1+\phi^2} + \frac{2\phi}{1+\phi^2}\right\} \frac{(\phi^4 - 1)^2}{(-10\gamma)(\phi^2)(\phi^4-3)} \tag{47}$$

Substituting in (44) we obtain $\frac{\partial L}{\partial Z_o}$ for KEYPS Function in terms of ϕ

b) Near Neutral Conditions

$$\psi_1 = \psi_2 = \psi_1' = \psi_2' = 0$$

Substituting in (41)

$$\frac{\partial L}{\partial Z_o} = \frac{L}{Z_o \ln (\frac{10}{Z_o})} \tag{48}$$

Integrating between Z1 and Z2 we obtain

$$\frac{L2}{L1} = \frac{\ln 10 - \ln Z1}{\ln 10 - \ln Z2} \tag{49}$$

c) Slightly Stable Conditions

$$\psi_1 = \psi_2 = \frac{-10\alpha}{L^2}$$

$$\psi_1' = \psi_2' = \frac{10\alpha}{L^2}$$

Substituting in (41) we obtain

$$\frac{\partial L}{\partial Z_o} = \frac{L/Z_o}{\ln(\frac{10}{Z_o}) + (\frac{\alpha}{L}) + (\frac{10\alpha}{L^3})} \tag{50}$$

which could be rearranged and integrated from Z1 to Z2 to get

$$L_2 \ln \frac{Z2}{10} - 10\alpha \ln L_2 + 235(\frac{1}{L_2})^2 = L_1 \ln \frac{Z1}{10} - 10\alpha \ln L_1 + 235(\frac{1}{L_1})^2 = A(L_1, Z_1) \tag{51}$$

where Z1 is initial roughness length, L_1 is the corresponding Monin-Obukov length, Z2 is the required roughness length, and L_2 is the corresponding Monin-Obukov length.

(51) is actually the functional dependence of L on Z_0 in a closed form for all log linear profiles, since the value of α can always be adjusted.

D. Strongly Stable Conditions

$$\phi_1 = \phi_2 = 1 + \alpha \quad , \quad \psi_1 = \psi_2 = 0$$

Hence from (36) and (38)

$$\frac{1}{u_*} \frac{\partial u_*}{\partial Z_o} = \frac{1}{Z_o} \ln\left(\frac{10}{Z_o}\right) \tag{52}$$

$$\frac{1}{T_*} \frac{\partial T_*}{\partial Z_o} = \frac{1}{Z_o} \ln\left(\frac{10}{Z_o}\right) \tag{53}$$

Substituting in (34) and integrating from Z1 to Z2 we obtain

$$\frac{L_2}{L_1} = \frac{\ln 10 - \ln Z1}{\ln 10 - \ln Z2} \tag{54}$$

Figure 1 shows the variation of L with respect to Z_o given an initial value of L at Z_o = .05 m., keeping the net radiation and ten m. level wind speed constant. As expected the value of $|L|$ increases with Z_o because as Z_o increases more mixing occurs in the boundary layer which shifts the profile towards neutral stability, i.e. towards higher $|L|$ values. Also the convergence of (1/L) to zero as Z_o approaches infinity

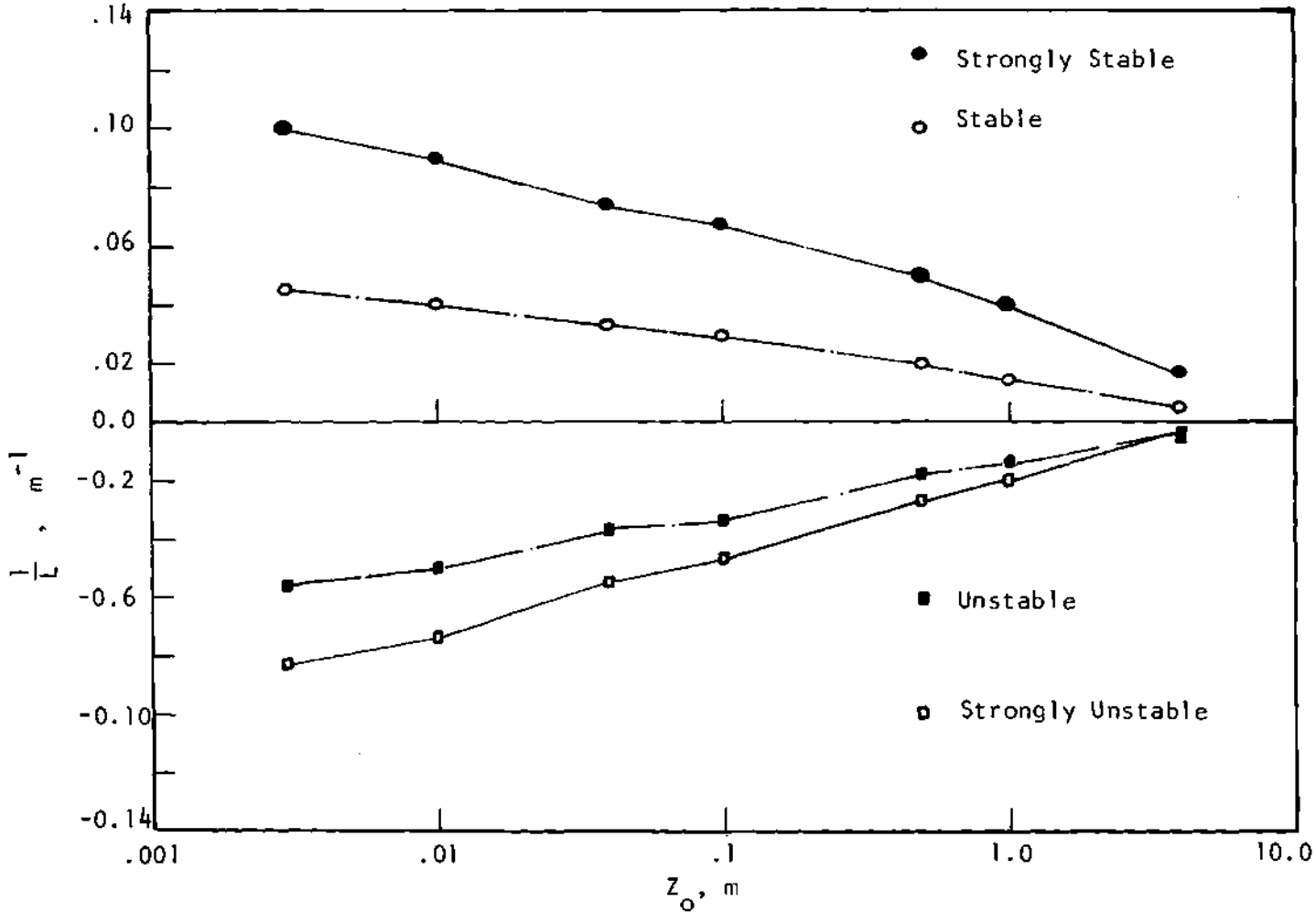

Figure 1. 1/L versus Z_o for Different Stability Regions.

is faster for unstable conditions due to the favorable mixing conditions that already exist for unstable stratification.

2.4 Net Solar Radiation

Since the atmospheric boundary layer is directly influenced by the net solar radiation penetrating the atmosphere the dependence of the Monin-Obukov length on radiation will be investigated for net radiation. Most National Weather Service Sites do not have instruments for measuring net radiation so far, sites have only a wind speed anemometer at one level. It becomes important to predict the total incident solar radiation based on position of the site (latitude), time of day and time of year. This "theoretical" solar intensity then has to be related to the net solar intensity through factors that are functions of cloud cover, cloud type, turbidity of the atmosphere and other factors.

The theoretical clear sky radiation could be directly estimated from tables in the ASHRAE Handbook of Fundamentals given for each latitude, or use different available theoretical models which will be referred to later.

For net radiation estimation Kimura (1969) related the clear sky radiation (I_{TH}) to net radiation (I_{THC}) through a cloud cover factor (CCF) where

$$I_{THC} = I_{TH} \cdot CCF$$

I_{THC} includes both direct and diffuse solar radiation, CCF is given for Ottawa in Table 1.

Table 1. Kimura Cloud Cover Factor

Month	sin β	p	Q	R
March	0.5 → 0.9	1.06	0.012	-0.0084
June	0.5 → 1.0	0.96	0.033	-0.0106
Sept.	0.5 → 0.9	0.95	0.030	-0.0108
Dec.	0.3 → 0.5	1.14	0.003	-0.0082

where $CCF = P + Q.CC + R(CC)^2$

CC is the amount of cloud on a scale from 0 to 10.

Also derived from a Boeing Company Report (1964) are the following six equations for estimation of net radiation,

$$CCM = 0.598 + .0026 \cdot TC + 0.0021 \cdot (TC)^2 - .0035(TC)^3, \quad CT = 0, \quad SALT \leq 45^\circ \quad (55)$$

$$CCM = .908 - .03214 \cdot TC + .0102 \cdot (TC)^2 - .00114(TC)^3, \quad CT = 0, \quad SALT > 45^\circ \quad (56)$$

$$CCM = .849 - .01277 \cdot TC + .0036 \cdot (TC)^2 - .00059(TC)^3, \quad CT = 1, \quad SALT \leq 45^\circ \quad (57)$$

$$CCM = 1.010 - .01394 \cdot TC + .00553 \cdot (TC)^2 - .00068(TC)^3, \quad CT = 1, \quad SALT > 45^\circ \quad (58)$$

$$CCM = 0.724 - .00652 \cdot TC + .00191 \cdot (TC)^2 - .00047(TC)^3, \quad CT \neq 0, \text{ or } 1, \quad SALT \leq 45^\circ \quad (59)$$

$$CCM = .959 - .02304 \cdot TC + .00787 \cdot (TC)^2 - .00091 \cdot (TC)^3, \quad CT \neq 0, \text{ or } 1, \quad SALT > 45^\circ \quad (60)$$

where CCM is the cloud cover modifier, and CT = 0 for stratus type cloud or equal to 1 for circostratus, TC = total amount of clouds at time t on a scale from 0 to 10, and $I_{THC} = I_{TH} \cdot CCM$.

The latest and most extensive research on net radiation estimation is the NOAA Solar Radiation Model which involves the prediction of clear sky radiation as a function of zenith angle of the sun and a correction factor for cloudiness, turbidity and less than the maximum duration of sunshine (See Appendix A).

2.5 Surface Roughness Estimation

An important part of the methodology will be an estimation of surface roughness length from topography and surface cover. An extensive amount of research has been conducted for this particular problem. Davenport (1965) gave the following estimates of roughness lengths for different types of terrains:

Table 2. Surface Roughness of Different Types of Terrain

Terrain type	Roughness length m.
Open sea	.0002 → .004
Flat open country	.02 → .06
Woodland, forest	.2 → 1.0
Urban area	1.0 → 6.0

Also Paeschke (1937) gave the following estimates after extensive analysis on natural crops:

Table 3. Roughness Lengths Associated with Different Crops

Crop	Z0 m.
Plane snow covered	.0049
Grassy surface	.0173
Flat country	.0214
Low grass	.032
High grass	.0394
Wheat	.045
Beets	.064

Wind tunnel tests were conducted by Plate and Quraishi (1965) and resulted in the following empirical formula for estimation of roughness lengths associated with different crops,

$$z_o = 0.15\ h_c, \tag{61}$$

where h_c is crop height.

The only crop listed by Paeshke which does not obey the experimental relation (61) is wheat which could be attributed to denseness of the crop.

2.6 Numerical Details

2.6.1 Data Description

a. The Kennedy Tower Data. The complete tower facility comprises two towers, one 18 m. and the other 150 m. high. The different levels on both towers are instrumented with wind and temperature sensors at levels 3, 18 m. for the small tower and 18, 30, 60, 90, 120, 150 m. for the large tower. Also wind speed, direction and net radiation are

recorded over a period of five years.

All the data profiles were supposed to be taken as a ten minute average centered around the hour point to filter out instantaneous disturbances and gusts.

The terrain surrounding the tower is homogeneous and covered with vegetation one to two m. high from (0 - 90°) clockwise. Another homogeneous zone with the same type of vegetation occurs in the 135-160° quadrant. The areas (230 - 300°), (90 - 135°), (160 - 180°) are covered with trees from 10 → 15 m tall. In the (180 - 230°) quadrant there is a body of water 225 m. from the tower.

The fact that two readings from the two towers are recorded at the same level will help to estimate the measurement error which will also relate to the accuracy of the model.

b. The Argonne Tower Data. The Argonne tower is 50 m. high, velocities are measured at levels 2.86, 5.72, 11.43, 28.6, 45.72 m. the temperature sensors are at five levels 1.68, 4.63, 10.36, 21.95, 43.89 m.

The terrain around Argonne tower is homogeneous and covered with sparse trees at 750 m. from the tower in the range (40 - 120°), from 120 - 230° it is clear land, from 320 - 360° there are dense trees at 550 m. from the tower.

2.6.2 Numerical Methods

i) Isolation of Neutral Profiles and Calculation of roughness lengths.

a. The hourly data that had more than two missing pieces of wind or

temperature information up to 60 m. or more than three missing values up to 150 m. were eliminated.

The given directions of the hourly profiles had to lie within the direction intervals prefixed according to the topography and vegetation of the surrounding terrain.

The temperature difference between two levels of measurements did not exceed 0.5°C otherwise the profile was considered anomalous.

A least square fit of the hourly temperature data with height was carried out, and the slope of the resulting best fit line was checked with dry adiabatic lapse rate (.0098°/m.) with tolerance of 0.003. The Richardson number was based on differencing velocity and temperature for the 3 and the 18 m. levels for the mean geometric height of 7.35

$$RI = \frac{9.806}{\bar{T}} \left(\frac{T(3) - T(1)}{H(3) - H(1)} + 0.0098\right) \left(\frac{H(3) - H(1)}{V(3) - V(1)}\right)^2 \qquad (62)$$

For Argonne the levels differenced were 2.86 and 45.72 m. for the geometric mean height of 9.9 m. If the magnitude of the Richardson number was less than 0.003 and the static temperature profile was within the neutral range, a least square fit with height was carried out to evaluate roughness lengths for different direction intervals.

The roughness lengths for each sector were averaged and the root mean square error was recorded.

b) The second method employed was suggested by Panofsky (private communication 1977). The roughness is evaluated for each direction and velocity class by least square fitting of the wind speed with logarithmic height. The velocity class is evaluated from wind speed at approximately 10 m.

level, then the roughness length is extrapolated to infinite velocity where mixing ensures neutral conditions.

ii) Roughness Length Check and Estimation of the Depth of the Similarity Layer. The stability range is divided into four main regions

Unstable	$RI \leq -.03$
Neutral	$-.03 < RI \leq .025$
Stable	$.025 < RI \leq .30$
Strongly Stable	$.30 < RI \leq 1.0$

The corresponding values of (1/L) are

Unstable	$(1/L) \leq -.003$
Neutral	$-.003 < (1/L) \leq .0025$
Stable	$.0025 < (1/L) \leq .162$
Strongly Stable	$.162 < (1/L) \leq .303$

The appropriate formula and roughness length for each sector and stability category were used to check the roughness length computed by each technique. The comparison was made by comparing the root mean square error between the predicted and given profile for each hour averaged over height.

The criterion for estimation of the depth of the similarity layer, which is the layer where similarity theory is successful in predicting the profile within a certain permissible error, is that the root mean square error is less than or equal to 1.2 m/s, since the root mean square error between the 18 m. level at the two towers in Kennedy Space Center averaged over five years turned out to be 0.65 m. with a maximum of 1.2 m/s and a minimum of 0.32 m/s.

If the average wind speed at 100 m. level is assumed to be 8 m/s, then the maximum permissible error is about 15%. The effect of a 15% error in wind speed prediction on the theoretical and extractable wind power is investigated in Appendix B.

Since the similarity layer is the layer where similarity laws apply within measurement errors, and the similarity theory applies only to the surface layer, then the depth of the similarity layer should be a good indication of the depth of the surface layer.

iii) The Monin-Obukov Length Evaluation. The evaluation of the Monin-Obukov length from Richardson number is direct from (15) or (18), (26), (29) for each hourly profile, then (1/L) was averaged for each direction interval, velocity class and net radiation class, also errors of the mean were calculated for each mean value. The root mean square error between predicted and given profile was calculated for each individual hourly profile. If the root mean square error in the unstable, neutral and stable regions exceeded 0.5 m/s or 0.9 m/s for the strong stability region where the theory is not expected to apply very well, the Monin-Obukov length calculated was considered as a first approximation and trial and error techniques were used for calculating the best fit Monin-Obukov length value.

iv) Solution of Equation (41). The Runge-Kutta technique was used.

v) Solution of Equation (9). Iterative techniques were used for solving the equation. The following table gives solution of equation (9) in tabular form to be referred to in case the methodology is used where no electronic computers are available.

Table 4. Solution of KEYPS Equation

(1/L)	Corresponding ϕ_1, Y = 10, Z = 10
0.0	1.0
-0.02	.701
-0.04	.585
-0.06	.520
-0.08	.476
-0.10	.444
-0.12	.419
-0.14	.399
-0.16	.382
-0.18	.367
-0.20	.355
-0.22	.344
-0.24	.334

CHAPTER III

DISCUSSION

3.1 Roughness Length Calculation and Estimation of Similarity Layer Thickness

3.1-1 Argonne Tower Data

According to the topography and surface cover around the tower the following direction intervals were chosen for Argonne.

1. 0 - 40°	2. 40 - 80°	3. 80 - 120°
4. 120 - 160°	5. 160 -190°	6. 190 - 230°
7. 230 - 270°	8. 270 - 320°	9. 320 - 380°

a) Results for Roughness Lengths Based on Richardson Number Isolation Method.

Table 5. Argonne Roughness Lengths Obtained by a Five Level Least Square Fit, $|Ri| < .03$

Direction Interval	Roughness Length (m)	Variation m
1	.016	.018 - .013
2	.033	.038 - .03
3	.049	.057 - .041
4	.121	.141 - .103
5	.031	.036 - .026
6	.028	.032 - .025
7	.051	.056 - .046
8	.042	.046 - .039
9	.012	.014 - .010

Table 6. Argonne Roughness Lengths Obtained by a Four Level Least Square Fit, $|RI| < .03$

Direction Interval	Roughness Length (m)	Variation in m.
1	.017	.019 - .015
2	.020	.022 - .018
3	.027	.032 - .023
4	.065	.075 - .056
5	.021	.023 - .018
6	.021	.023 - .019
7	.045	.049 - .042
8	.024	.026 - .022
9	.009	.011 - .008

b) Results for Roughness Lengths Calculated by Extrapolation to Neutral Conditions. The ten m. level velocity intervals are: 1, 2.5, 3.5, 4.5, 5.5, 6.5, 7.5, 8.5 m/s.

Table 7. Argonne Roughness Lengths Obtained by a Five Level Least Square Fit, Using Extrapolation Technique

Direction Interval	1	2	3	4	5	6	7	8	9
Roughness Length, m.	.008	.007	.007	.018	.012	.008	.019	.010	.002

Table 8. Argonne Roughness Lengths Obtained by a Four Level Least Square Fit, Using Extrapolation Technique

Direction Interval	1	2	3	4	5	6	7	8	9
Roughness Length, m.	.005	.012	.014	.025	.016	.009	.018	.015	.002

Figures 2 and 3 show how the aerodynamic roughness length (the roughness length that would minimize the error between mean predicted profile using the logarithmic law and actual data profile) asymptotically approaches the actual roughness length at very high wind speeds (i.e. 1/V tending to zero). Similar graphs have been drawn for the remaining direction intervals and the results are given in Table 5 and Table 6 for five level and four level least square fit respectively.

c) Determination of the Optimum Roughness Lengths. Figures 4 and 5 show the average wind speed at different direction intervals for all levels compared with the average predicted wind speed for neutral conditions using different roughness lengths obtained for the same direction intervals by different approaches.

The figures in the graphs represent the root mean square error between calculated and actual profiles averaged over height for each stability region.

Similar graphs have been drawn for the remaining seven direction intervals. By examining all nine graphs and choosing roughness lengths that would minimize the root mean square error between average predicted and given wind speed, the following set of optimum roughness lengths for Argonne is suggested in Table 9.

Table 9. Argonne Optimum Roughness Lengths

Direction Interval	1	2	3	4	5	6	7	8	9
Roughness Length, m.	.017	.033	.049	.065	.031	.028	.051	.042	.012

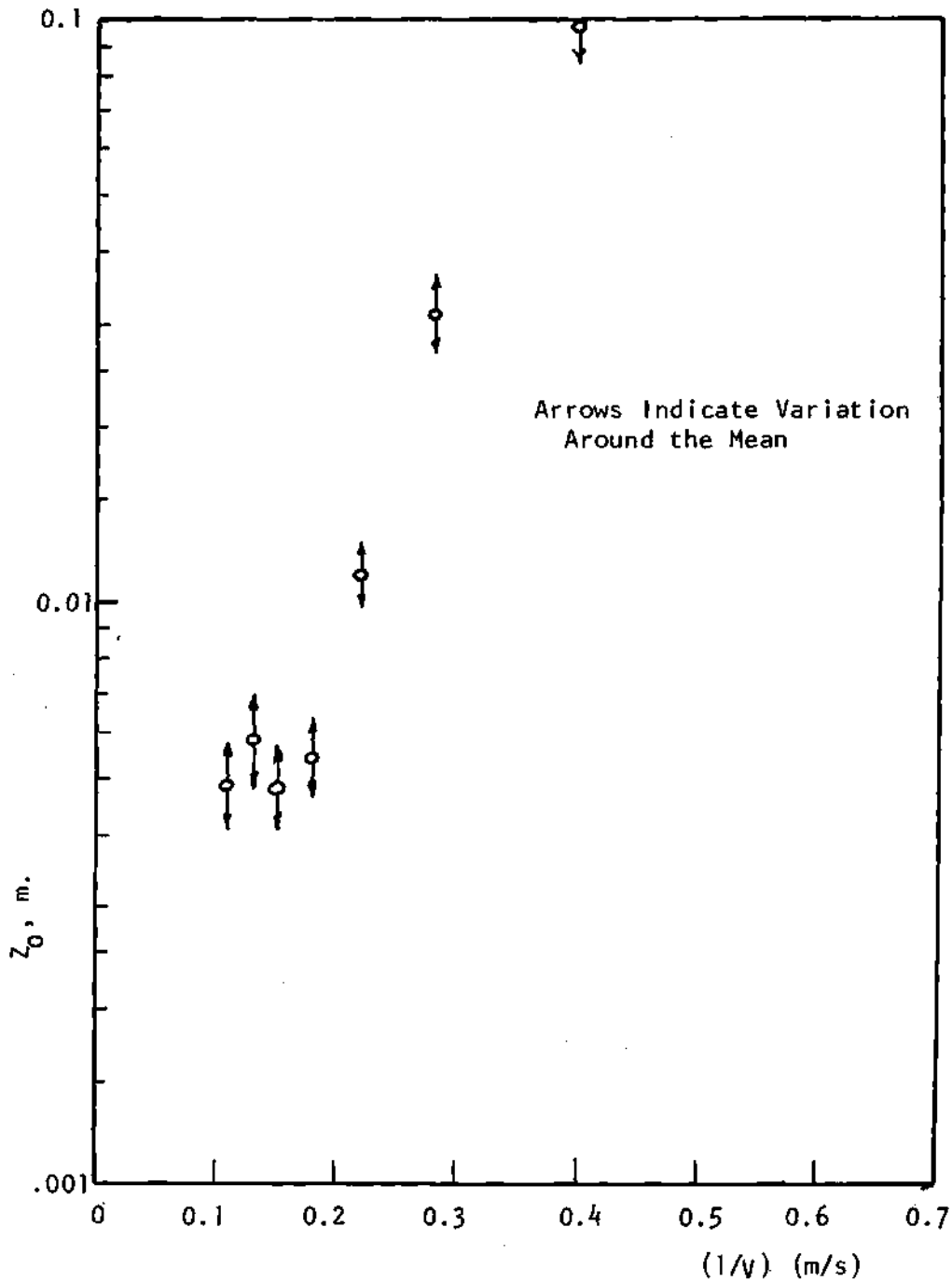

Figure 2. Argonne Aerodynamic Roughness Length for Direction 1, 5 Level Least Square Fit.

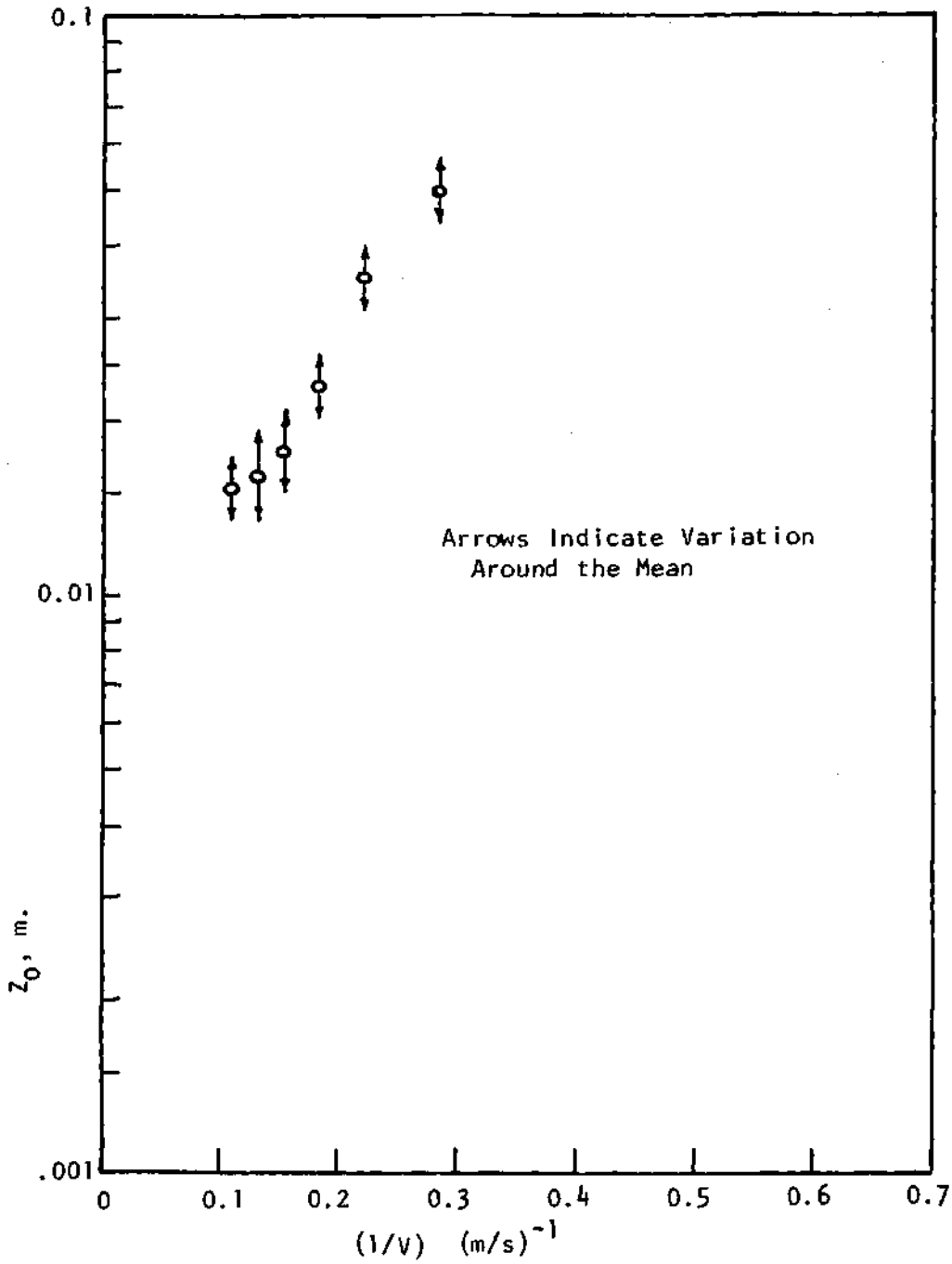

Figure 3. Argonne Aerodynamic Roughness Length for Direction 5,5 Level Least Square Fit.

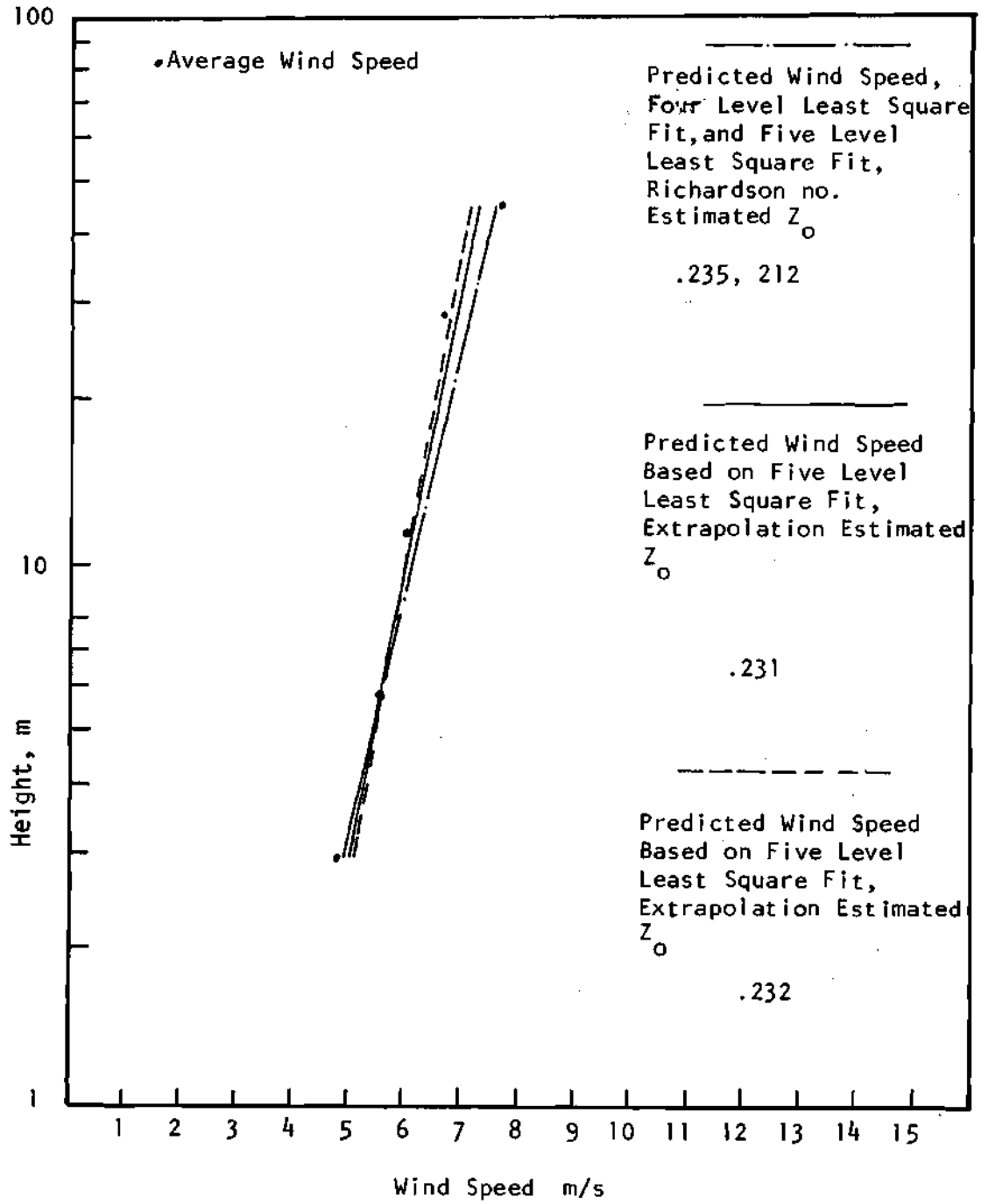

Figure 4. Argonne Average Wind Speed Against Predicted Wind Speed Based on Different Roughness Length Estimates for Direction 1.

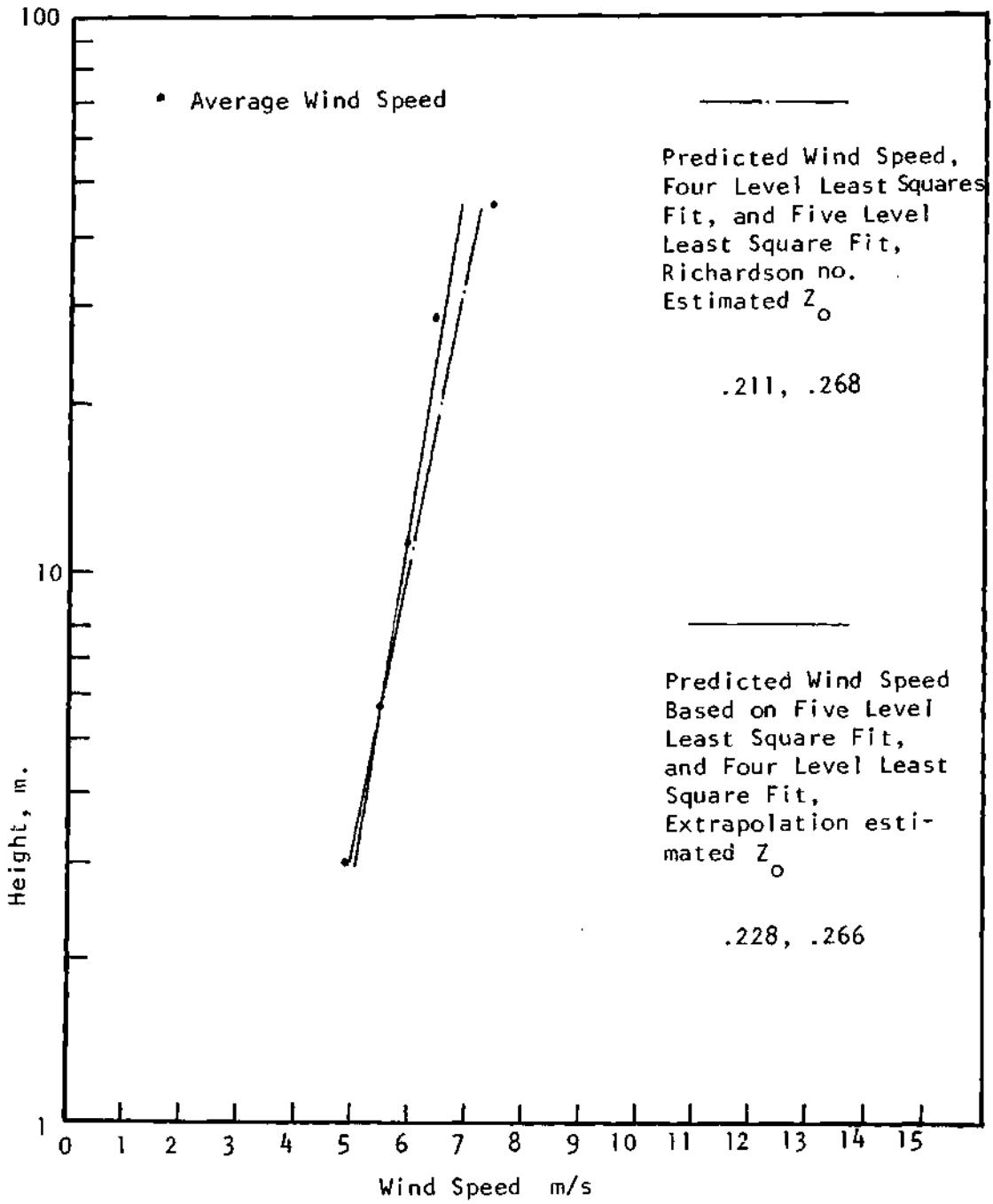

Figure 5. Argonne Average Wind Speed Against Predicted Wind Speed Based on Different Roughness Length Estimates, for Direction 9.

Comments

(i) The optimum roughness lengths for Argonne were all based on Richardson number selection technique.

(ii) The variation of roughness length with direction is smooth and agrees well with what is expected from topography and land cover in Argonne.

(iii) All points for average data wind speed roughly lie on a straight line on a semi-logarithmic scale which proves the validity of the methods used for isolation of neutral profiles.

(iv) The range of variation of roughness lengths around the tower is not very wide but still it is wide enough to demonstrate the effect of change of roughness on the Monin-Obukov length.

d) Similarity Layer Thickness. Figures 6, 7, and 8 show the root mean square error for each height (absissa) for the four stability classes for different directions. Similar graphs have been plotted for the remaining six direction intervals.

Comments

i) The Argonne tower height is all within the similarity layer since the root mean square error never exceeded 1.5 m/s, which in turn suggests that the inertial sublayer for Argonne extends to 50 m. for all directions and stability regions.

ii) As expected the errors for the strongly stable case are noticeably larger than the errors of the unstable, neutral, and stable cases. That is because turbulence in the strongly stable stratification diminishes and the different layers tend to act separately from each other.

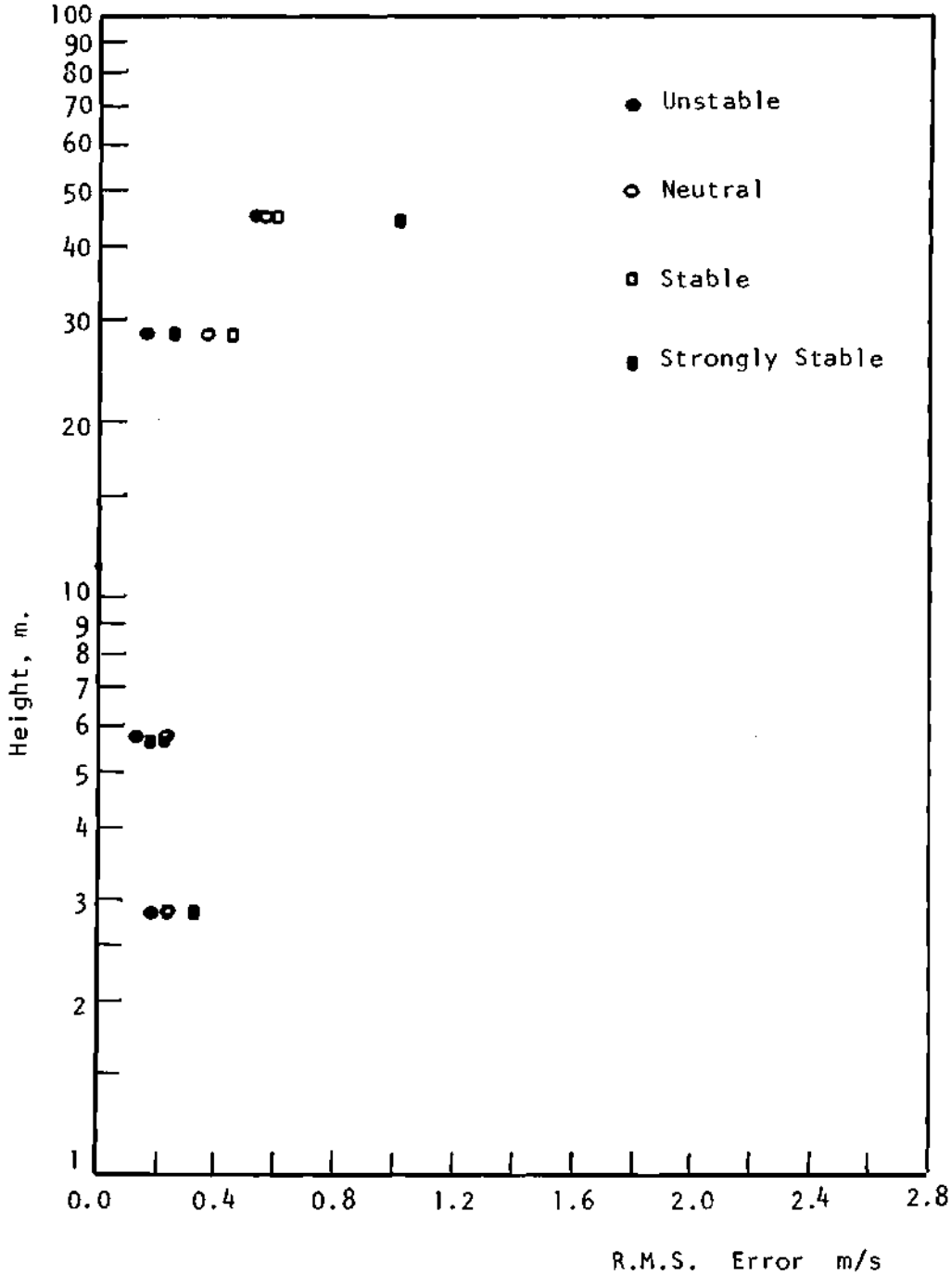

Figure 6. R.M.S. Error for Argonne Data, Direction 1.

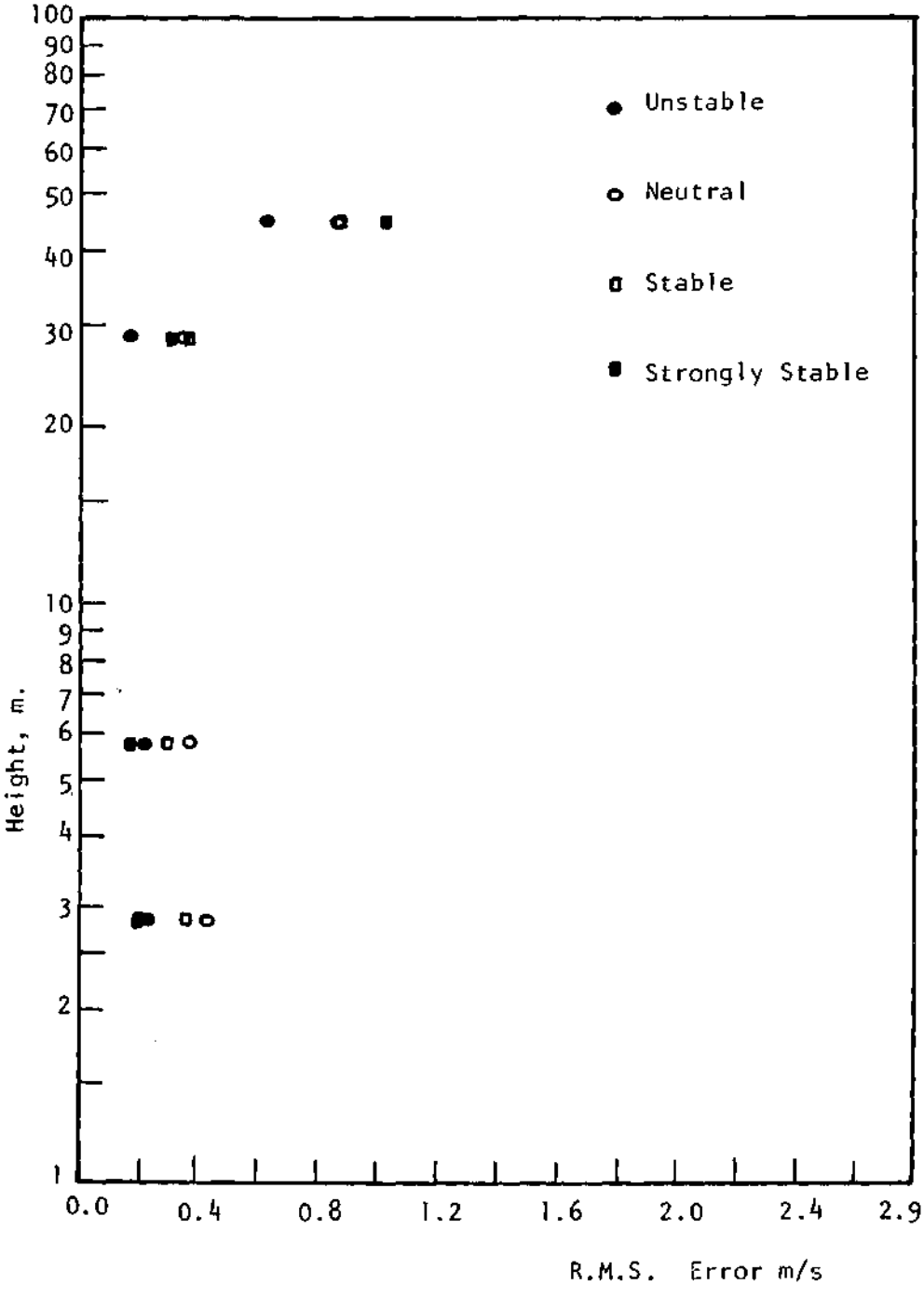

Figure 7. R.M.S. Error for Argonne Data, Direction 5.

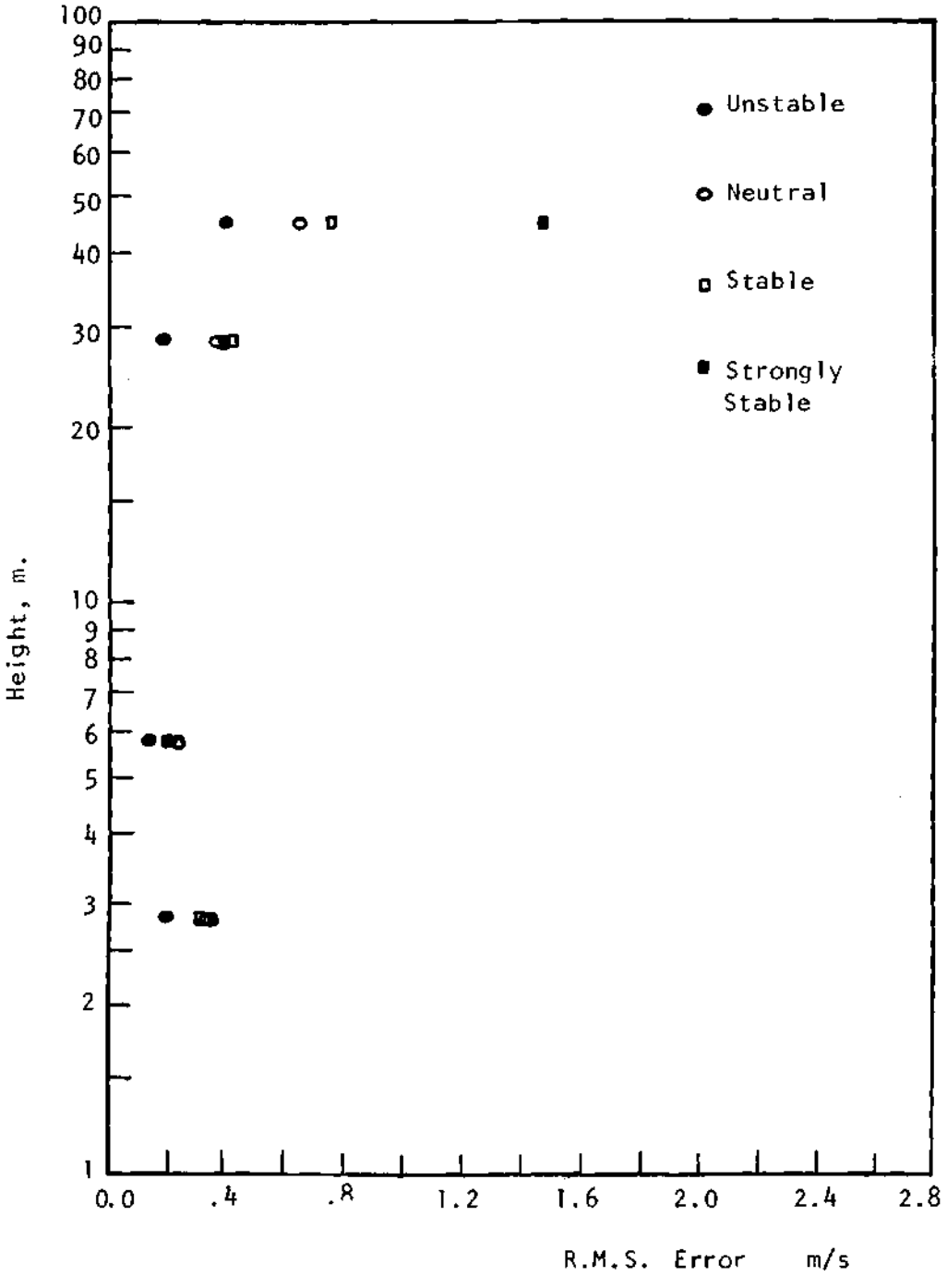

Figure 8. R.M.S. Error for Argonne Data, Direction 9.

3.1-2 Kennedy Tower Data

All the above analysis for Argonne data was repeated for Kennedy and the results for Kennedy roughness lengths were consistently smaller than those obtained by Fichtl (1969) and Panofsky (1973). Also the similarity layer thickness was smaller than expected (see Figure 9).

But by examining Figures 10, 11, and 12 and similar graphs that were plotted for the remaining two direction intervals where the average wind speed for neutral conditions were plotted against height on a semi-logarithmic scale, we can see that all the points lie on a straight line, which still proves the validity of the isolation techniques used, except for the wind speed at the three m. level which seems to be always on the higher side.

There are different explanations for this phenomenon. Since the area just around the tower is covered only with mowed grass, then just around the tower there is a sudden decrease in roughness length which could be responsible for the creation of an internal boundary layer with smaller roughness length, i.e. higher wind speed. Also, as has been discussed before since the viscous sublayer in the atmospheric boundary layer could extend up to five roughness lengths, there is a possibility that the three m. level could be in the viscous sublayer since Kennedy has a high roughness.

Also during the course of isolating the neutral profile, no neutral profiles were found for the first three years, which was an anomalous result. Later in a private conversation with Fichtl it was found that the first three years of temperature data were not taken as ten minute

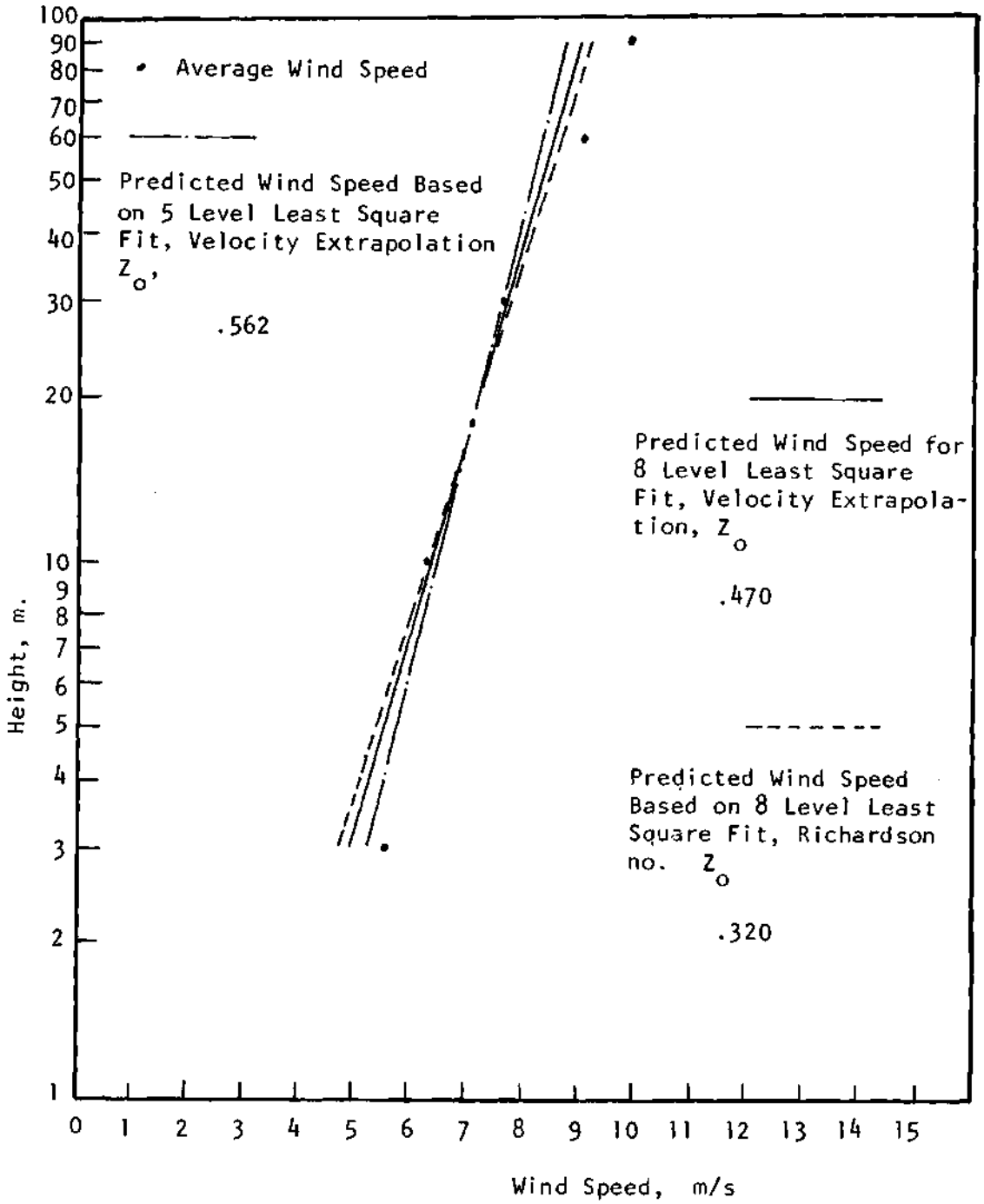

Figure 9. Kennedy Average Wind Speed Against Predicted Wind Speed Based on Different Roughness Length Estimates, Direction 2, 1st Level Included.

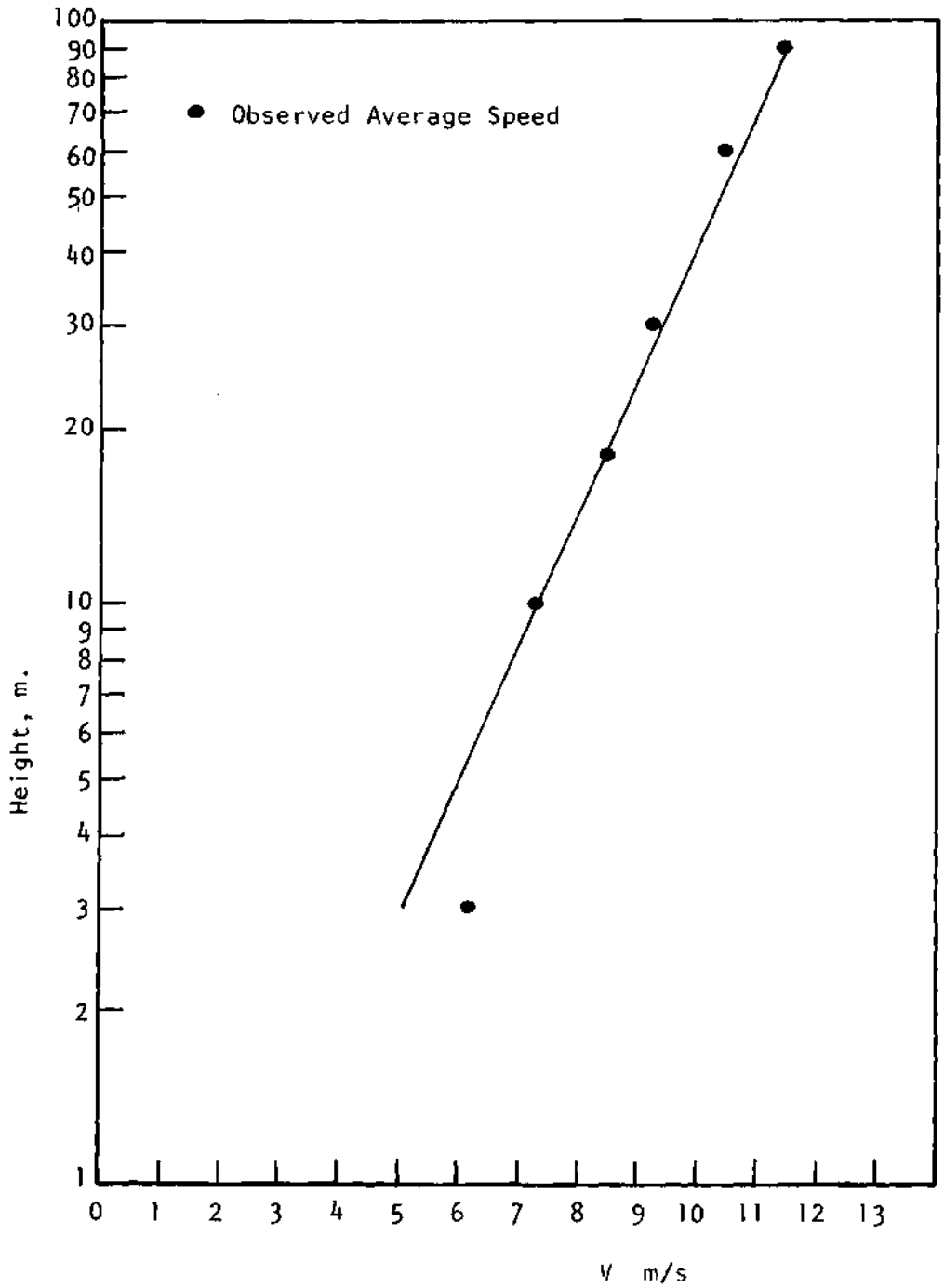

Figure 10. Kennedy Average Wind Speed for Neutral Stability, Direction 1.

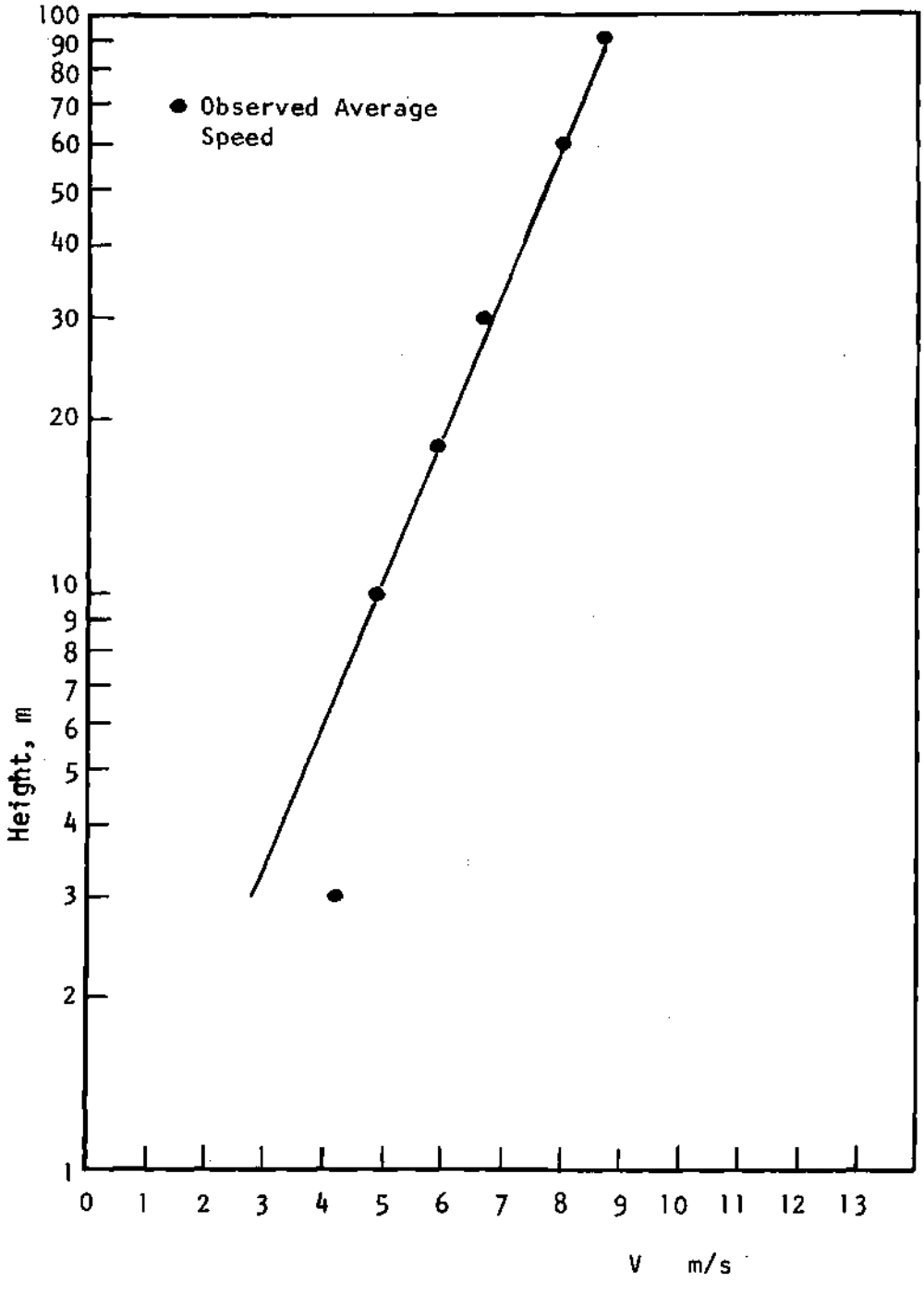

Figure 11. Kennedy Average Wind Speed for Neutral Stability, Direction 1.

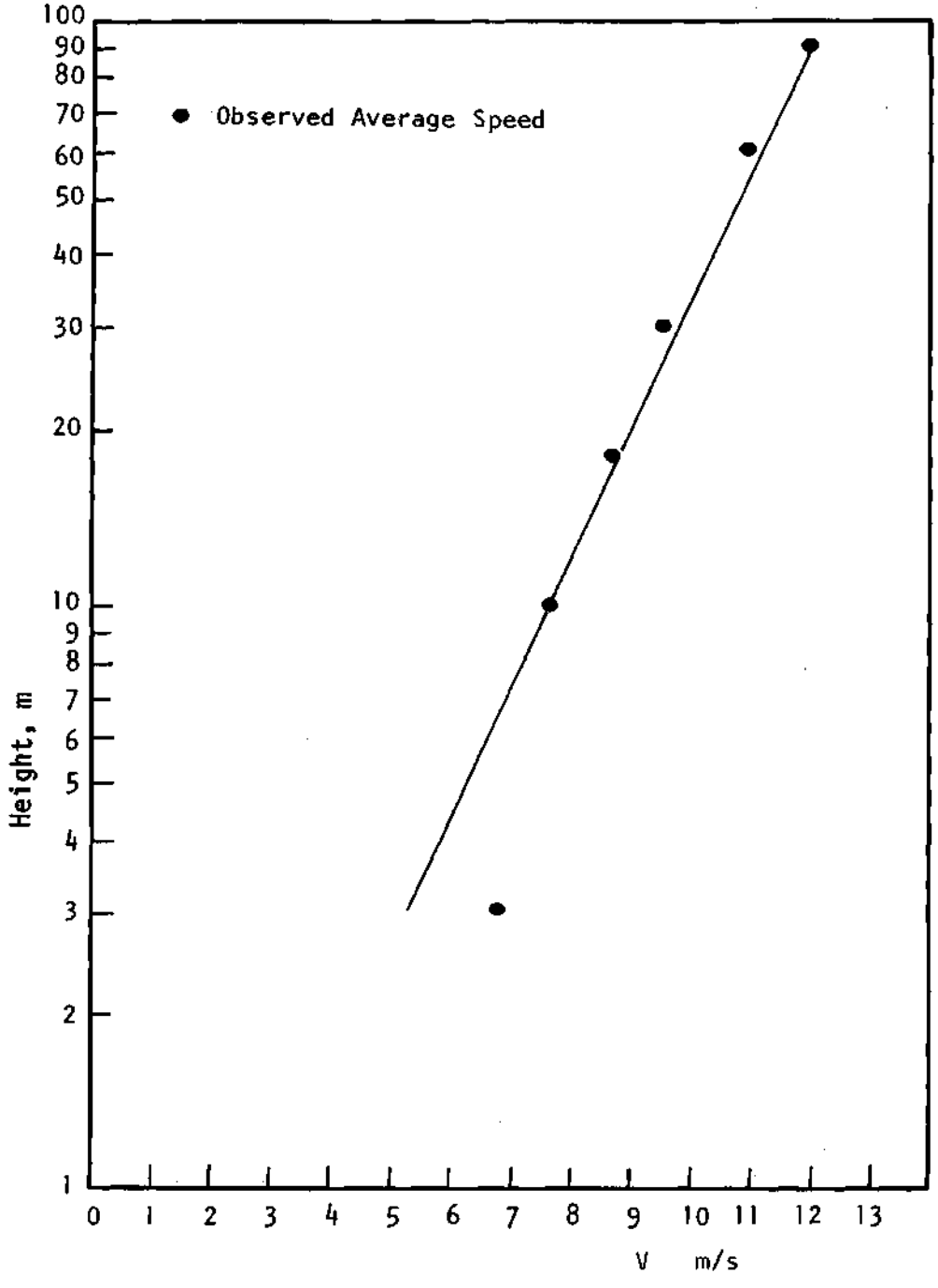

Figure 12. Kennedy Average Wind Speed for Neutral Stability, Direction 5.

average temperature, rather instantaneous temperature data was taken around the hour point.

Figure 13 shows a schematic representation of the development of internal boundary layers.

Consequently the whole procedure was repeated again disregarding the three m. level wind speed and the first three years of data for the Kennedy tower.

The following direction intervals were chosen for Kennedy tower based on topography and land cover.

1. (0 - 90°) 2. (90 - 180°) 3. (180 - 230°)

4. (230 - 315°) 5. (315 - 360°)

a) Results for Roughness Lengths Based on Richardson Number Isolation Method.

Table 10. Kennedy Roughness Lengths Obtained By an Eight Level Least Square Fit, $|RI| < .03$

Direction Interval	Roughness Length (m)	Variation in (m)
1	.272	.306 - .242
2	.692	.746 - .643
3	1.136	1.247 - 1.035
4	1.056	1.207 - .925
5	.274	.307 - .245

b) Results for Roughness Lengths Based on Extrapolation Method.

Kennedy: Ten m. velocity intervals (3.5, 4.5, 5.5, 6.5, 7.5, 8.5, 9.5, 10.5 →) m/s.

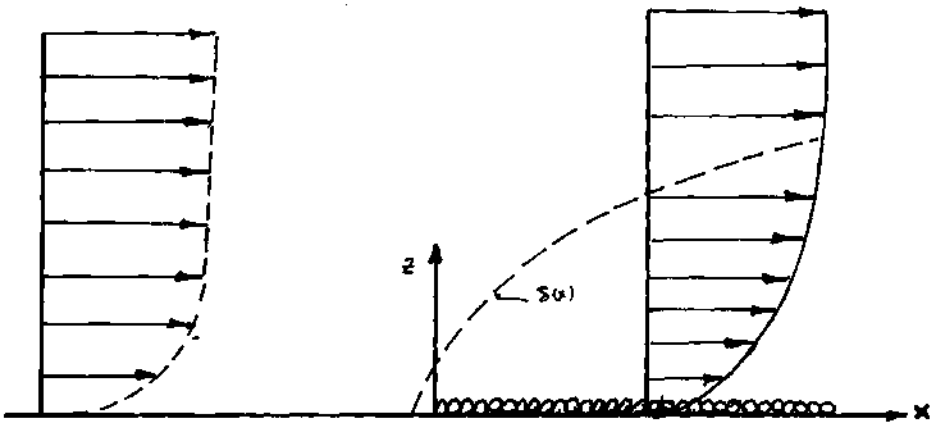

Figure 13. Schematic Representation of the Development of Internal Boundary Layer, Flow from Smooth to Rough.

Table 11. Kennedy Roughness Lengths Obtained by an Eight Level Least Square Fit, Using Extrapolation Technique

Direction Interval	1	2	3	4	5
Roughness Length, m.	.270	.40	.23	.64	.25

Figure 14 shows the convergence of aerodynamic roughness length at high velocities for direction five. Similar graphs to Figure 14 have been plotted for the remaining four direction intervals.

c) Determination of the Optimum Roughness Lengths. Similar figures to Figure 9 were plotted for the five direction intervals, Figure 15 and 16. By examining all five graphs the optimum roughness lengths that would minimize the error between observed and predicted mean wind speeds were estimated as a function of direction.

Table 12. Kennedy Optimum Roughness Lengths

Direction Interval	1	2	3	4	5
Roughness Length, m.	.272	.692	1.14	1.06	.274

Comments

i) Still the optimum roughness lengths are based on the Richardson number method. Hence in case the temperature profile is available, the Richardson number based method is recommended, but if the temperature profile is not available, the extrapolation method could be used since the errors associated with it are not significantly larger than the Richardson number based method. Also the aerodynamic roughness length

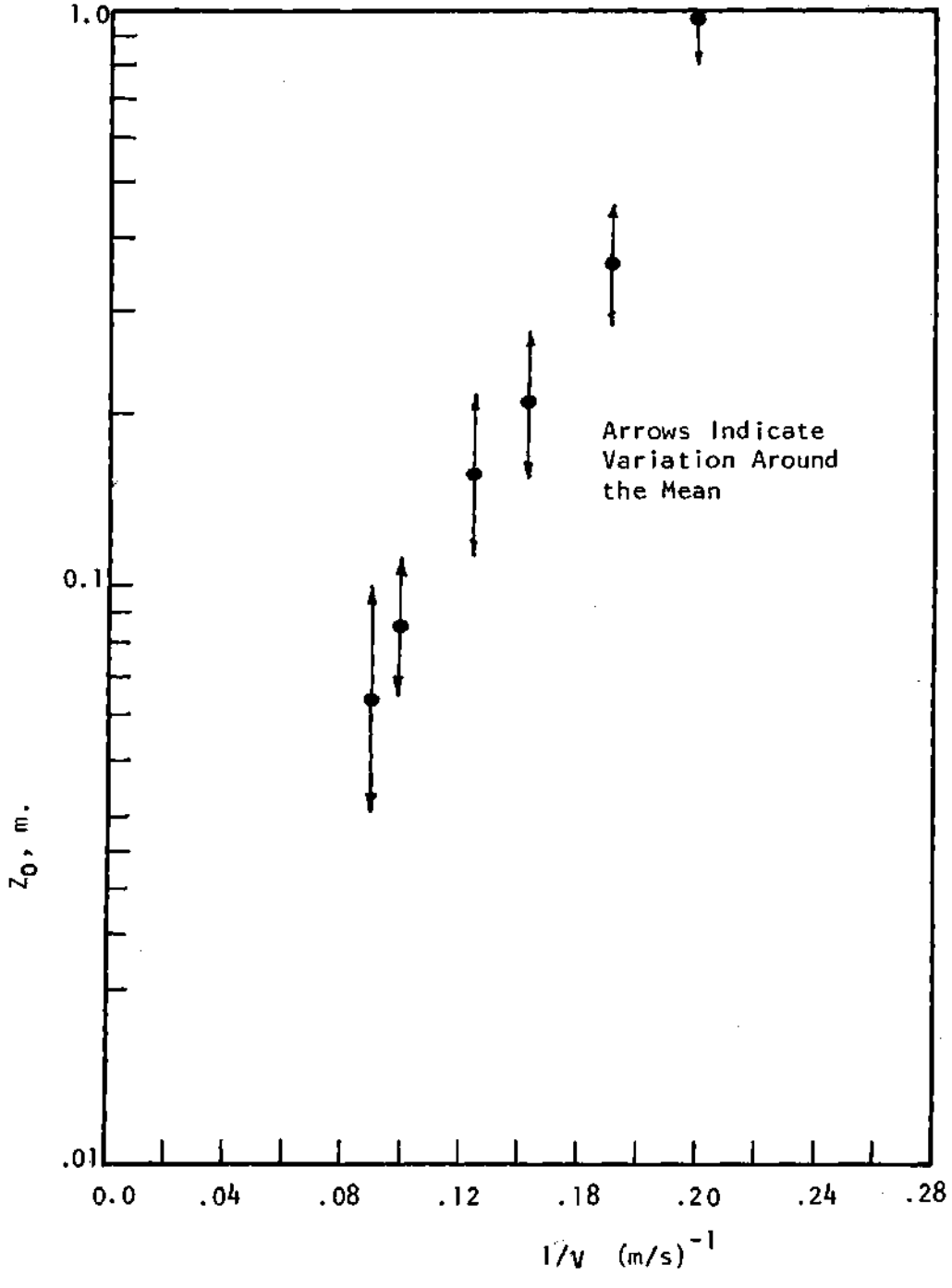

Figure 14. Kennedy Aerodynamic Roughness Length, for Direction 5,8 Level Least Square Fit, 3 m. Level Omitted.

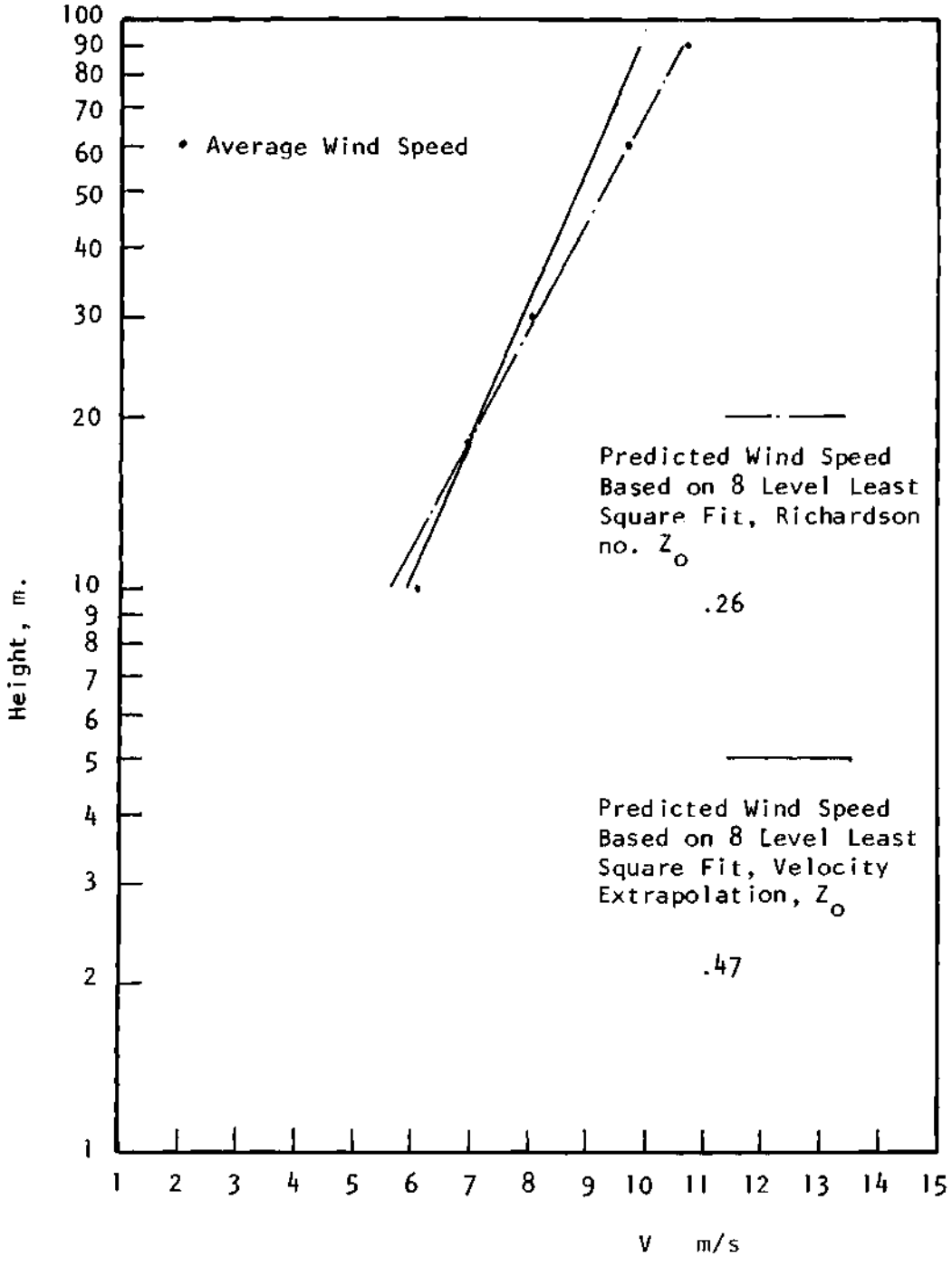

Figure 15. Kennedy Average Wind Speed Against Predicted Wind Speed Based on Different Roughness Length Estimates for Direction 2.

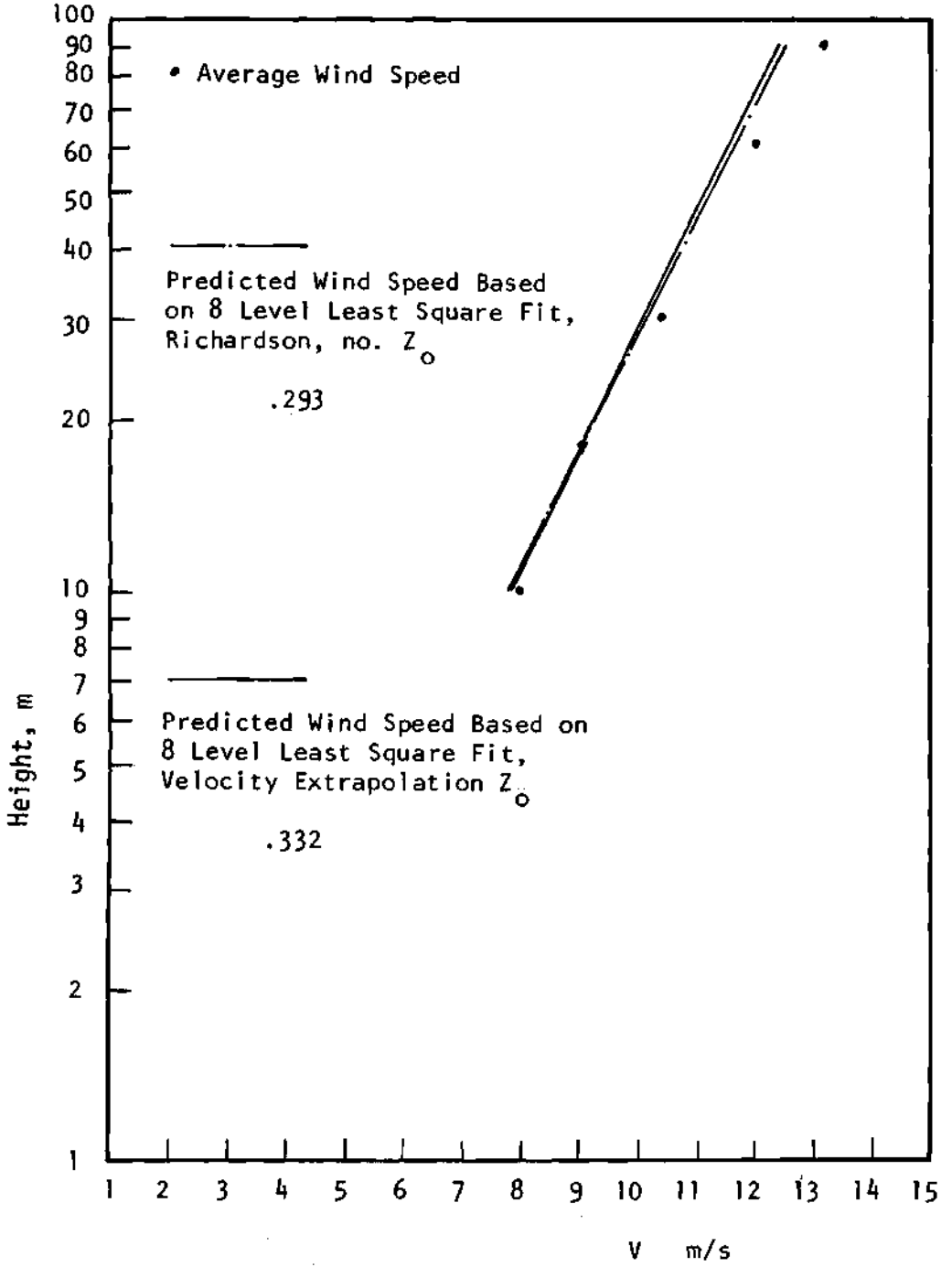

Figure 16. Kennedy Average Wind Speed Against Predicted Wind Speed Based on Different Roughness Length Estimates for Direction 5.

extrapolation technique underestimates in most cases the roughness length which could be due to the inaccuracy involved in dispensing with the temperature profile.

(ii) The variation of roughness length with direction is smooth and agrees well with the topography and land cover.

(iii) Figure 15 shows the average calculated wind speed versus the observed average wind speed against height for the newly estimated roughness length disregarding the three m. level, for the same direction given in Figure 9. The roughness length in Figure 9 for direction two is 0.9 m. It changed to .692 after elimination of the three m. level while the maximum error in profile prediction changed from .9 m/s to .5 m/s. For direction five the roughness length changed from .034 m. to .274 m. and the maximum error in profile prediction changed from .9 m/s to .4 m/s. Hence the profiles are relatively insensitive to changes in roughness lengths. This is very important to mention since the methodology intended to be proposed involves estimation of roughness lengths based on topography and land cover which may involve some error.

(iv) Other estimates for Kennedy roughness lengths were given by Panofsky (1973) and Fichtl (1969).

d) Similarity Layer Thickness. Figures 17 and 18 are similar to Figure 6 except it is for Kennedy tower data, also similar graphs have been plotted for the remaining three direction intervals.

Comments

i) As expected the root mean square errors are larger for stable cases which implies that the similarity layer is thicker for unstable and neutral stratification than for stable stratification.

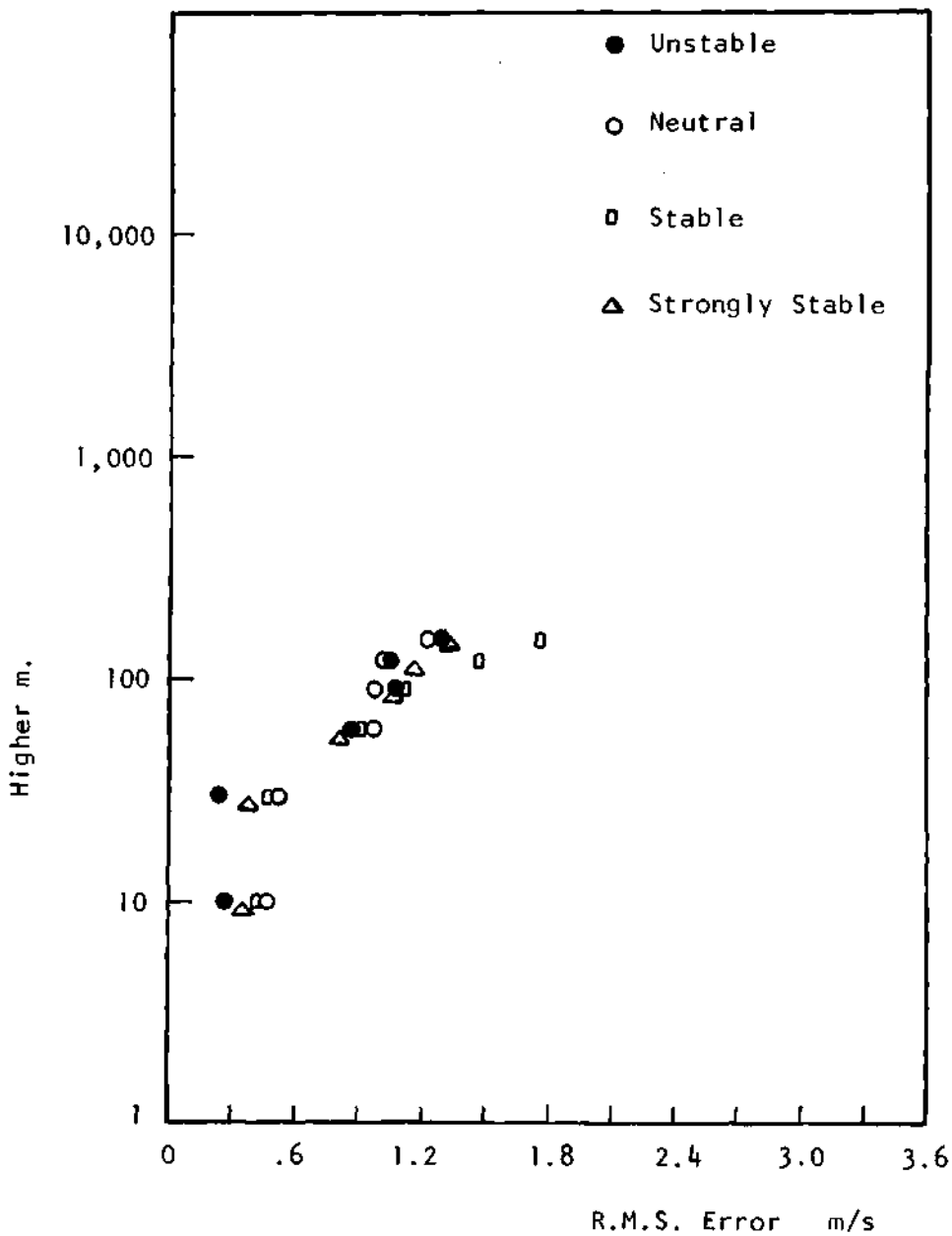

Figure 17. R.M.S. Error for Kennedy Data, Direction 1.

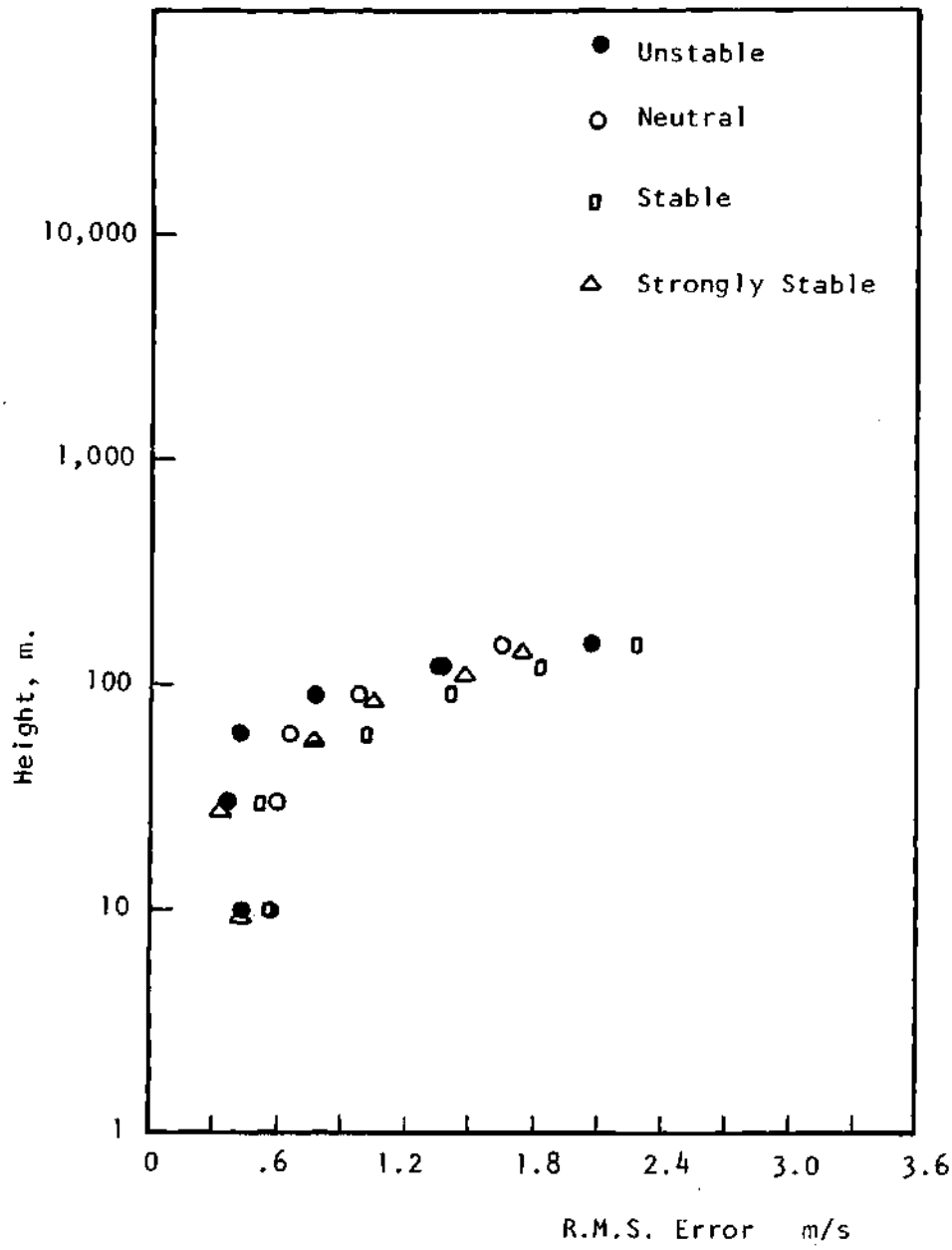

Figure 18. R.M.S. Error for Kennedy Data, Direction 3.

ii) By examining all graphs for all directions the similarity layer for Kennedy extends up to 90 - 120 m. except for direction four, it extends to 60 - 120 m.

iii) The errors for the stable stratification are consistently larger than the errors for strongly stable stratification, only for Kennedy data.

3.2 Determination of Arbitrary Constants for Best Fit and Comparison Between Bussinger and KEYPS Formulae for Unstable Conditions

Table 13 shows the error associated with Bussinger and KEYPS Formulae for different heights in Argonne data, the error is the root mean square error between the hourly observed and predicted profile averaged over all unstable profiles and all directions for each height.

Table 13. Comparison Between Bussinger and KEYPS Formulae

Height Level No.	1	2	3	4	5
Bussinger Error m/s	.262	.236	0	.258	.432
KEYPS Error m/s	.265	.235	0	.258	.452

Table 13 shows that both Bussinger and KEYPS functions work equally well for unstable conditions. The KEYPS formulation will be used in our model.

Table 14 shows the root mean square error between the hourly observed and predicted data profiles averaged over direction and height associated with different values of γ in KEYPS Function (equation (9)) for Kennedy and Argonne data.

Table 14. Optimization of Arbitrary Constant γ

γ		4	5	6	7	8	9	10	11	12
Argonne error	m/s	.1498	.1486	.1488	.1497	.1511	.1527	.1547	.1568	.1589
Kennedy error	m/s	.421	.422	.441	.459	.475	.489	.503	.576	.527

Table 14 shows clearly how insensitive the KEYPS function is to variation in the arbitrary constant γ. The value of γ suggested by Paulson (1970) will be utilized, $\gamma = 10$.

Webb's expansion coefficient α is the value of the first power coefficient in a Taylor expansion which was estimated by Bussinger to be 4.7 and from 4.5 - 5.2 by Webb. The value of this constant is of importance to evaluate not only because of the accuracy of the model in the stable region, but also due to the relationship between the critical Richardson number and α (equation (29)). The accurate estimation of the critical Richardson number will shed more light on the decay of turbulence in the atmospheric boundary layer.

The following two Figures, 19 and 20, show the root mean square error between hourly predicted and observed data profiles averaged over direction and height against the corresponding value of α for Argonne and Kennedy data respectively.

As can be seen from the graphs the value of α that minimizes the error for Argonne is 2.0 while for Kennedy it is between (1.5 and 2.0).

The value of 2.0 will be adopted. This value of α implies a critical Richardson number for Argonne and Kennedy data of 0.5 which is

considerably higher than the value suggested before by Webb and Bussinger. This means that turbulence in the atmospheric boundary layer can be self-sustaining for higher Richardson numbers.

3.3 Monin-Obukov Length

A major objective for this research work is to be able to determine with minimum error the value of the Universal Monin-Obukov Length associated with a certain roughness length for different ten m. level wind speeds and net radiation values. Hence by using (41) we can obtain L for any wind speed, net radiation class and roughness length. As mentioned in (2.5-2) the Richardson number is used to evaluate L for each profile and then the profile is reproduced and the root mean square error between the predicted and given profile is calculated and averaged over height. If the error is within measurement error, the value of L is accepted, otherwise the value of L is considered as a first approximation and an iterative technique around the starting value of L is used to find the value of L that would minimize the error.

i) Argonne Data

Statistical Introduction

Table 15. Hourly Profiles Statistics

Total Number of Profiles	Unstable	Neutral	Stable	Very Stable
23158	7899	2276	11553	1430

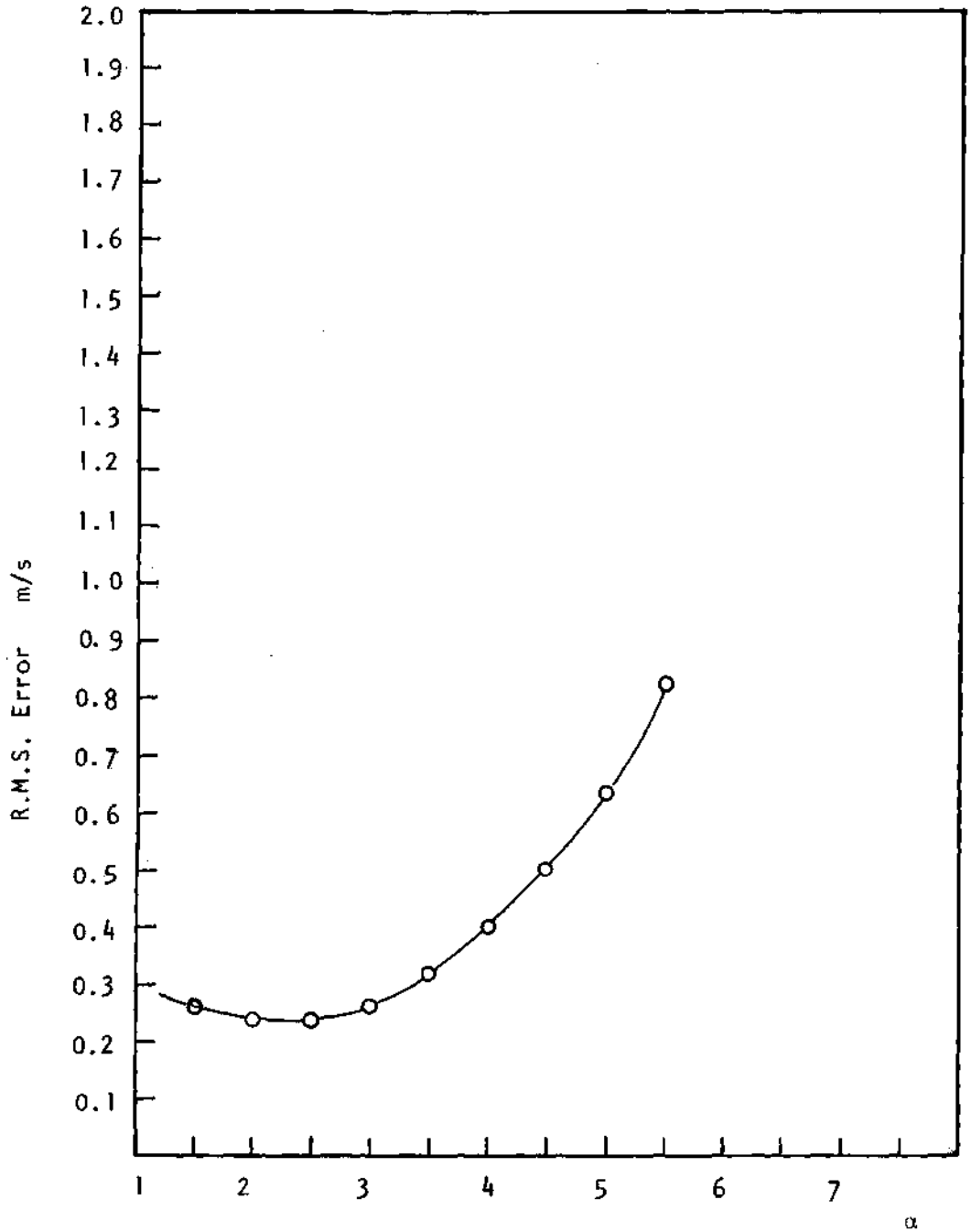

Figure 19. Argonne R.M.S. Error Averaged Over Height and Direction against α.

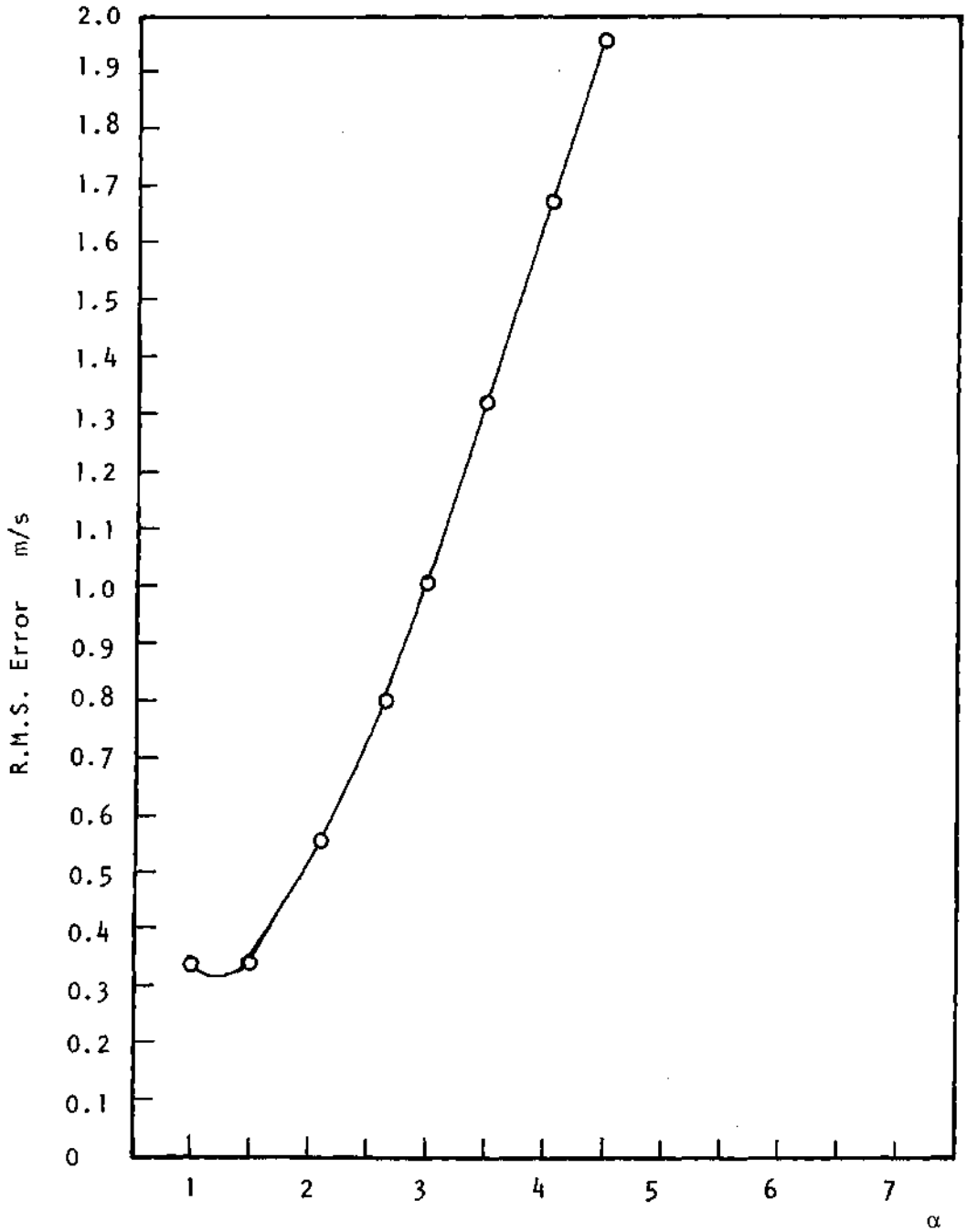

Figure 20. Kennedy R.M.S. Error Averaged Over Height and Direction Against α.

Number of profiles where the theoretical value of the Monin Obukov length predicted the profile within measurement error	18685
Number of profiles that required iteration	3817
Total number of profiles after optimization	22502
Unstable	7899
Neutral	2101
Stable	11186
Very Stable	1316
Number of hourly data that did not predict the observed profiles within measurement error	656

The next table shows the root mean square error averaged over height and direction for each stability region.

Table 16. Average R.M.S. Error for Each Stability Region

Stability Region	R.M.S. Error
Unstable	.567
Neutral	.338
Stable	.372
Very Stable	.579

Figure 21 shows the value of (1/L) versus wind speed for different net radiation classes, averaged over direction. These values of (1/L) correspond to an average roughness of .03 m. The graph shows how accurately the Monin-Obukov length, extracted from the data, using our model, follows the expected physical dependence on net radiation and wind speed.

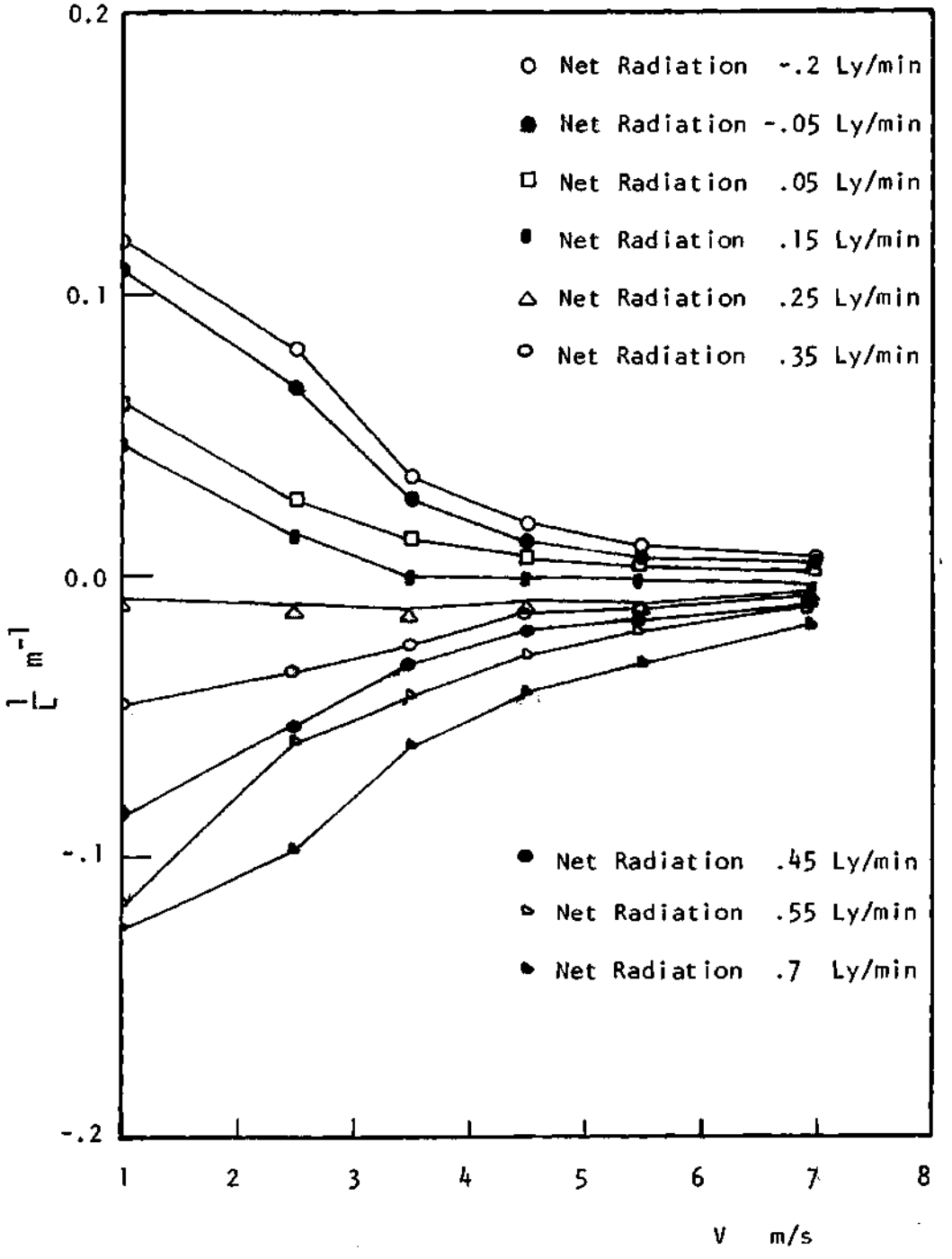

Figure 21. (1/L) Versus Wind Speed for Different Radiation Classes.

Increasing wind speed implies higher wind shear and dominant neutral conditions which implies higher values of L. On the other hand increasing radiation level has a destabilizing effect on the atmospheric boundary layer which implies lower values of L and vice versa.

Figure 22 shows the scatter of the calculated (1/L) around the mean value for Argonne data. The error bars indicate the error of the mean, the figures on the graph indicate the number of observations for each value of (1/L) for a given net radiation class ($< -.1$ cal/cm^2/min), roughness length (.42), and for each wind speed.

Another interesting extraction from Argonne data is shown in Figure 23 where the friction velocity (shear stress at the ground) is plotted against wind speed for different net radiation classes for the average Argonne roughness. Again the variation of friction velocity with wind speed follows exactly the expected physical dependence, since shear stress at the ground increases with increasing turbulence which is due to the increase in wind shear (wind speed). It also decreases with increasing radiation due to upward transfer of momentum resulting from surface heating.

The accuracy of the above two graphs indicate the effectiveness of the model used and the accuracy of measurement for Argonne tower data.

Figure 23 shows the variation of the Monin-Obukov length with roughness length for a given net radiation class for all wind speed classes. Similar graphs for different net radiation classes show the same trend. High values of roughness lengths introduce more turbulence in the atmospheric boundary layer which causes more mixing that shifts the stability towards neutral conditions, i.e. higher values of L.

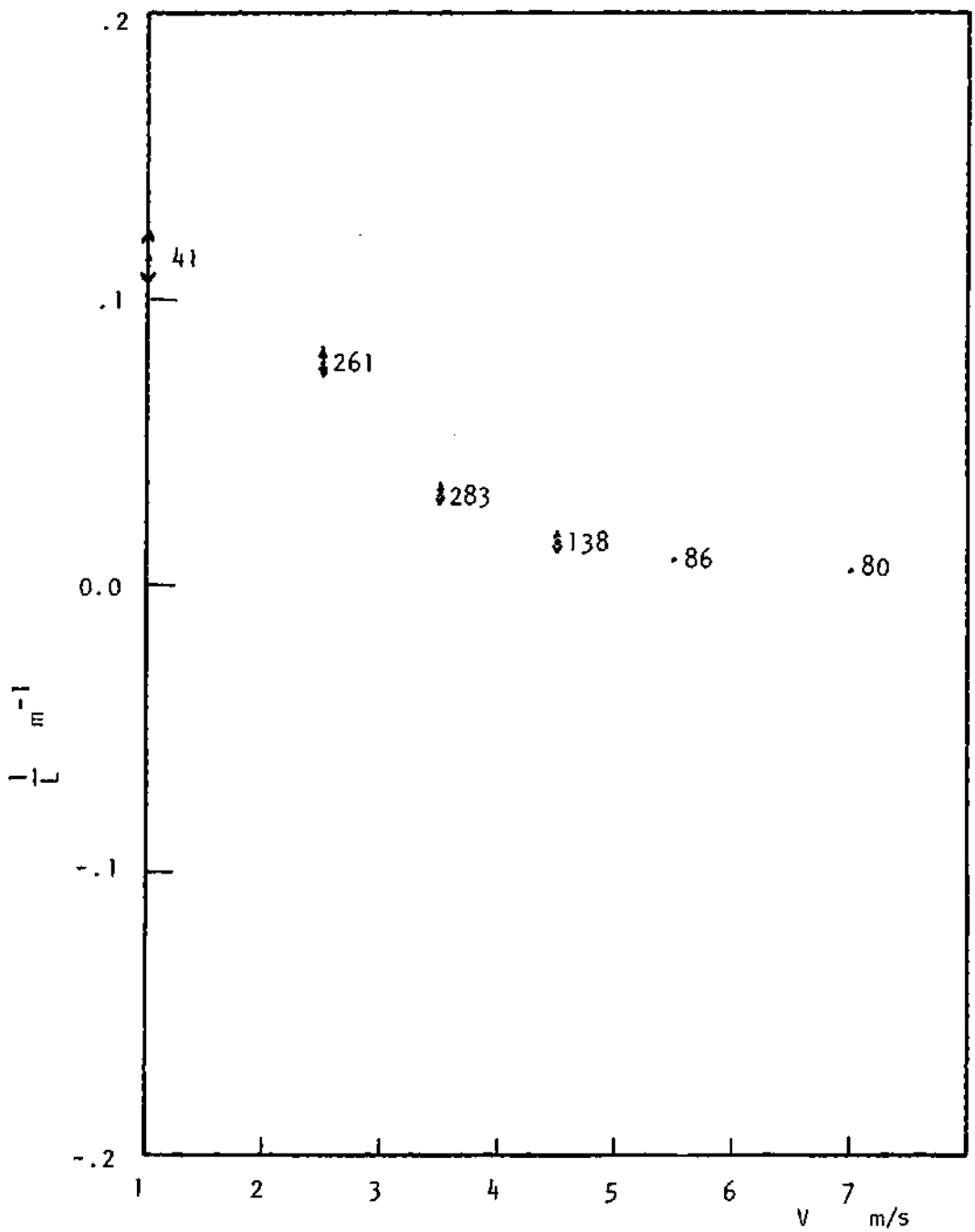

Figure 22. Scatter of 1/L Around the Mean

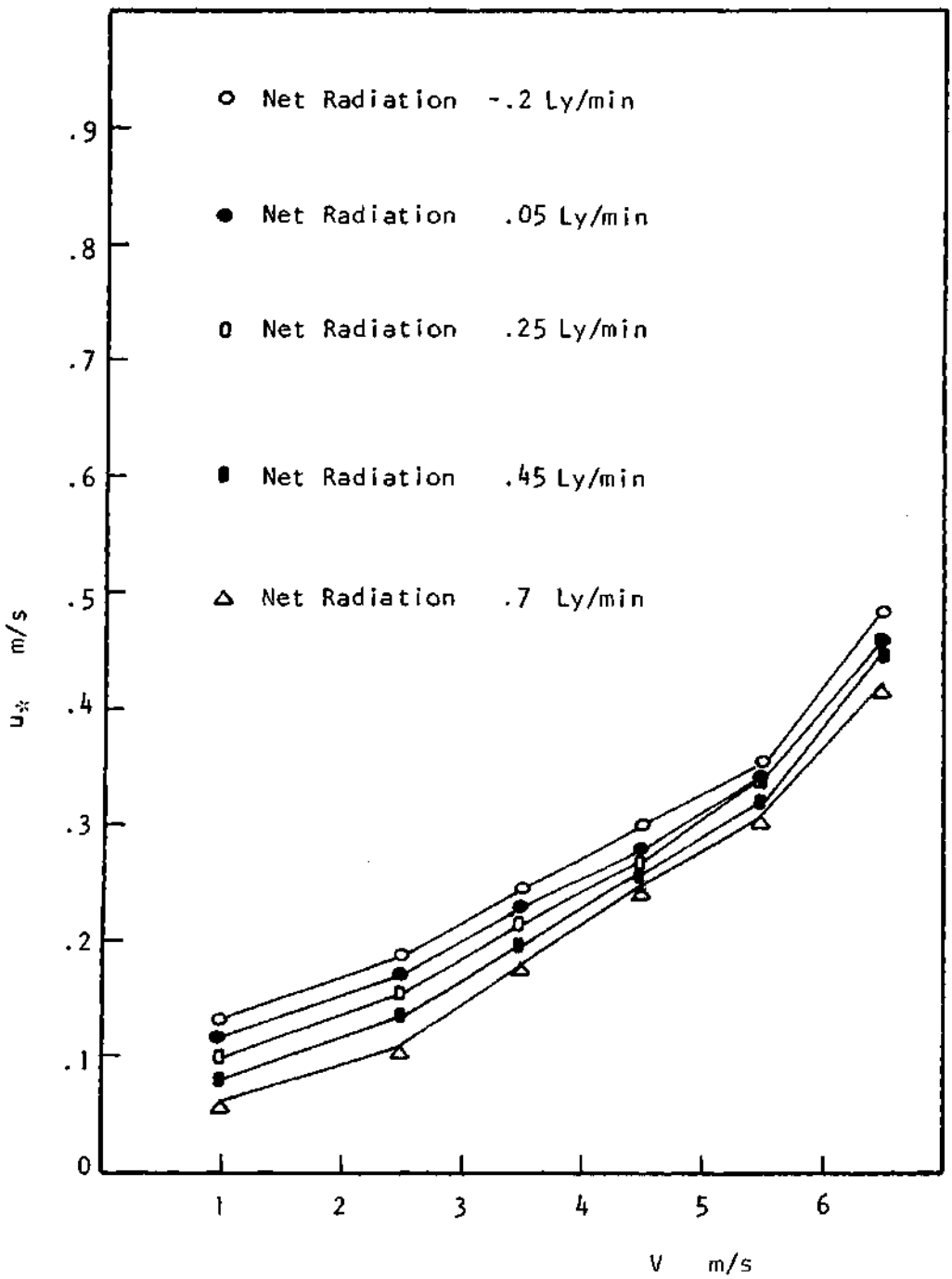

Figure 23. u_* Versus Wind Speed for Different Radiation Classes.

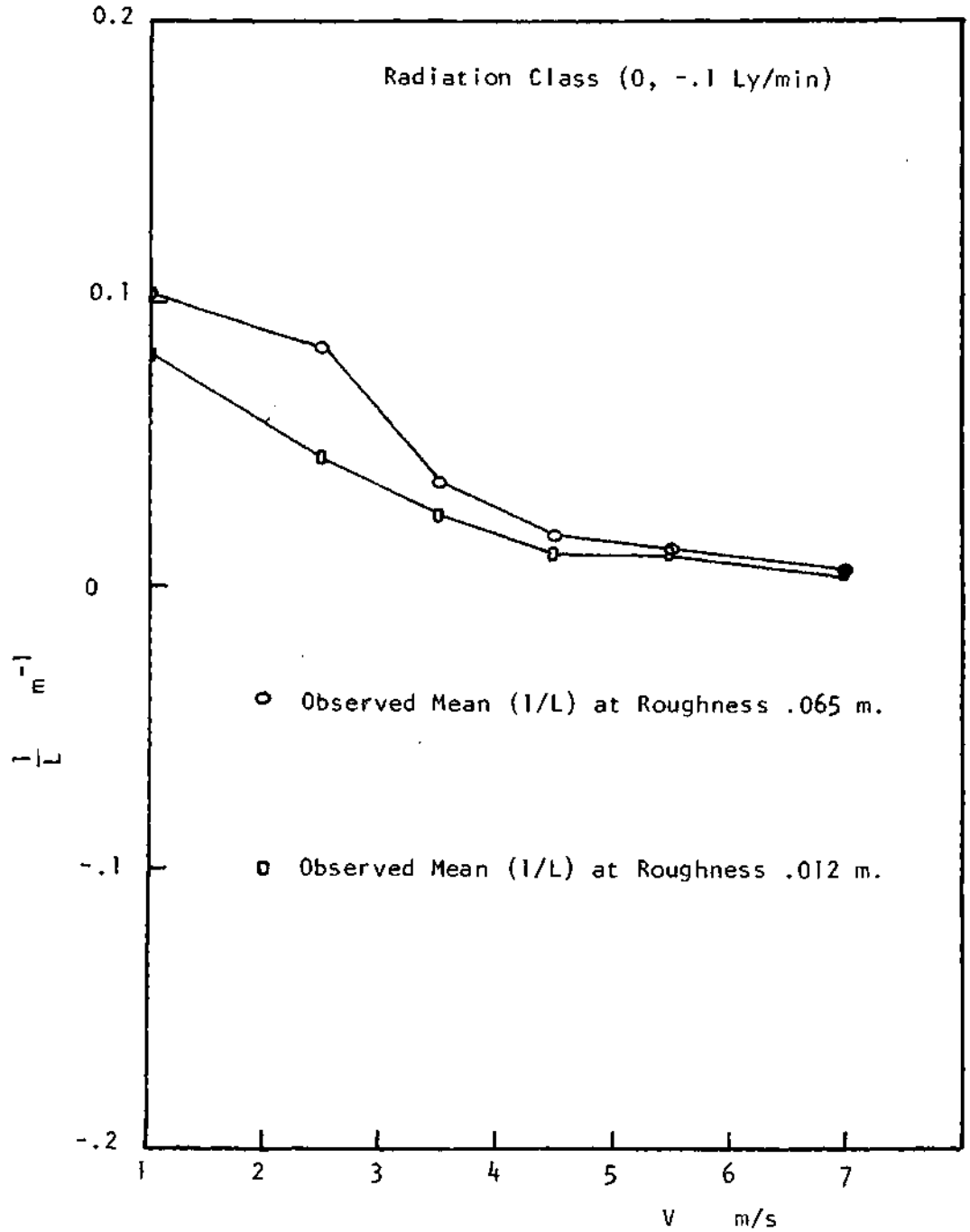

Figure 24. Sample Variation of (1/L) with Wind Speed and Roughness Length for a Given Net Radiation Class.

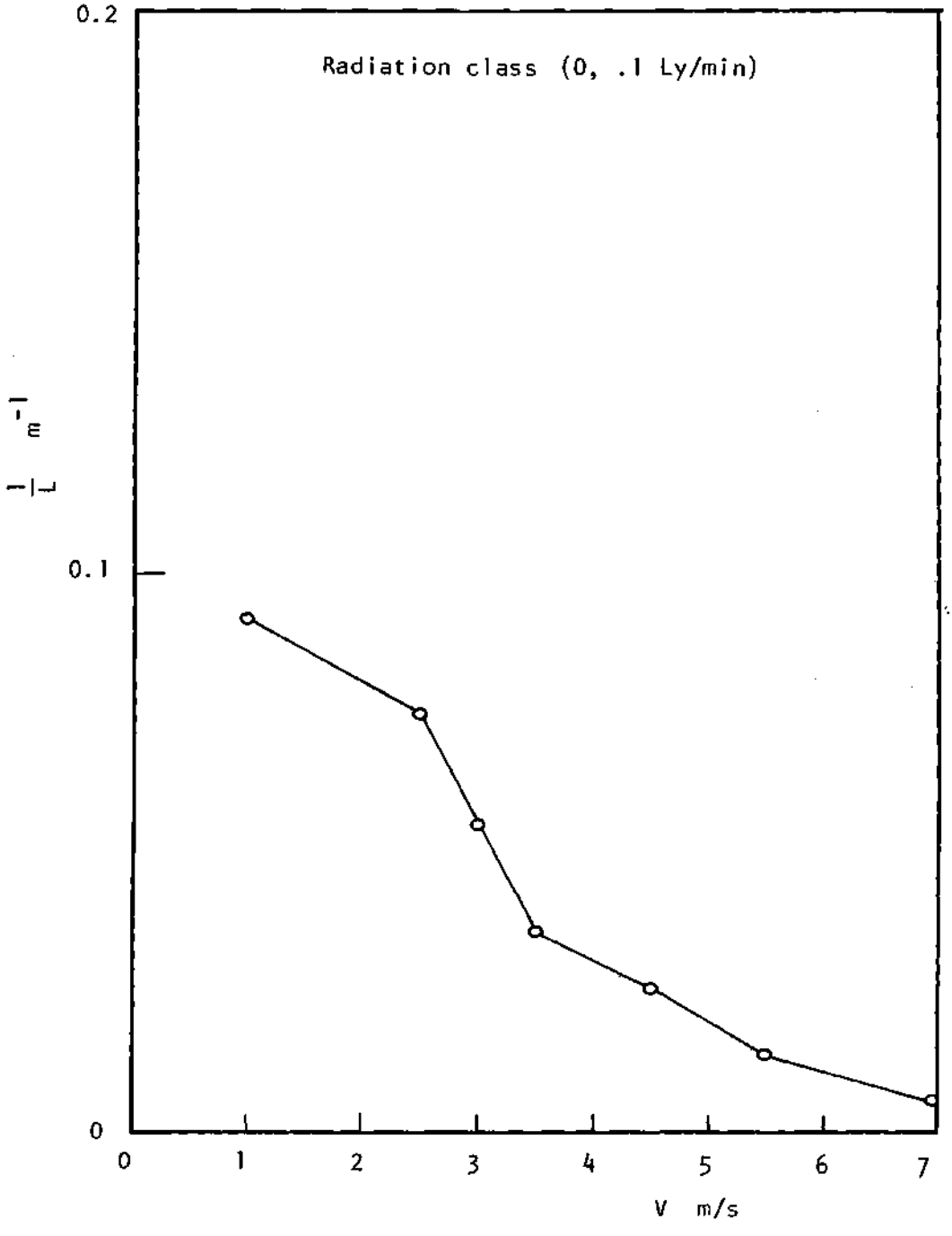

Figure 25. Mean (1/L) Versus Wind Speed for Stable Stratification based on Kennedy data.

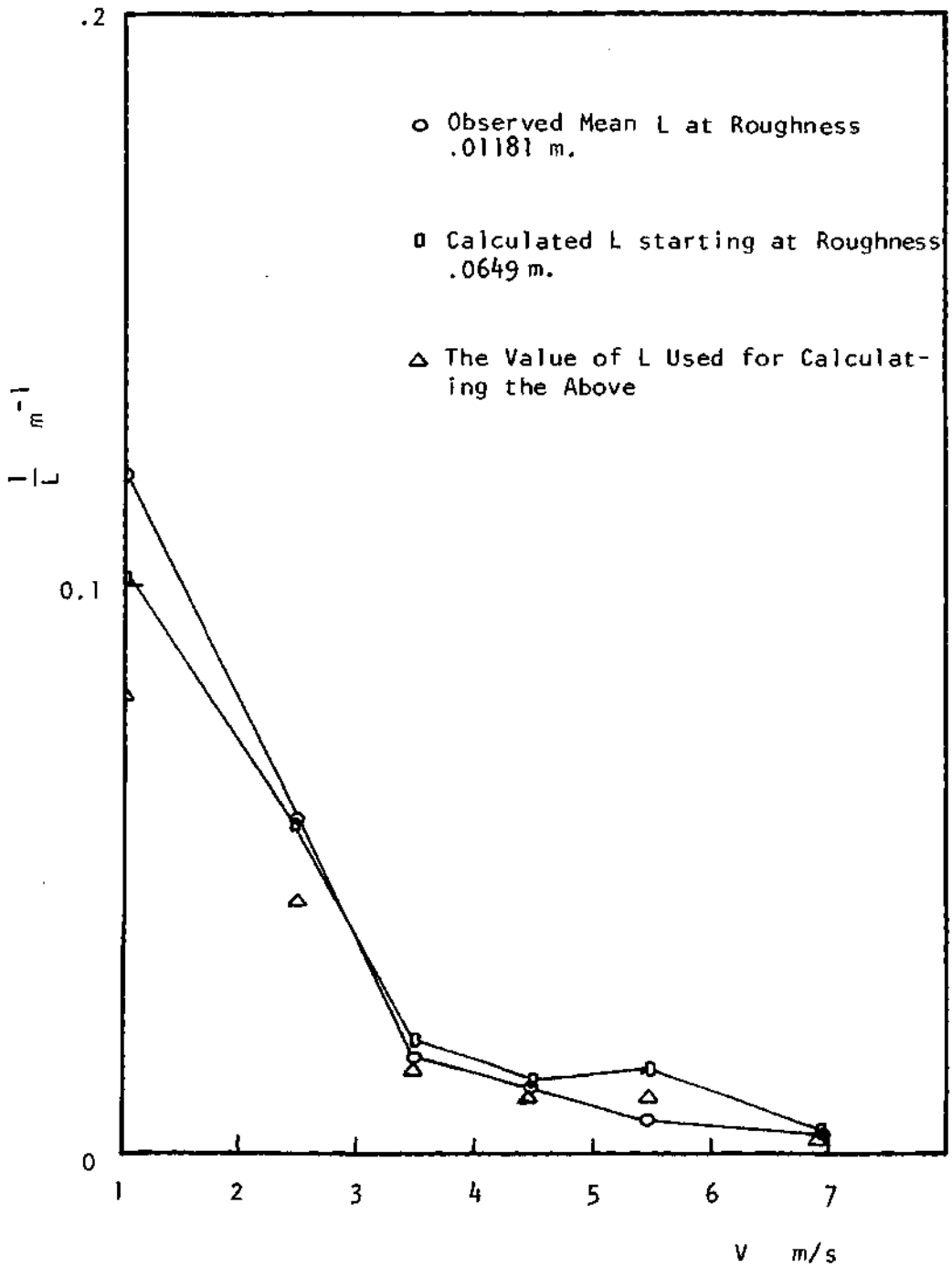

Figure 26. Mean (1/L) Versus Predicted (1/L) Based on Argonne Data for Stable Stratification.

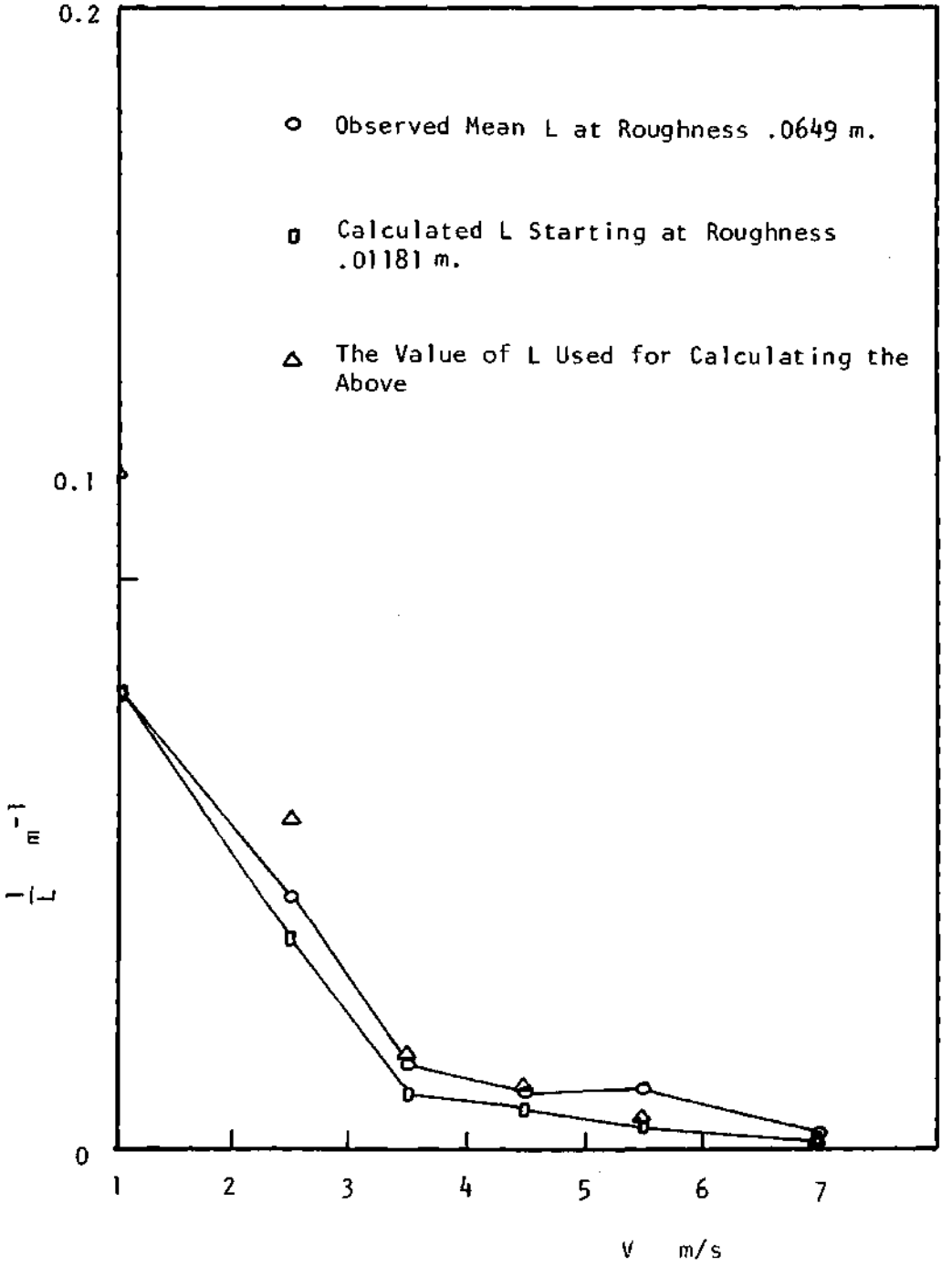

Figure 27. Mean (1/L) Versus Predicted (1/L) Based on Argonne Data for Stable Stratification with Reversed Initial Values.

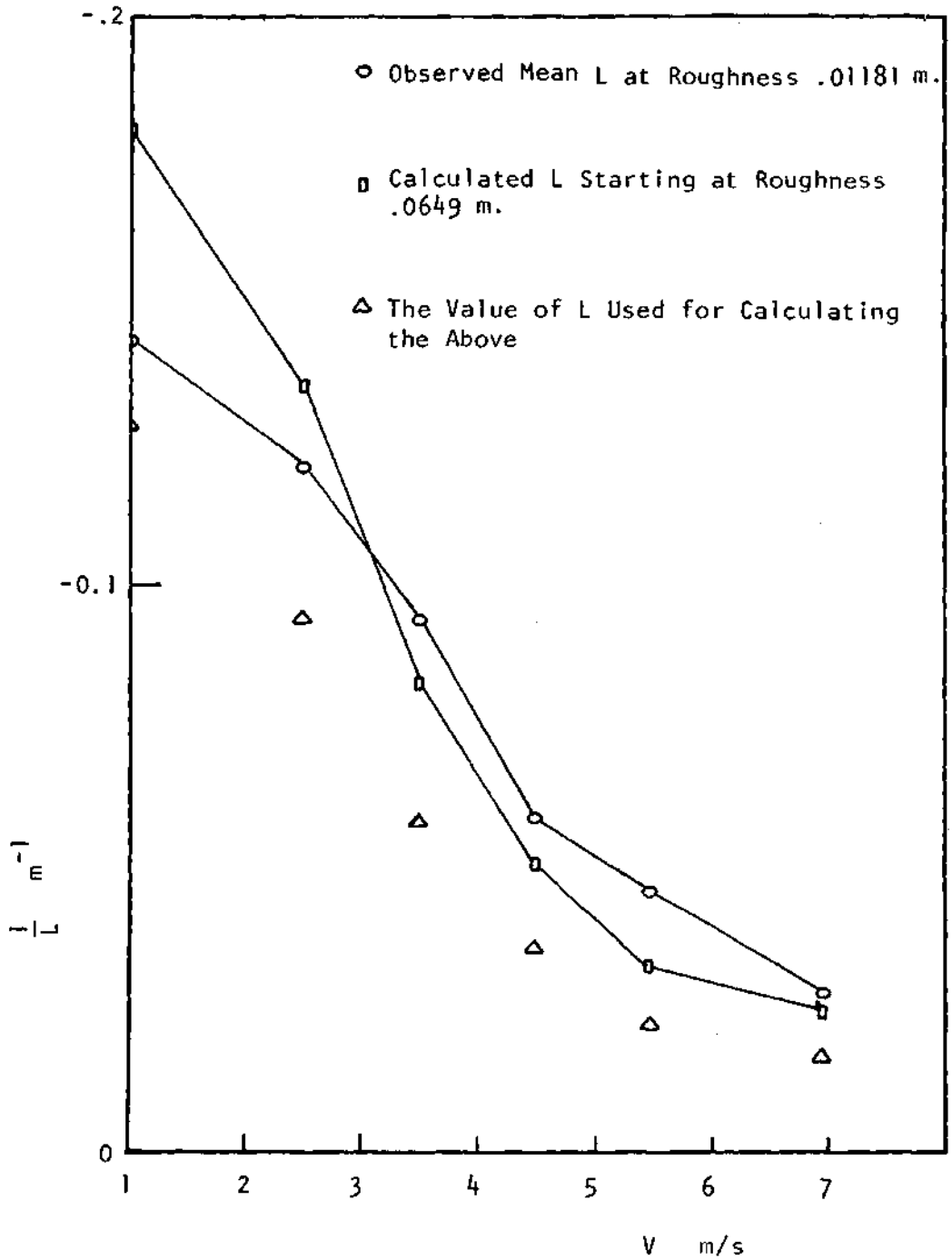

Figure 28. Mean (1/L) Versus Predicted (1/L) Based on Argonne Data for Unstable Stratification.

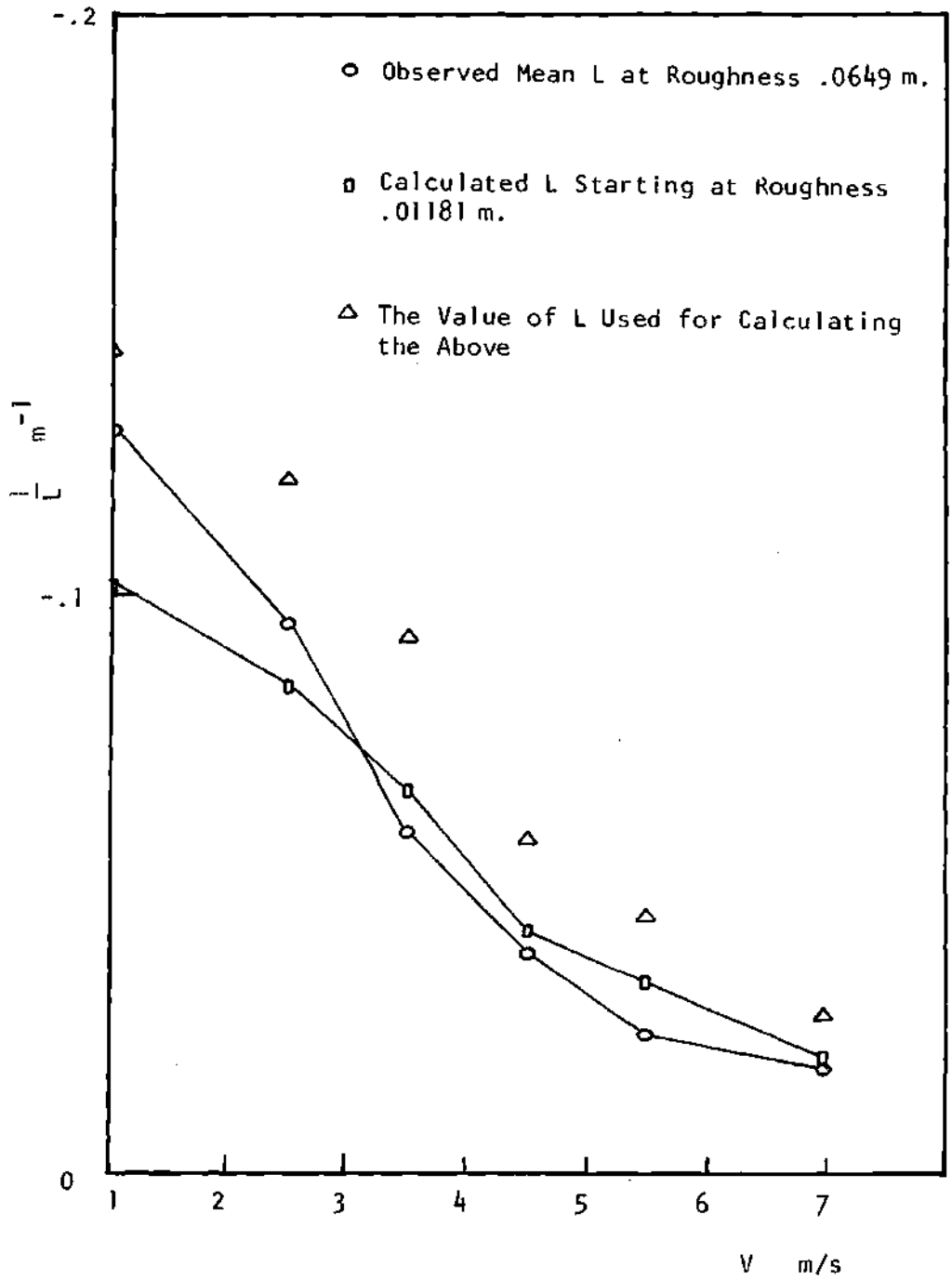

Figure 29. Mean (1/L) Versus Predicted (1/L) Based on Argonne Data for Unstable Stratification with Reversed Initial Values.

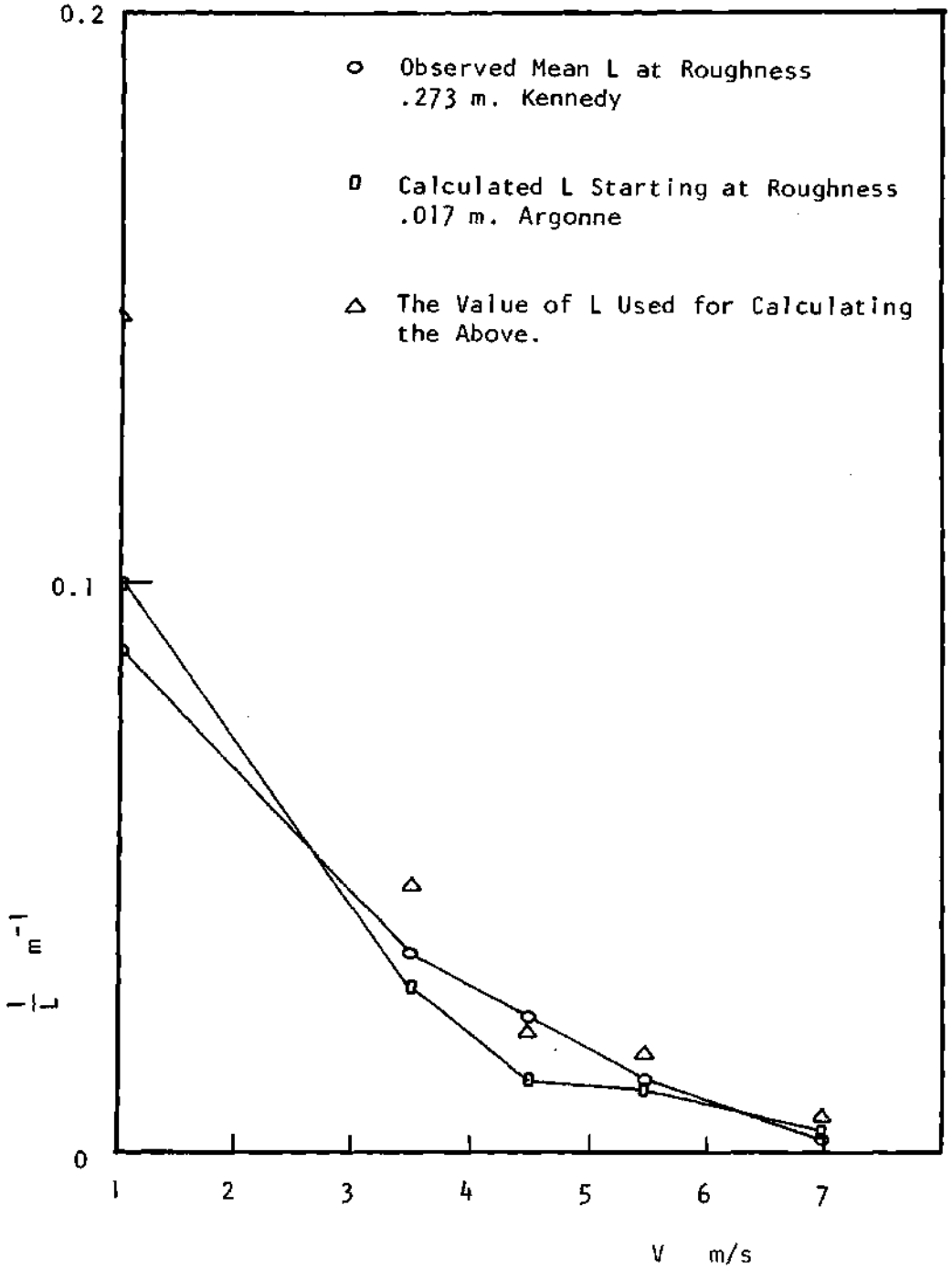

Figure 30. Mean (1/L) Based on Kennedy Data Versus Predicted (1/L) Using Initial Values for (1/L) Based on Argonne Data, Stable.

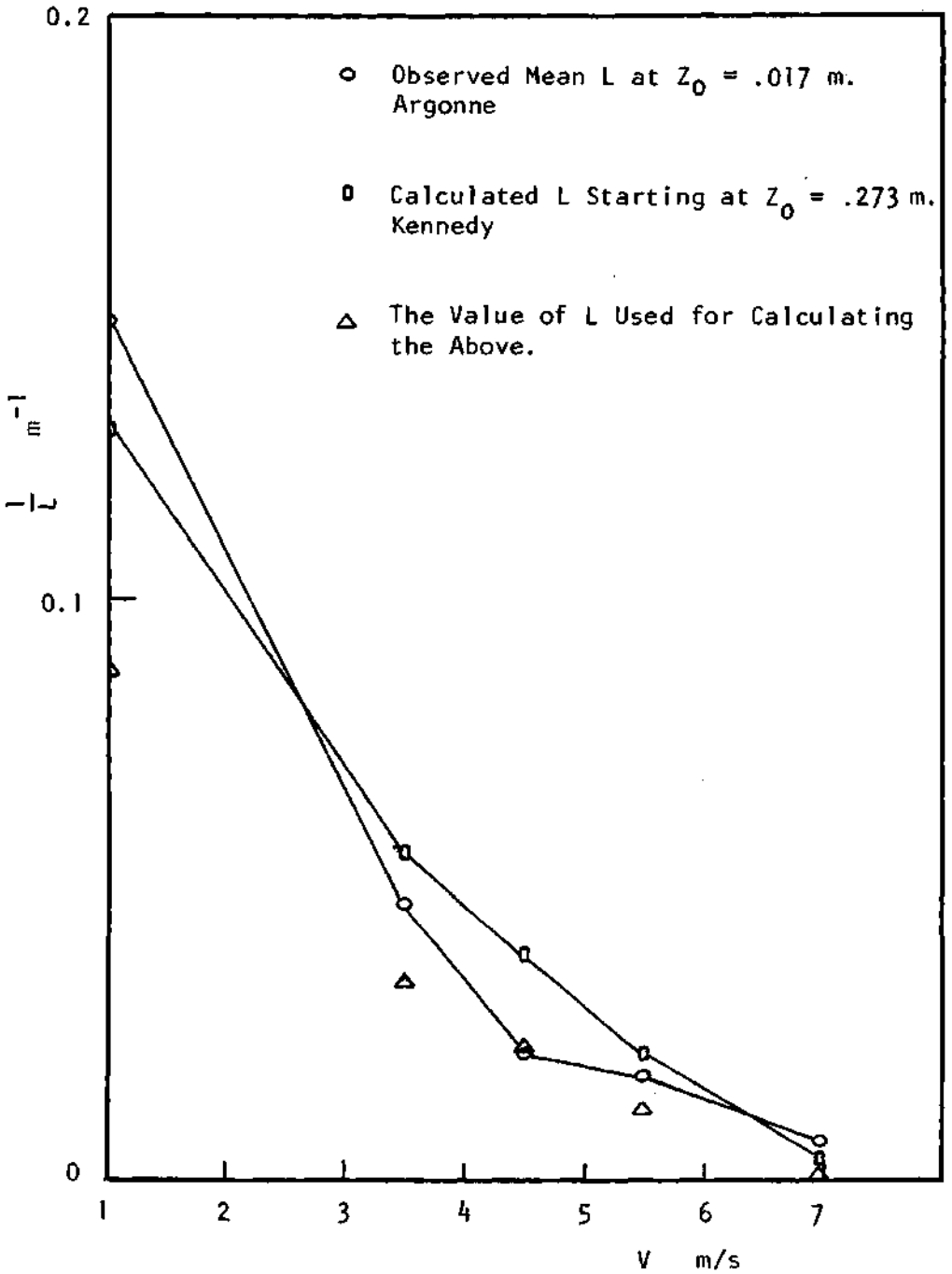

Figure 31. Mean (1/L) Based on Argonne Data Versus Predicted (1/L) Using Initial Values for (1/L) Based on Kennedy Data, Stable.

the same net radiation and wind speed classes, but at a different surface roughness value

△The value of the Monin-Obukov length used for calculating the above. The associated roughness length is given on the graphs.

Figures 26 and 27 show the agreement between predicted and observed (1/L) for the stable stratification. Initial values for (1/L) are given at higher roughness length than comparison roughness length (Figure 26), and lower roughness length than comparison roughness length (Figure 27).

Figures 28 and 29 show the agreement between predicted and observed (1/L) for unstable stratification. Initial values of (1/L) are given at higher roughness length than comparison roughness length (Figure 28), and lower roughness length than comparison roughness length (Figure 29).

Figures 30 and 31 are of particular importance since the change of roughness value from Kennedy to Argonne is quite considerable, besides two different sets of tower data were used, yet the calculated values of L are quite close to the values of L extracted from the profiles.

In general the graphs show a good agreement except for very high values of (1/L) which could be partly due to the singular behavior of (1/L) as L approaches zero. Also an error could arise from the sparsity of the profiles at certain direction classes since the average direction class has not been used yet.

3.5 Universal Values of the Monin-Obukov Length

The question of which values of the Monin-Obukov length would be used as initial conditions in equation (41) had to be resolved. In terms of sufficiency of data, then the average roughness for Argonne

would be adequate. As a check on this choice we had to check if the values of the Monin-Obukov length for the Argonne average roughness when used as initial conditions could reproduce the mean values of the Monin-Obukov length extracted from the profiles in different direction intervals both in Argonne and Kennedy data.

Figures 32 and 33 show the agreement between the average values of L extracted from the profiles and the values calculated for unstable stratification for roughness lengths of .07, and .05 m. respectively. The initial values of L were average Argonne values for average roughness.

Figures 34 and 35 are the same as above except two different direction intervals were used, roughness lengths were taken as .05, .07 m., respectively and the stable region was considered.

Figure 36 is of particular importance since the average roughness Monin-Obukov length of Argonne was used to predict the Monin-Obukov length for a different tower (Kennedy) and a much higher roughness length (1.0 m).

The agreement seems to be acceptable, hence the average Argonne roughness Monin-Obukov lengths were used to establish the universal values of Monin-Obukov length as a function of wind speed, net radiation and roughness length.

Figures 37 through 41 show the values of the Monin-Obukov length (absissa) against roughness length (ordinate) for different wind speed classes at a certain net radiation class. Every figure represents a single radiation class.

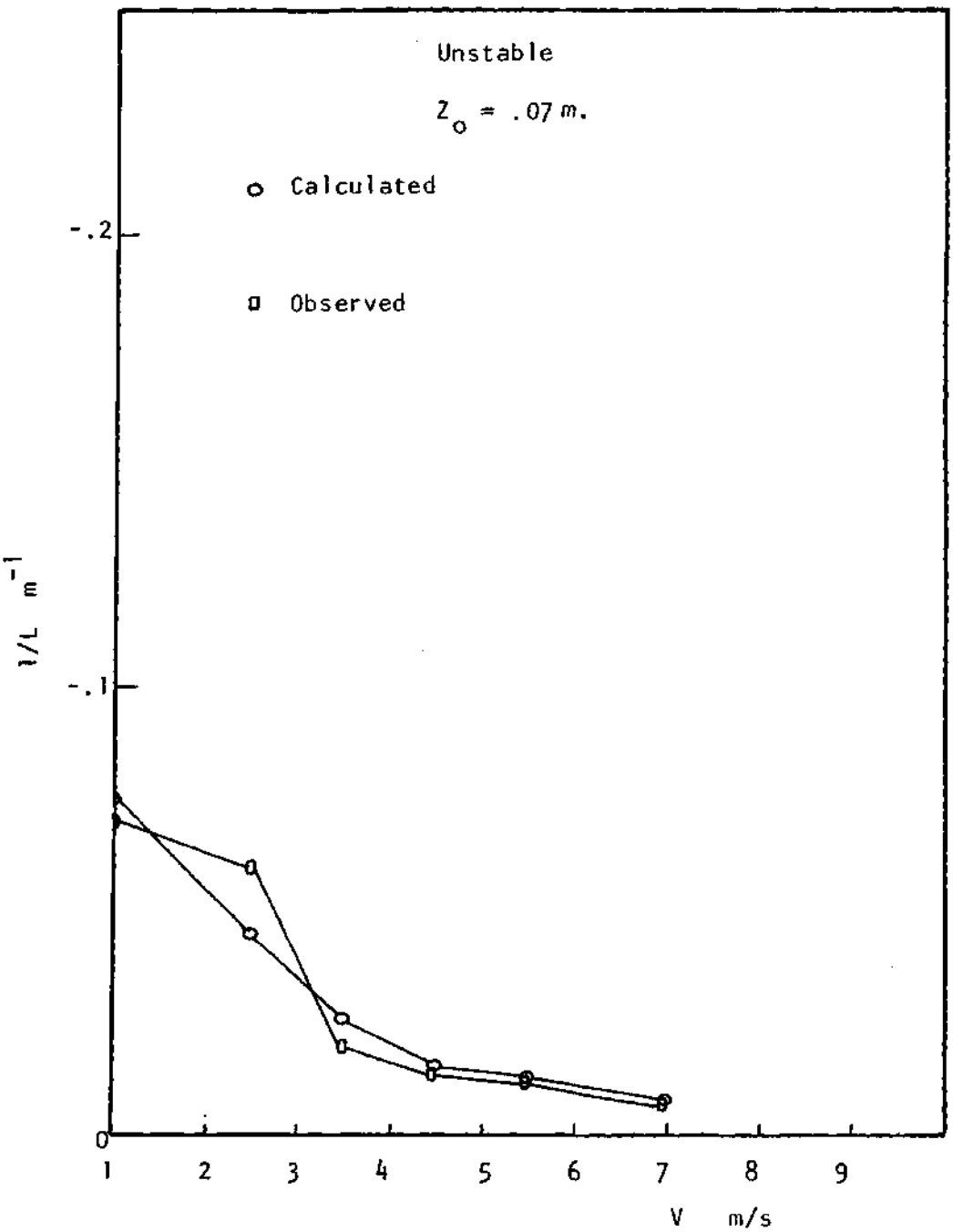

Figure 32. Average (1/L) Versus Predicted (1/L) for Unstable Stratification, Z_o = .07, Using Universal (1/L) for Initial Values.

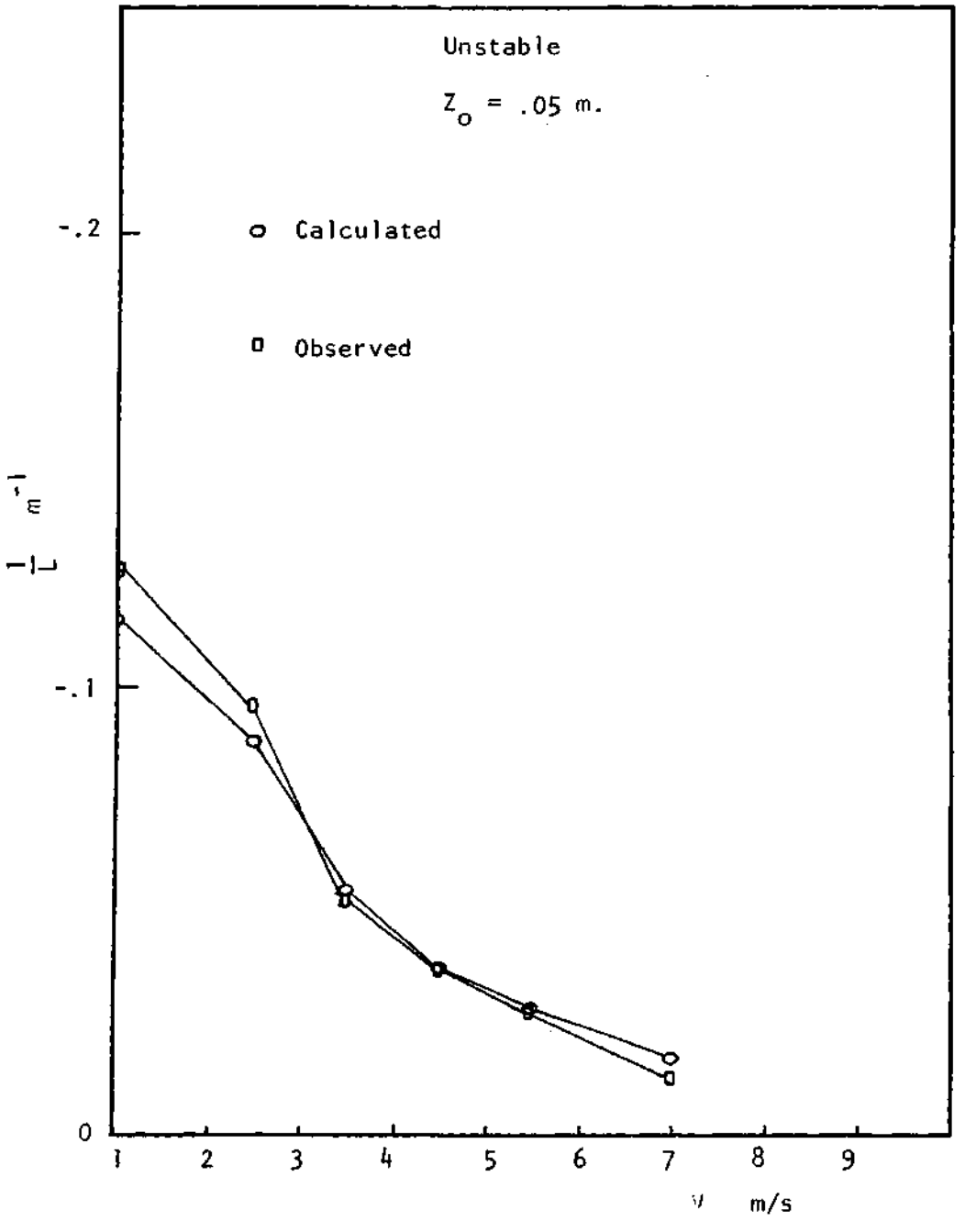

Figure 33. Average 1/L Versus Predicted (1/L) for Unstable Stratification, Z_o = .05, Using Universal (1/L) for Initial Values.

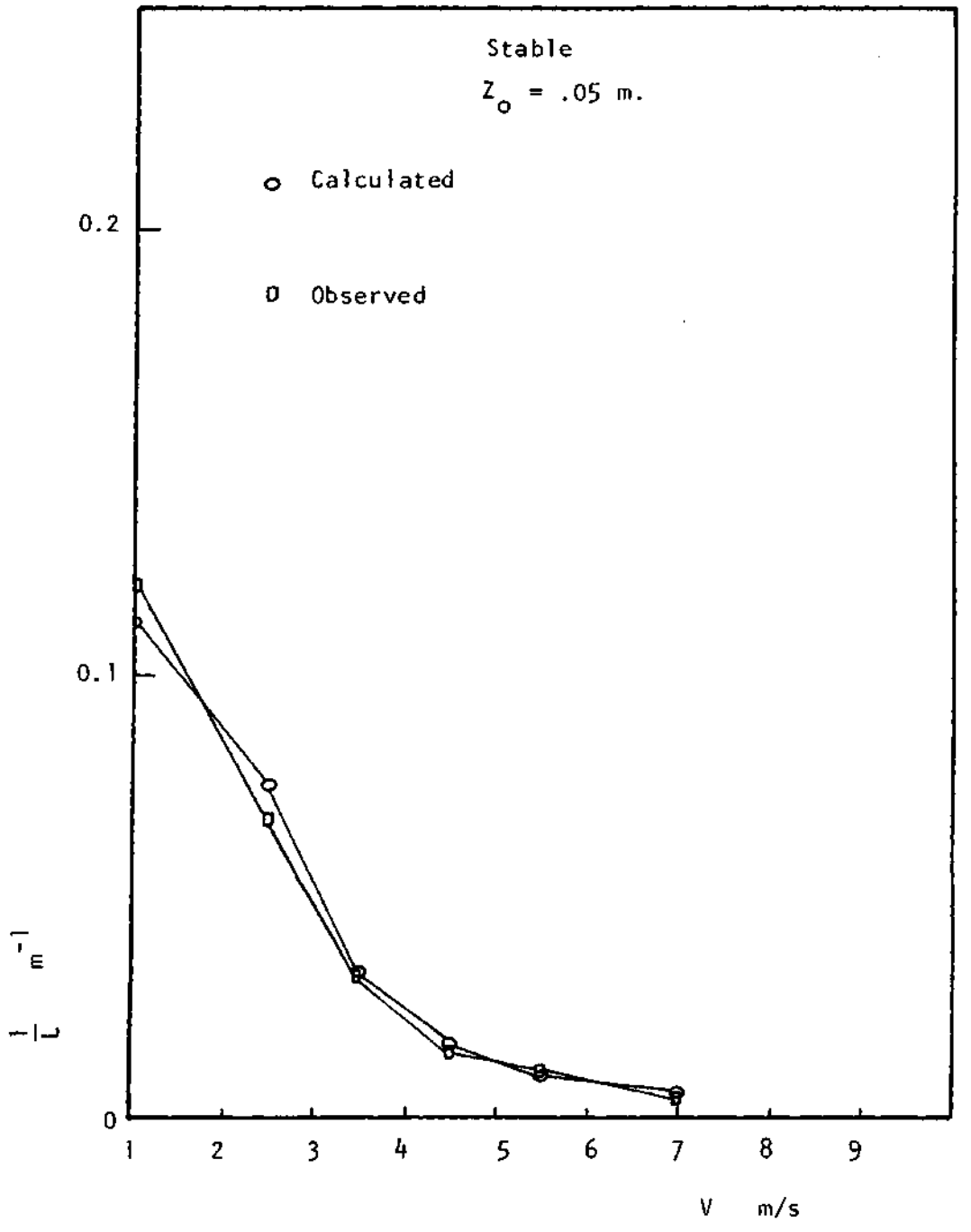

Figure 34. Average (1/L) Versus Predicted (1/L) for Stable Stratification, Z_o = .05, Using Universal (1/L) for Initial Values.

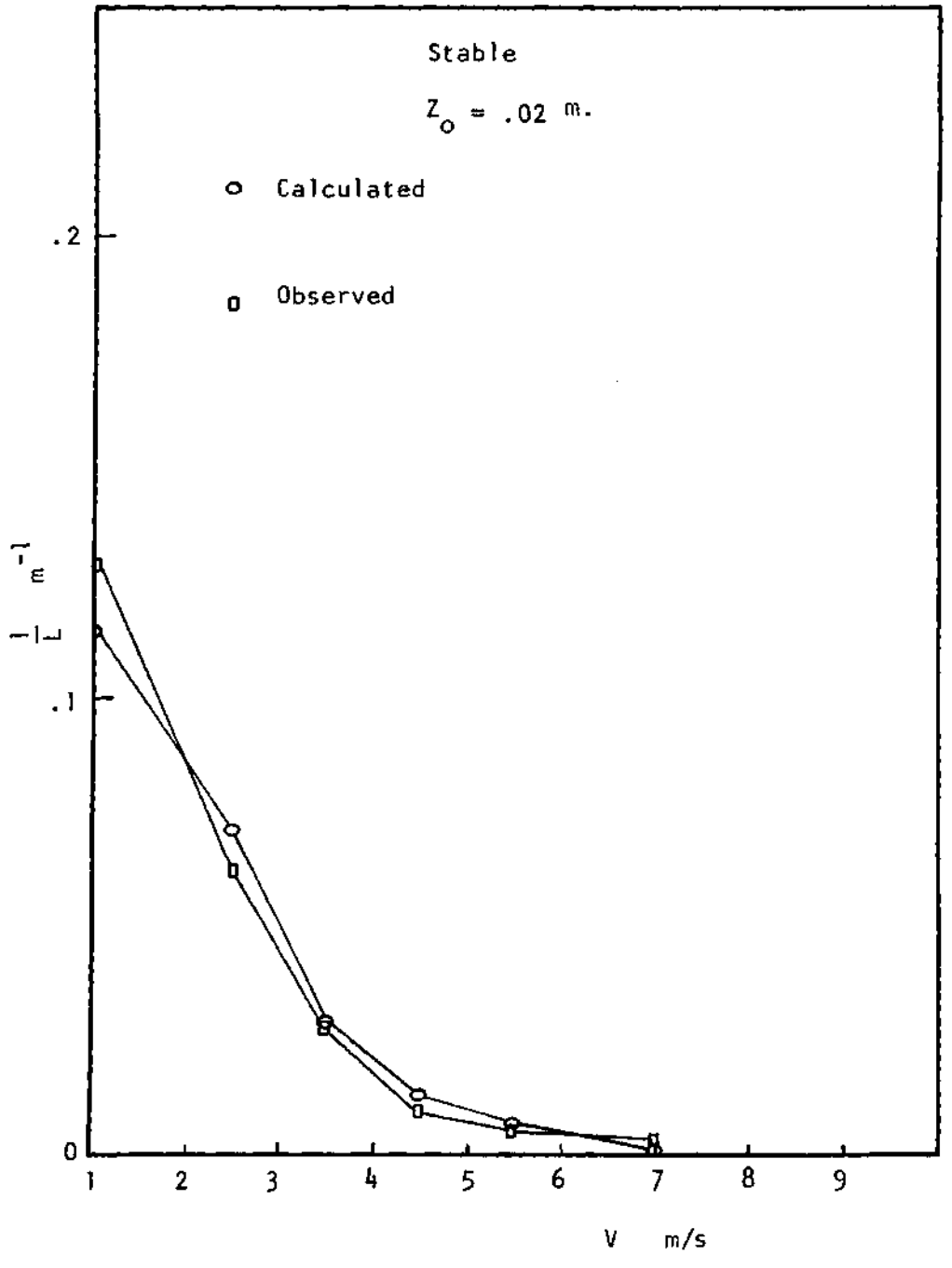

Figure 35. Average (1/L) versus Predicted (1/L) for Stable Stratification, Z_o = .02, Using Universal (1/L) for Initial Values.

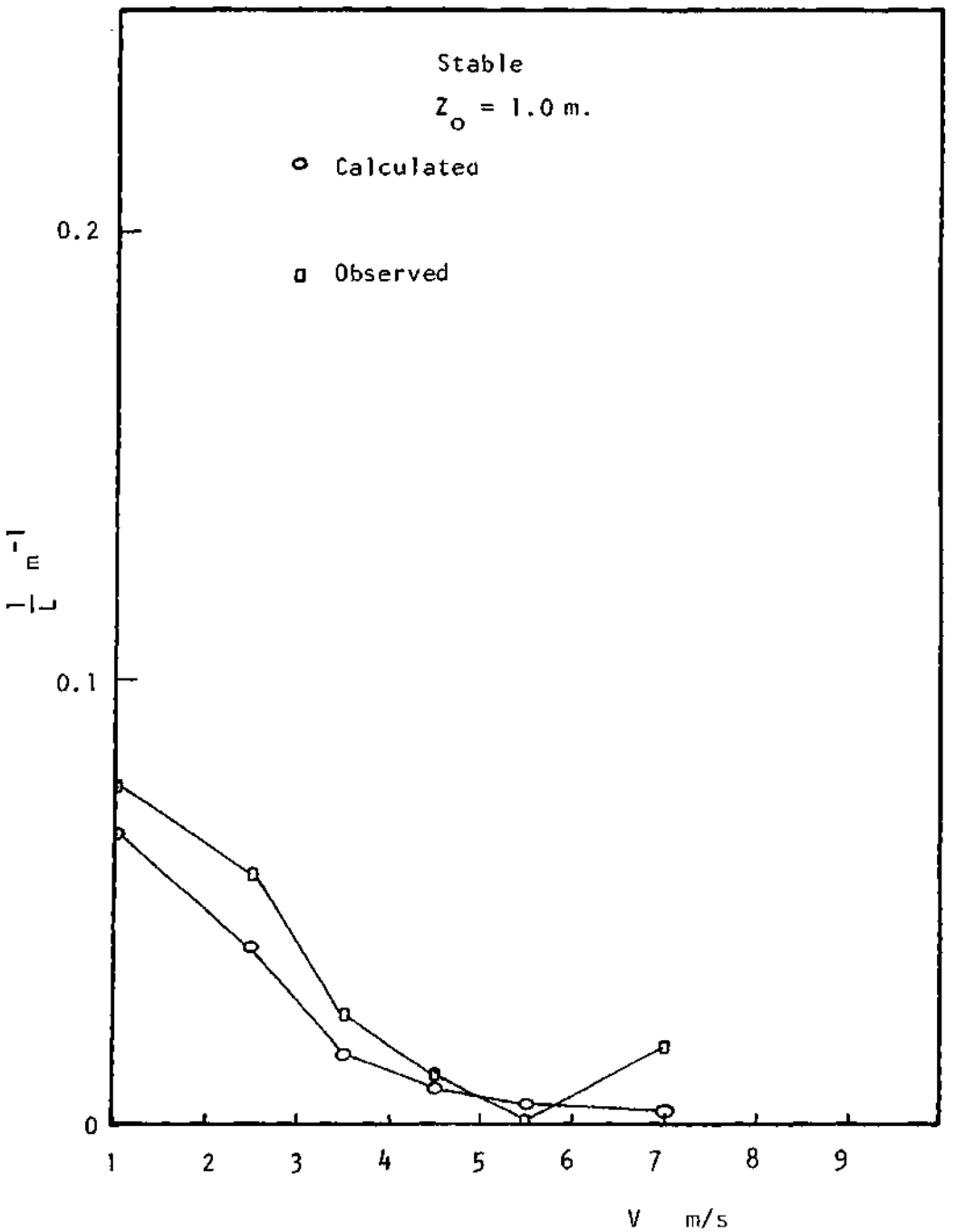

Figure 36. Average (1/L) Versus Predicted (1/L) for Stable Stratification, Z_o = 1.0, Using Universal (1/L) for Initial Values.

o	wind speed (0,2 m/s)
•	wind speed (2,3 m/s)
▫	wind speed (3,4 m/s)
▪	wind speed (4,5 m/s)
△	wind speed (5,6 m/s)
▲	wind speed (> 6 m/s)

The graphs show how (1/L) systematically decreases with the increase of roughness length due to the increased production of turbulence associated with the increase in roughness length which shifts L towards neutral conditions, i.e. $|1/L|$ tends to zero.

Also $|1/L|$ systematically decreases with the increase of the ten m. level wind speed due to neutral conditions created due to mixing associated with higher wind speeds.

Also (1/L) decreases with increasing net radiation due to the destabilizing effect of solar radiation on the atmospheric boundary layer.

The same information is given in tables for easier access for wind energy applications.

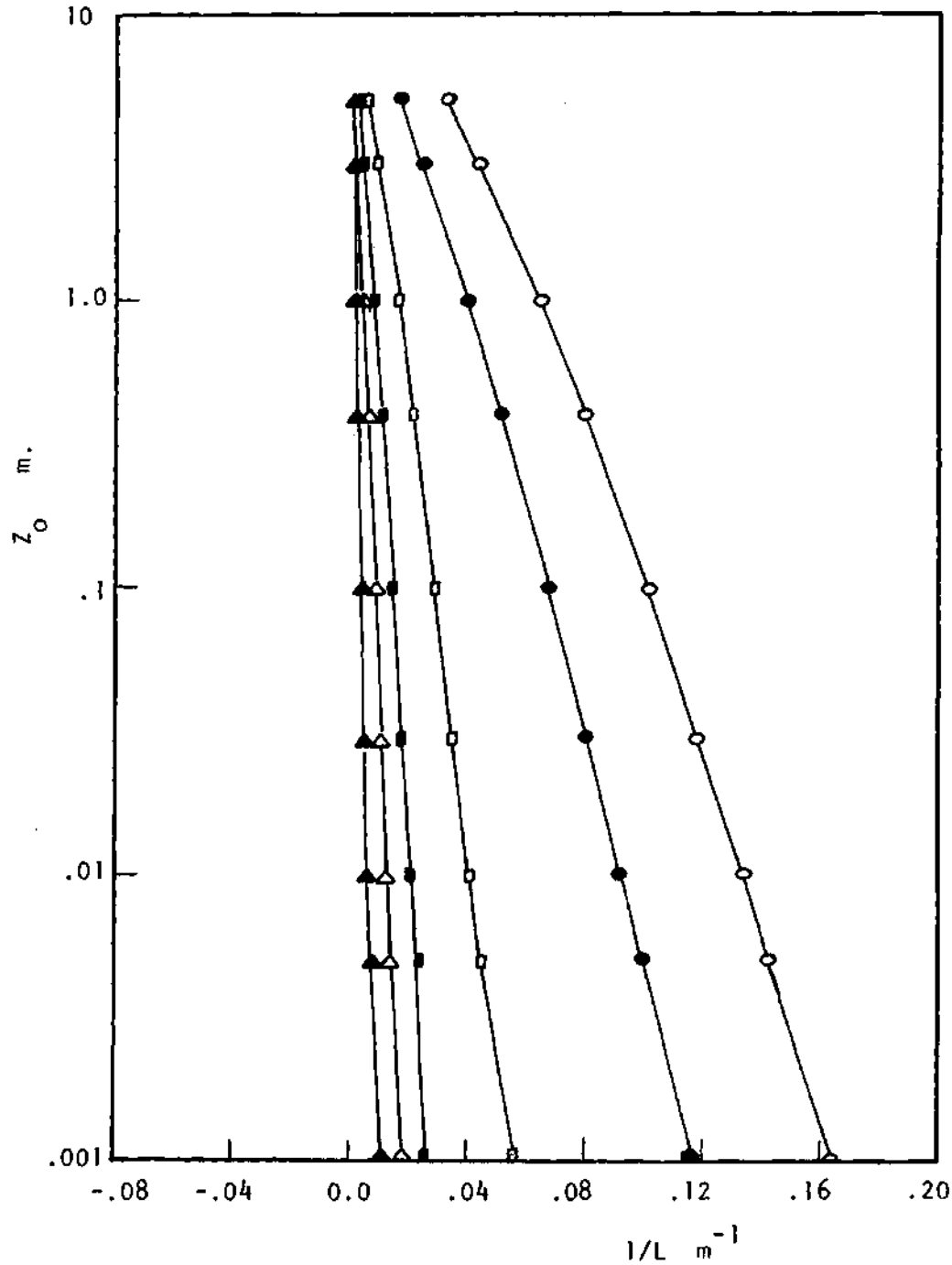

Figure 37. 1/L Versus Wind Speed for Radiation Class 1.

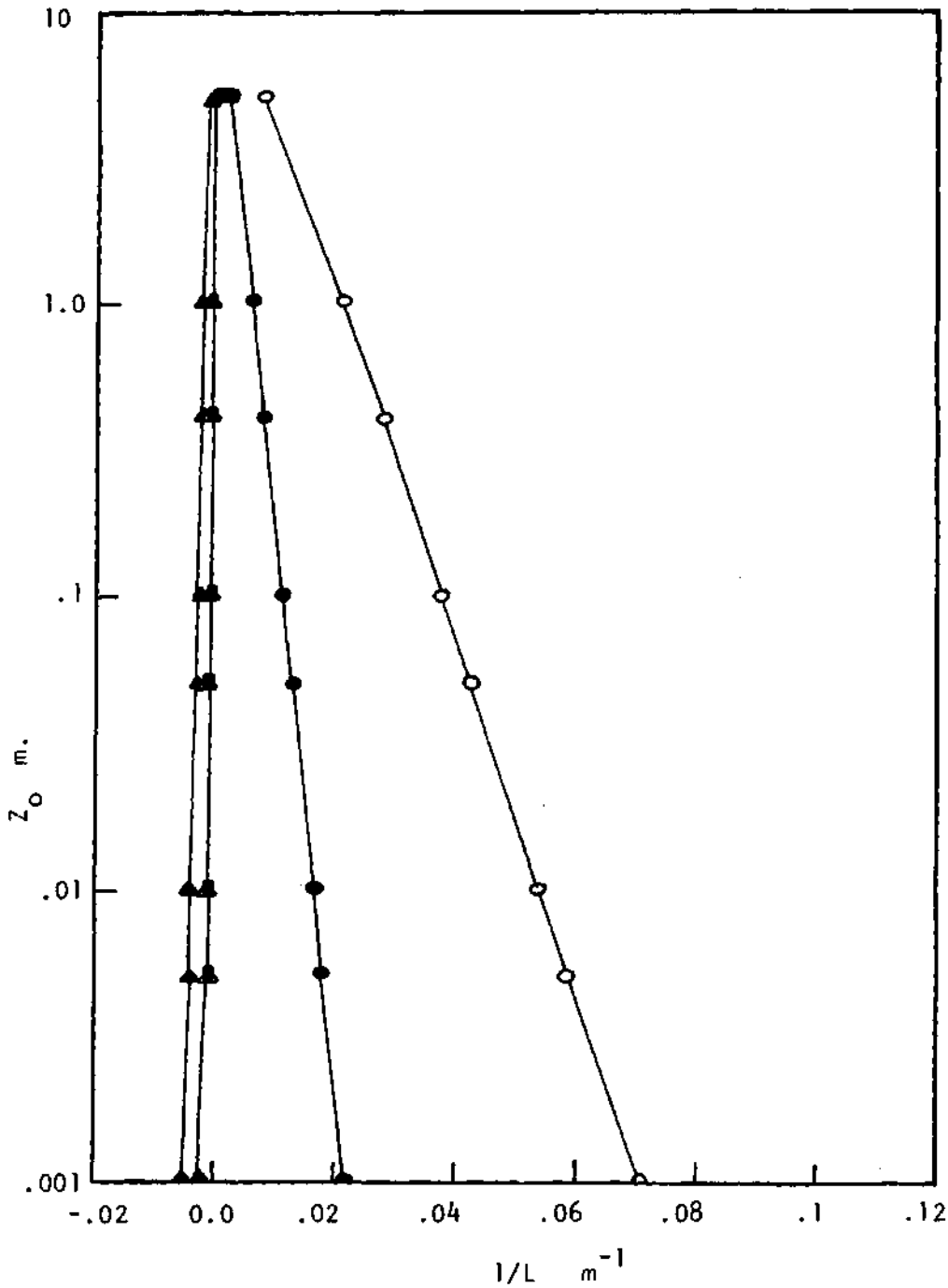

Figure 38. 1/L Versus Wind Speed for Radiation Class 3.

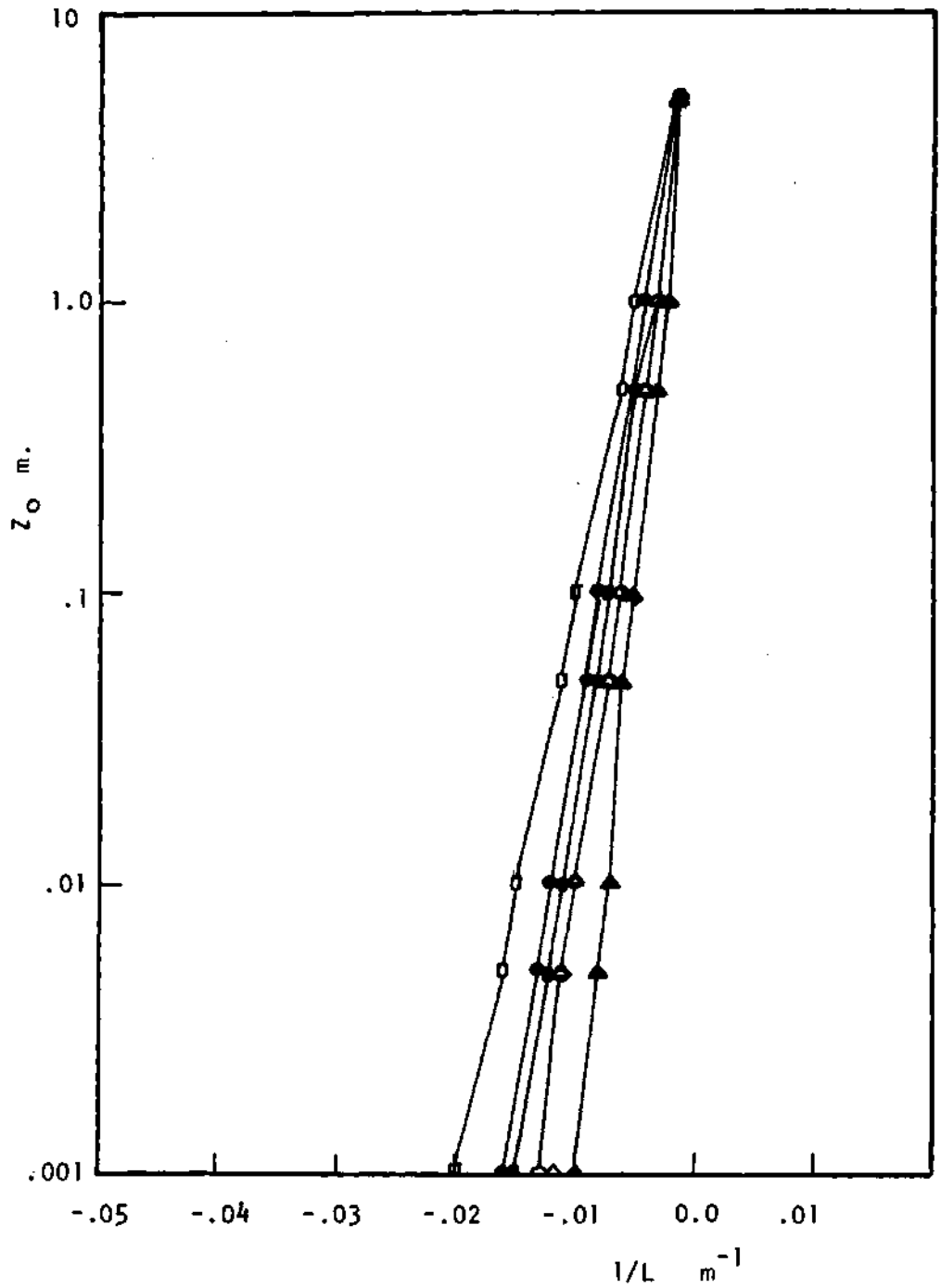

Figure 39. 1/L Versus Wind Speed for Reduction Class 5.

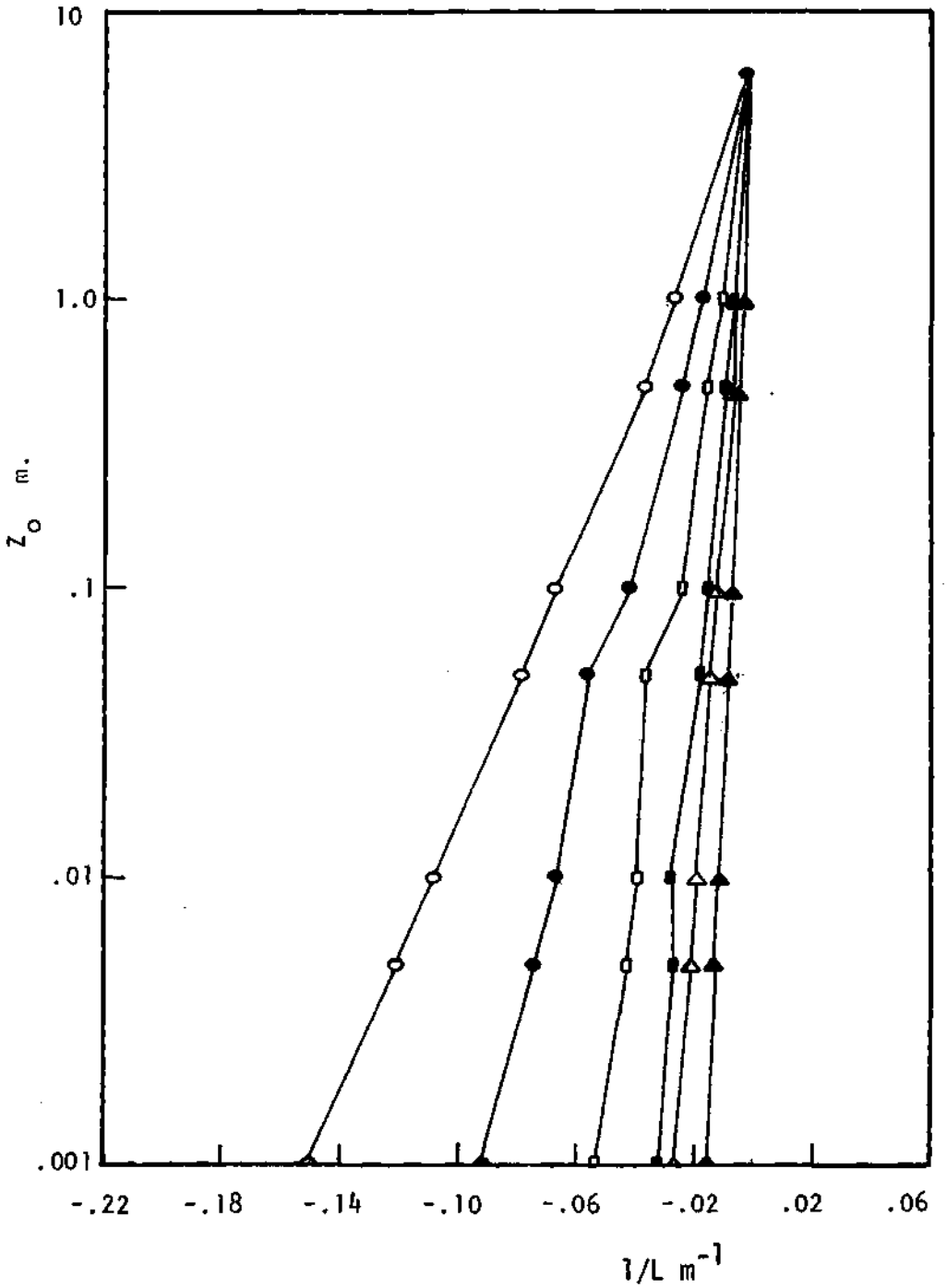

Figure 40. 1/L Versus Wind Speed for Radiation Class 7.

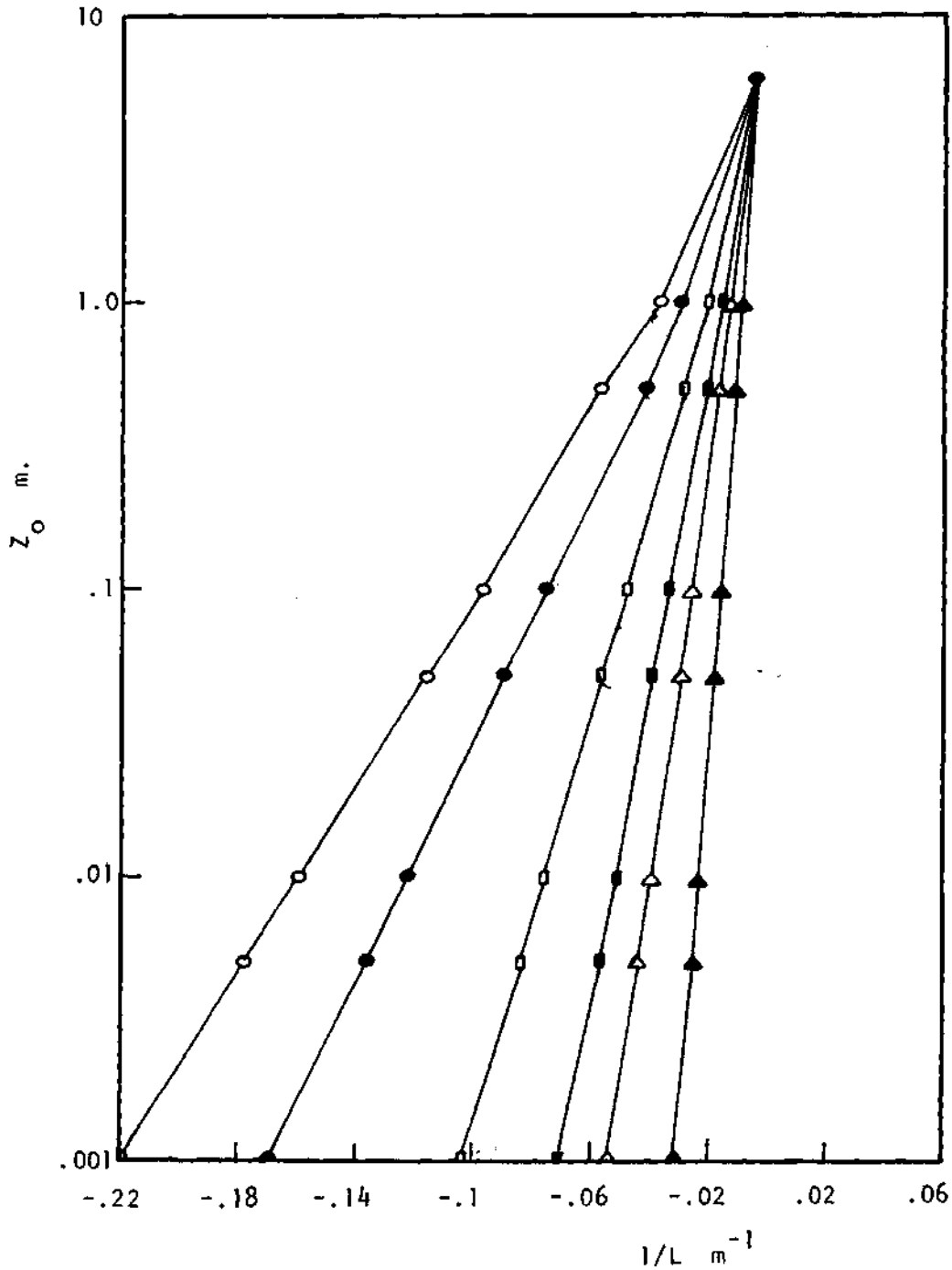

Figure 41. 1/L Versus Wind Speed for Radiation Class 9.

Table 17. Universal Monin-Obukov Length for Different Net Radiation, Wind Speed Classes, and Roughness Lengths

Tabulated Values are (1/L), m^{-1}

Net. Rad. Ly/min. Wind Speed m/s	<-.1	(-.1,0)	(0,.1)	(.1,.2)	(.2,.3)	(.3,.4)	(.4,.5)	(.5,.6)	(>.6)
				Z_o = .001 m.					
(0,2) m/s	.163	.151	.087	.069	-.013	-.078	-.149	-.204	-.220
(2,3) m/s	.116	.098	.042	.022	-.016	-.057	-.090	-.102	-.168
(3,4) m/s	.053	.042	.021	-.002	-.020	-.040	-.052	-.073	-.102
(4,5) m/s	.028	.019	.010	-.002	-.015	-.021	-.031	-.047	-.069
(5,6) m/s	.017	.010	.005	-.002	-.013	-.016	-.025	-.035	-.052
(> 6) m/s	.010	.005	.002	-.005	-.010	-.011	-.015	-.020	-.030
				Z_o = .005 m.					
(0,2) m/s	.143	.132	.074	.059	-.010	-.063	-.120	-.164	-.177
(2,3) m/s	.100	.084	.035	.018	-.013	-.046	-.073	-.083	-.135
(3,4) m/s	.045	.035	.017	-.001	-.016	-.033	-.042	-.059	-.083
(4,5) m/s	.024	.016	.008	-.001	-.012	-.017	-.026	-.038	-.056
(5,6) m/s	.014	.008	.004	-.001	-.011	-.013	-.020	-.028	-.042
(> 6) m/s	.008	.004	.001	-.004	-.008	-.009	-.012	-.016	-.024
				Z_o = .01 m.					
(0,2) m/s	.134	.123	.069	.054	-.010	-.057	-.107	-.146	-.158
(2,3) m/s	.092	.078	.032	.017	-.012	-.042	-.066	-.074	-.121
(3,4) m/s	.041	.032	.016	-.001	-.015	-.029	-.038	-.053	-.074
(4,5) m/s	.021	.014	.007	-.001	-.011	-.016	-.023	-.034	-.050
(5,6) m/s	.013	.007	.004	-.001	-.010	-.012	-.018	-.026	-.038
(> 6) m/s	.007	.004	.001	-.004	-.007	-.009	-.011	-.015	-.022

Table 17. (Continued)

Net Rad. Ly/min. Wind Speed m/s	<-.1	(-.1,0)	(0,.1)	(.1,.2)	(.2,.3)	(.3,.4)	(.4,.5)	(.5,.6)	(>.6)
				Z_o = .02 m.					
(0,2) m/s	.125	.114	.063	.049	-.009	-.050	-.095	-.129	-.139
(2,3) m/s	.085	.071	.029	.015	-.011	-.037	-.058	-.066	-.107
(3,4) m/s	.038	.029	.014	-.001	-.013	-.026	-.034	-.047	-.066
(4,5) m/s	.020	.013	.007	-.001	-.010	-.014	-.021	-.031	-.045
(5,6) m/s	.012	.007	.003	-.001	-.009	-.011	-.016	-.023	-.034
(> 6) m/s	.007	.003	.001	-.003	-.007	-.008	-.010	-.013	-.020
				Z_o = 0.03 m.					
(0,2) m/s	.119	.109	.060	.047	-.008	-.047	-.087	-.119	-.128
(2,3) m/s	.081	.068	.027	.014	-.010	-.035	-.053	-.061	-.094
(3,4) m/s	.035	.027	.013	-.001	-.012	-.024	-.031	-.044	-.061
(4,5) m/s	.018	.012	.006	-.001	-.009	-.013	-.019	-.028	-.042
(5,6) m/s	.011	.006	.003	-.001	-.008	-.01	-.015	-.021	-.031
(> 6) m/s	.006	.003	.001	-.003	-.006	-.007	-.009	-.012	-.018
				Z_o = .04 m.					
(0,2) m/s	.115	.105	.057	.045	-.008	-.044	-.082	-.112	-.120
(2,3) m/s	.078	.065	.026	.014	-.010	-.033	-.051	-.057	-.093
(3,4) m/s	.034	.026	.013	-.001	-.012	-.023	-.030	-.041	-.057
(4,5) m/s	.017	.012	.006	-.001	-.009	-.013	-.018	-.027	-.039
(5,6) m/s	.011	.006	.003	-.001	-.008	-.010	-.014	-.020	-.030
(> 6) m/s	.006	.003	.001	-.003	-.006	-.007	-.009	-.012	-.017
				Z_o = .05 m.					
(0,2) m/s	.112	.102	.055	.043	-.007	-.042	-.078	-.106	-.114
(2,3) m/s	.075	.063	.025	.013	-.009	-.031	-.048	-.055	-.088
(3,4) m/s	.033	.025	.012	-.001	-.011	-.022	-.028	-.039	-.055
(4,5) m/s	.017	.011	.006	-.001	-.008	-.012	-.017	-.026	-.038
(5,6) m/s	.010	.006	.003	-.001	-.007	-.009	-.014	-.019	-.028
(> 6) m/s	.006	.003	.001	-.003	-.006	-.007	-.008	-.011	-.017

Table 17. (Continued)

Net Rad. Ly/min. Wind Speed m/s	<-.1	(-.1,0)	(0,.1)	(.1,.2)	(.2,.3)	(.3,.4)	(.4,.5)	(.5,.6)	(>.6)
				Z_o = .07 m.					
(0,2) m/s	.107	.098	.052	.041	-.007	-.039	-.072	-.097	-.105
(2,3) m/s	.072	.060	.024	.012	-.009	-.029	-.045	-.051	-.081
(3,4) m/s	.031	.024	.011	-.001	-.010	-.021	-.026	-.036	-.051
(4,5) m/s	.016	.010	.005	-.001	-.008	-.011	-.016	-.024	-.035
(5,6) m/s	.010	.005	.003	-.001	-.007	-.009	-.013	-.018	-.026
(> 6) m/s	.005	.003	.001	-.003	-.005	-.006	-.008	-.010	-.015
				Z_o = .09 m.					
(0,2) m/s	.103	.094	.050	.039	-.007	-.037	-.068	-.091	-.098
(2,3) m/s	.069	.057	.023	.012	-.008	-.027	-.042	-.048	-.076
(3,4) m/s	.029	.023	.011	-.001	-.010	-.019	-.025	-.034	-.048
(4,5) m/s	.015	.010	.005	-.001	-.007	-.011	-.015	-.023	-.033
(5,6) m/s	.009	.005	.003	-.001	-.007	-.008	-.012	-.017	-.025
(> 6) m/s	.005	.003	.001	-.003	-.005	-.006	-.007	-.010	-.015
				Z_o = .1 m.					
(0,2) m/s	.102	.093	.049	.038	-.006	-.036	-.066	-.086	-.095
(2,3) m/s	.068	.056	.022	.011	-.008	-.027	-.041	-.046	-.074
(3,4) m/s	.029	.022	.011	-.001	-.010	-.019	-.024	-.033	-.046
(4,5) m/s	.015	.010	.005	-.001	-.007	-.010	-.015	-.022	-.032
(5,6) m/s	.009	.005	.002	-.001	-.006	-.008	-.012	-.017	-.024
(> 6) m/s	.005	.002	.001	-.002	-.005	-.006	- 007	-.010	-.014

Table 17. (Continued)

Net Rad. Ly/min. Wind Speed m/s	<-.1	(-.1,0)	(0,.1)	(.1,.2)	(.2,.3)	(.3,.4)	(.4,.5)	(.5,.6)	(>.6)
				Z_o = .15 m					
(0,2) m/s	.096	.087	.046	.035	-.006	-.032	-.058	-.078	-.084
(2,3) m/s	.063	.052	.020	.010	-.007	-.024	-.037	-.041	-.065
(3,4) m/s	.027	.020	.010	-.001	-.009	-.017	-.022	-.030	-.041
(4,5) m/s	.013	.009	.004	-.001	-.007	-.009	-.014	-.020	-.029
(5,6) m/s	.008	.004	.002	-.001	-.006	-.007	-.011	-.015	-.022
(> 6) m/s	.004	.002	.001	-.002	-.004	-.005	-.007	-.009	-.013
				Z_o = .2 m.					
(0,2) m/s	.091	.083	.043	.033	-.005	-.029	-.053	-.071	-.076
(2,3) m/s	.060	.049	.019	.010	-.007	-.022	-.034	-.038	-.059
(3,4) m/s	.025	.019	.009	-.001	-.008	-.016	-.020	-.028	-.038
(4,5) m/s	.013	.008	.004	-.001	-.006	-.009	-.013	-.018	-.026
(5,6) m/s	.008	.004	.002	-.001	-.005	-.007	-.010	-.014	-.020
(> 6) m/s	.004	.002	.001	-.002	-.004	-.005	-.006	-.080	-.012
				Z_o = .25 m.					
(0,2) m/s	.088	.079	.041	.032	-.005	-.027	-.049	-.005	-.070
(2,3) m/s	.057	.047	.018	.009	-.006	-.020	-.031	-.035	-.055
(3,4) m/s	.023	.018	.009	-.001	-.008	-.015	-.019	-.026	-.035
(4,5) m/s	.011	.007	.004	-.001	-.006	-.008	-.011	-.017	-.025
(5,6) m/s	.007	.004	.002	-.001	-.005	-.006	-.009	-.012	-.018
(>6) m/s	.004	.002	.001	-.002	-.004	-.004	-.005	-.007	-.011

Table 17. (Continued)

Net Rad. Ly/min. Wind Speed m/s	<-.1	(-.1,0)	(0,.1)	(.1,.2)	(.2,.3)	(.3,.4)	(.4,.5)	(.5,.6)	(>.6)
				Z_o = .30 m.					
(0,2) m/s	.085	.077	.039	.030	-.005	-.026	-.046	-.060	-.065
(2,3) m/s	.055	.045	.017	.009	-.006	-.019	-.029	-.033	-.051
(3,4) m/s	.023	.017	.008	-.001	-.007	-.014	-.018	-.024	-.033
(4,5) m/s	.011	.008	.004	-.001	-.005	-.008	-.011	-.016	-.023
(5,6) m/s	.007	.004	.002	-.001	-.005	-.006	-.009	-.012	-.018
(> 6) m/s	.004	.002	.001	-.002	-.004	-.004	-.005	-.007	-.011
				Z_o = .35 m.					
(0,2) m/s	.082	.074	.038	.029	-.005	-.024	-.043	-.057	-.060
(2,3) m/s	.053	.044	.017	.008	-.006	-.018	-.028	-.031	-.048
(3,4) m/s	.022	.017	.008	-.001	-.007	-.013	-.017	-.023	-.031
(4,5) m/s	.011	.007	.004	-.001	-.0057	-.007	-.011	-.015	-.022
(5,6) m/s	.007	.004	.002	-.001	-.0046	-.006	-.008	-.012	-.017
(> 6) m/s	.004	.002	.001	-.002	-.003	-.004	-.005	-.007	-.010
				Z_o = .4 m.					
(0,2) m/s	.08	.072	.037	.028	-.004	-.023	-.040	-.053	-.057
(2,3) m/s	.052	.042	.016	.008	-.005	-.017	-.026	-.030	-.045
(3,4) m/s	.021	.016	.008	-.001	-.007	-.013	-.016	-.022	-.029
(4,5) m/s	.011	.007	.003	-.001	-.005	-.007	-.010	-.015	-.021
(5,6) m/s	.006	.003	.002	-.001	-.004	-.005	-.008	-.011	-.016
(> 6) m/s	.003	.002	.001	-.002	-.003	-.004	-.005	-.007	-.010

Table 17. (Continued)

Net Rad. Ly/min. Wind Speed m/s	<-.1	(-.1,0)	(0,.1)	(.1,.2)	(.2,.3)	(.3,.4)	(.4,.5)	(.5,.6)	(>.6)
				Z_o = .45 m.					
(0,2) m/s	.078	.071	.035	.027	-.004	-.022	-.038	-.050	-.053
(2,3) m/s	.050	.041	.015	.008	-.005	-.017	-.025	-.028	-.043
(3,4) m/s	.020	.015	.007	-.001	-.006	-.012	-.015	-.021	-.028
(4,5) m/s	.010	.007	.003	-.001	-.005	-.007	-.010	-.014	-.020
(5,6) m/s	.006	.003	.002	-.001	-.004	-.005	-.008	-.011	-.015
(>6) m/s	.003	.002	.001	-.002	-.003	-.004	-.005	-.006	-.009
				Z_o = .5 m.					
(0,2) m/s	.077	.069	.035	.026	-.004	-.021	-.036	-.047	-.050
(2,3) m/s	.044	.040	.015	.008	-.005	-.016	-.024	-.027	-.040
(3,4) m/s	.020	.015	.007	-.001	-.006	-.012	-.015	-.020	-.027
(4,5) m/s	.010	.006	.003	-.001	-.005	-.007	-.009	-.013	-.019
(5,6) m/s	.006	.003	.002	-.001	-.004	-.005	-.007	-.010	-.015
(>6) m/s	.003	.002	.001	-.002	-.003	-.004	-.005	-.006	-.009
				Z_o = .55 m.					
(0,2) m/s	.075	.067	.034	.026	-.004	-.02	-.035	-.045	-.048
(2,3) m/s	.048	.039	.015	.007	-.005	-.015	-.023	-.025	-.038
(3,4) m/s	.019	.015	.007	-.001	-.006	-.011	-.014	-.019	-.025
(4,5) m/s	.010	.006	.003	-.001	-.004	-.006	-.009	-.013	-.018
(5,6) m/s	.006	.003	.002	-.001	-.004	-.005	-.007	-.010	-.014
(>6) m/s	.003	.002	.001	-.002	-.003	-.003	-.004	-.006	-.009

Table 17. (Continued)

Net Rad. Ly/min. Wind Speed m/s	<-.1	(-.1,0)	(0,.1)	(.1,.2)	(.2,.3)	(.3,.4)	(.4,.5)	(.5,.6)	(>.6)
					Z_o = .6 m.				
(0,2) m/s	.074	.066	.033	.025	-.004	-.019	-.034	-.043	-.046
(2,3) m/s	.047	.038	.015	.007	-.005	-.015	-.022	-.024	-.037
(3,4) m/s	.019	.015	.007	-.001	-.006	-.011	-.014	-.018	-.024
(4,5) m/s	.010	.006	.003	-.001	-.004	-.006	-.009	-.013	-.017
(5,6) m/s	.006	.003	.002	-.001	-.004	-.005	-.007	-.010	-.014
(>6) m/s	.003	.002	.001	-.002	-.003	-.003	-.004	-.006	-.009
					Z_o = .7 m.				
(0,2) m/s	.071	.063	.032	.024	-.004	-.018	-.031	-.040	-.043
(2,3) m/s	.045	.036	.014	.006	-.005	-.014	-.021	-.023	-.034
(3,4) m/s	.018	.014	.006	-.001	-.006	-.010	-.013	-.017	-.023
(4,5) m/s	.010	.006	.003	-.001	-.004	-.006	-.008	-.012	-.016
(5,6) m/s	.006	.003	.002	-.001	-.004	-.005	-.006	-.010	-.013
(>6) m/s	.003	.002	.001	-.002	-.003	-.003	-.004	-.006	-.008
					Z_o = .8 m.				
(0,2) m/s	.069	.061	.03	.023	-.004	-.017	-.029	-.037	-.040
(2,3) m/s	.043	.035	.013	.006	-.004	-.013	-.020	-.021	-.032
(3,4) m/s	.017	.013	.006	-.001	-.005	-.010	-.012	-.016	-.021
(4,5) m/s	.009	.005	.003	-.001	-.004	-.005	-.008	-.011	-.015
(5,6) m/s	.005	.003	.002	-.001	-.004	-.004	-.006	-.009	-.012
(>6) m/s	.003	.002	.001	-.002	-.003	-.003	-.004	-.005	-.008

Table 17. (Continued)

Net Rad. Ly/min. Wind Speed m/s	<-.1	(-.1,0)	(0,.1)	(.1,.2)	(.2,.3)	(.3,.4)	(.4,.5)	(.5,.6)	(>.6)
				Z_o = .9 m.					
(0,2) m/s	.067	.059	.029	.022	-.003	-.016	-.028	-.035	-.037
(2,3) m/s	.042	.034	.013	.006	-.004	-.012	-.018	-.020	-.030
(3,4) m/s	.016	.013	.006	-.001	-.005	-.009	-.011	-.015	-.020
(4,5) m/s	.008	.005	.003	-.001	-.003	-.005	-.007	-.011	-.015
(5,6) m/s	.005	.003	.002	-.001	-.003	-.004	-.006	-.008	-.011
(>6) m/s	.003	.002	.001	-.002	-.003	-.003	-.003	-.005	-.007
				Z_o = 1.0 m.					
(0,2) m/s	.065	.057	.028	.021	-.003	-.015	-.026	-.033	-.035
(2,3) m/s	.040	.033	.012	.006	-.004	-.012	-.017	-.019	-.028
(3,4) m/s	.016	.012	.006	-.001	-.005	-.009	-.011	-.015	-.019
(4,5) m/s	.008	.005	.0023	-.001	-.003	-.005	-.007	-.010	-.014
(5,6) m/s	.005	.002	.0015	-.001	-.003	-.004	-.006	-.008	-.011
(>6) m/s	.002	.002	.001	-.002	-.002	-.002	-.003	-.005	-.007
				Z_o = 2 m.					
(0,2) m/s	.052	.045	.021	.016	-.002	-.010	-.016	-.020	-.021
(2,3) m/s	.031	.025	.009	.004	-.003	-.008	-.011	-.012	-.017
(3,4) m/s	.012	.009	.004	-.001	-.003	-.006	-.007	-.010	-.012
(4,5) m/s	.006	.004	.002	- 001	-.002	-.003	-.005	-.007	-.009
(5,6) m/s	.004	.001	.001	-.001	-.002	-.003	-.004	-.005	-.007
(>6) m/s	.001	.001	.001	-.001	-.001	-.001	-.002	-.003	-.005

Table 17. (Continued)

Net Rad. Ly/min Wind Speed m/s	<-.1	(-.1,0)	(0,.1)	(.1,.2)	(.2,.3)	(.3,.4)	(.4,.5)	(.5,.6)	(>.6)
				Z_o = 3 m.					
(0,2) m/s	.044	.038	.017	.012	-.002	-.007	-.01	-.012	-.013
(2,3) m/s	.025	.020	.007	.003	-.002	-.006	-.007	-.008	-.011
(3,4) m/s	.009	.007	.003	-.001	-.003	-.004	-.005	-.007	-.008
(4,5) m/s	.004	.003	.001	-.001	-.002	-.003	-.003	-.005	-.006
(5,6) m/s	.003	.001	.001	-.001	-.002	-.002	-.003	-.004	-.005
(> 6) m/s	.001	.001	.001	-.001	-.001	-.001	-.002	-.003	-.003
				Z_o = 4 m.					
(0,2) m/s	.038	.032	.014	.010	-.001	-.005	-.006	-.007	-.007
(2,3) m/s	.021	.016	.005	.603	-.002	-.004	-.005	-.005	-.006
(3,4) m/s	.007	.005	.003	0.0	-.002	-.003	-.004	-.005	-.005
(4,5) m/s	.003	.002	.001	0.0	-.001	-.002	-.003	-.003	-.004
(5,6) m/s	.002	.001	.001	0.0	-.001	-.002	-.002	-.003	-.004
(> 6) m/s	.001	.001	.00	.001	-.001	-.001	-.001	-.002	-.003
				Z_o = 5 m.					
(0,2) m/s	.033	.027	.011	.008	-.001	-.003	-.003	-.003	-.003
(2,3) m/s	.017	.013	.004	.002	-.001	-.003	-.003	-.003	-.003
(3,4) m/s	.006	.004	.002	0.0	-.001	-.002	-.002	-.003	-.003
(4,5) m/s	.003	.002	.001	0.0	-.001	-.001	-.002	-.002	-.003
(5,6) m/s	.002	.001	.001	0.0	-.001	-.001	-.002	-.002	-.002
(> 6) m/s	.001	.001	0.0	-.001	-.001	-.001	-.001	-.001	-.002

3.6 Methodology Suggested for Projection of Wind Speed with Height

a. Most of the National Weather Service meteorological stations have the anemometer heights around 6 - 10 m. level, but in case it is not exactly 10 m. then the following equation could be used to adapt the wind speed to the 10 m. level taken from Justus and Mikhail (1976)

$$\frac{V_2}{V_1} = \left(\frac{Z_2}{Z_1}\right)^n \tag{63}$$

where

$$n = (0.37 - .0881 \cdot \ln V_1)/(1 - .0881 \cdot \ln(Z_1/10)) \tag{64}$$

where V_1 is the wind speed at height Z_1 and V_2 is the wind speed at height Z_2.

The error associated with using these statistics based equations for adapting wind speed to the ten m. level will not be too large, since most anemometer heights will be near the ten m. level.

b. If a net radiation measuring instrument is available then the net radiation is recorded. Otherwise the information about time of day and year and location can be used to determine the theoretical solar radiation which could be related to net radiation through a cloud cover factor (see p. 25-27, and Appendix A).

c. Estimate the roughness length based on the type of terrain and surface cover (2.5).

d. Use net radiation, ten m. level wind speed, and roughness length to estimate the Monin-Obukov length (see Table 17).

e. An alternate method for evaluation of Monin-Obukov length is using ten m. level wind speed, estimated insolation in three categories (strong, moderate, light), and cloud cover observation to obtain Pasquill-Gifford stability category (Table 19), then from estimated roughness length and Pasquill stability category the value of 1/L can be estimated from Figure 48.

f. Determine stability category using the value of the Monin-Obukov length (see 2.5-2).

g. Use equation (10) to project wind speed with height, substituting for ψ_1 from (21) or determine ϕ_1 from Table 2 and substitute in (14) for unstable conditions. For stable stratification determine ψ_1 from (27). For neutral and strong stability $\psi_1 = 0$.

3.7 Verification of the Suggested Methodology

To estimate the accuracy of the methodology suggested it was put to test for Argonne and Kennedy data. For each hourly profile the direction was used to determine the roughness that has already been estimated as a function of direction, also the ten m. level wind speed and net radiation were extracted from the hourly data and used to determine L; from equation (41) L was adapted to the local roughness length. L was fed into the model to predict the wind speed profile. The root mean square error between predicted and observed profiles was calculated as a function of direction, height, and stability class.

Figures 40 through 45 show the r.m.s error against height for each stability at selected direction intervals for Argonne and Kennedy data respectively. The figures on the graphs are the root mean square errors for that particular direction interval averaged over height for

each stability region. The root mean square errors for these graphs are naturally larger than those indicated by Figures 6, 7, 17 which is expected since in this case a set of L values for each wind speed and net radiation class at a certain roughness is fed into the program and modified at each direction interval for the appropriate roughness using (41) rather than extracted from the profiles.

The maximum r.m.s. error for all heights and stabilities averaged over direction, is 0.7 m/s, which shows that within the height of the Argonne tower (≈ 50 m.) the theory predicts the profile within measurement error.

Kennedy data shows that the maximum r.m.s. error is always around 1.5 m/s up to 100 m. which is still within the range of accuracy expected from this model, bearing in mind that the error between the average predicted and observed wind speed is almost half the r.m.s. error which represents the instantaneous deviations of the predicted value from the observed one. The anomalous behavior observed is that the r.m.s. error for the unstable region is higher than that for stable and neutral regions, for all direction intervals. This was not expected since the unstable region adheres better to the similarity theory than does the stable region.

This anomalous behavior confirms the previously mentioned observation about the inaccuracy of the radiation data for the unstable region (daytime radiation).

Disregarding the high r.m.s. error values associated with unstable stratification for Kennedy, the max r.m.s. error values observed for all heights less than or equal to 90 m. and different

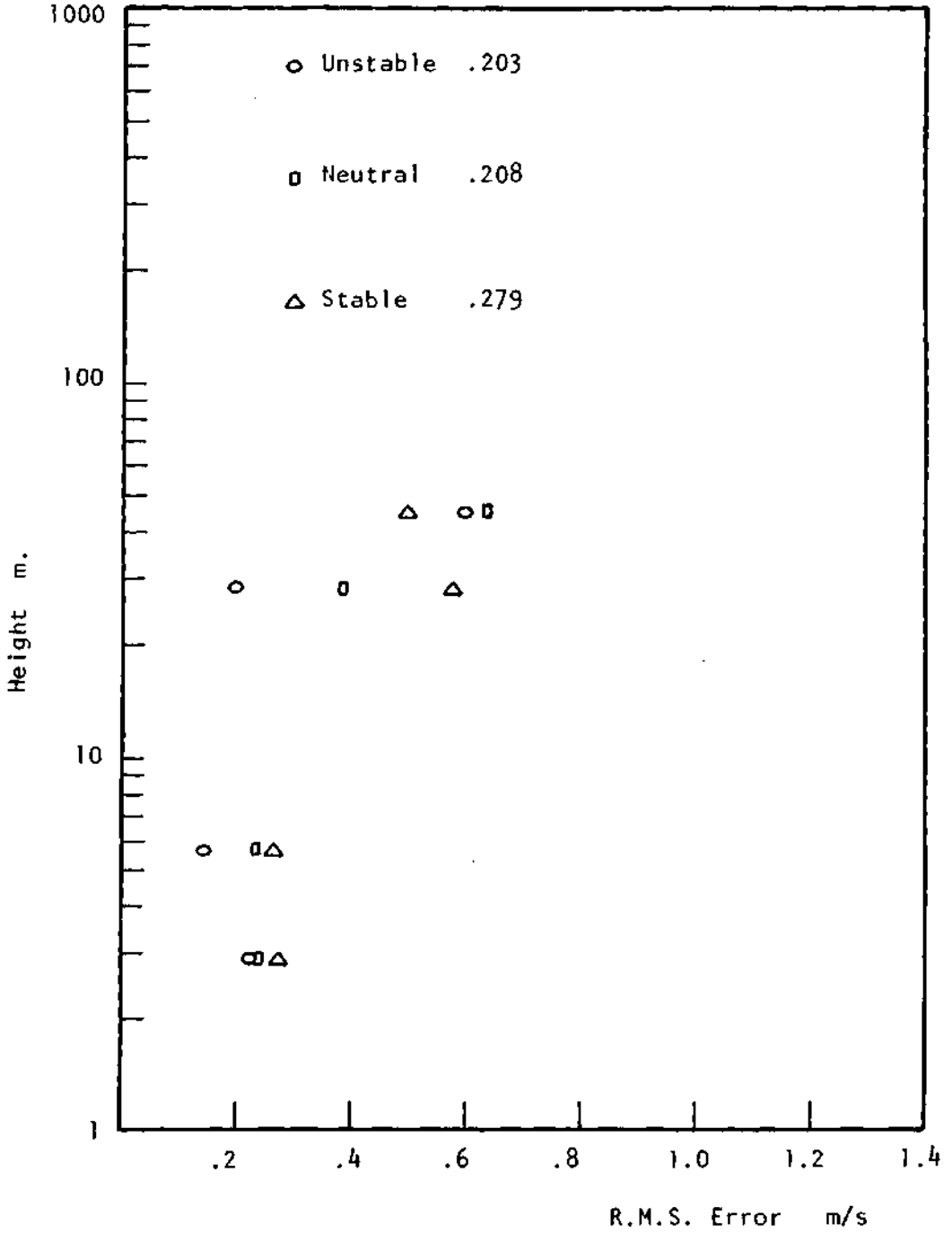

Figure 42. R.M.S. Error for Wind Speed Prediction of Argonne Data, Direction 1.

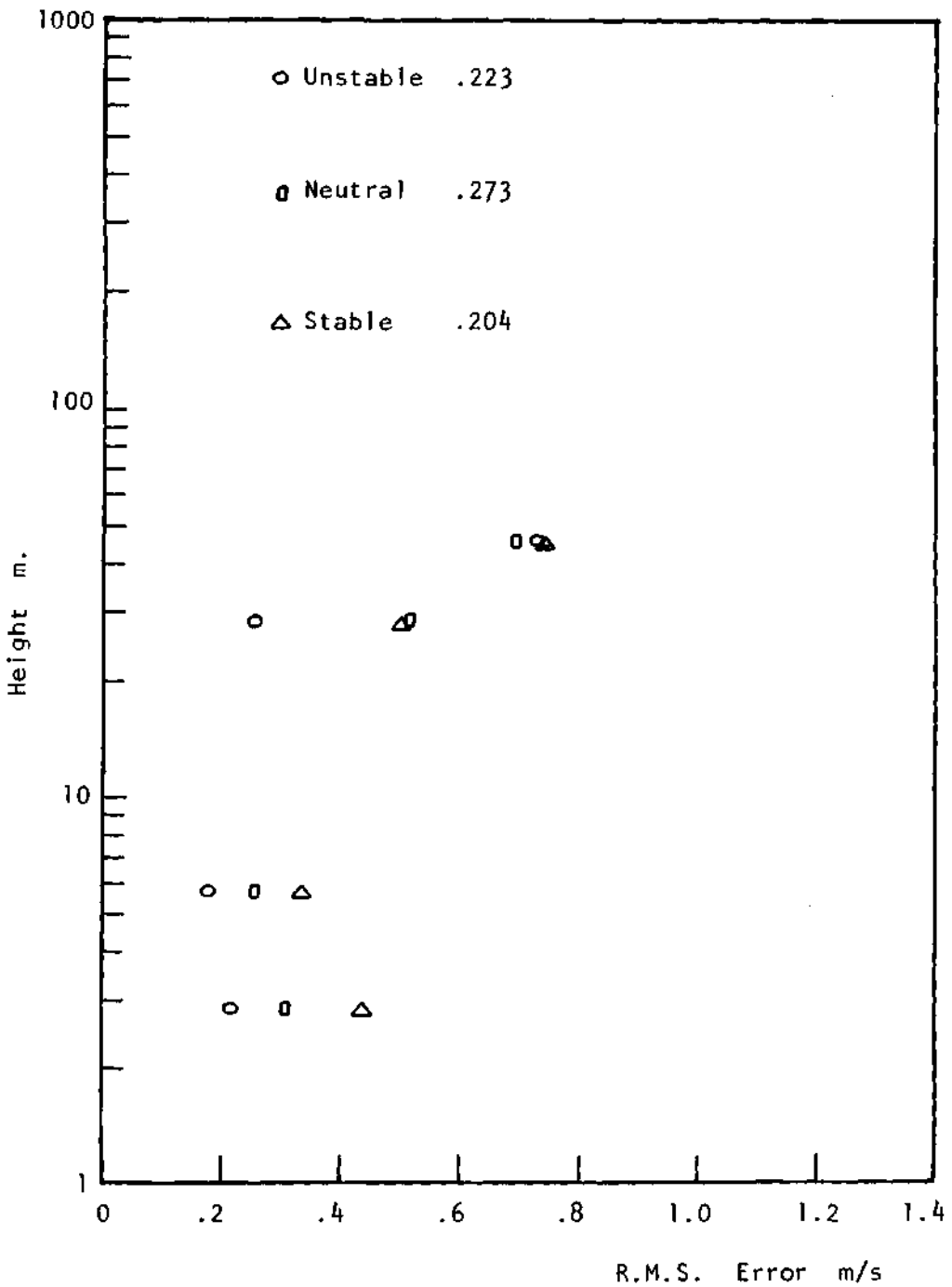

Figure 43. R.M.S. Error for Wind Speed Prediction of Argonne Data, Direction 3.

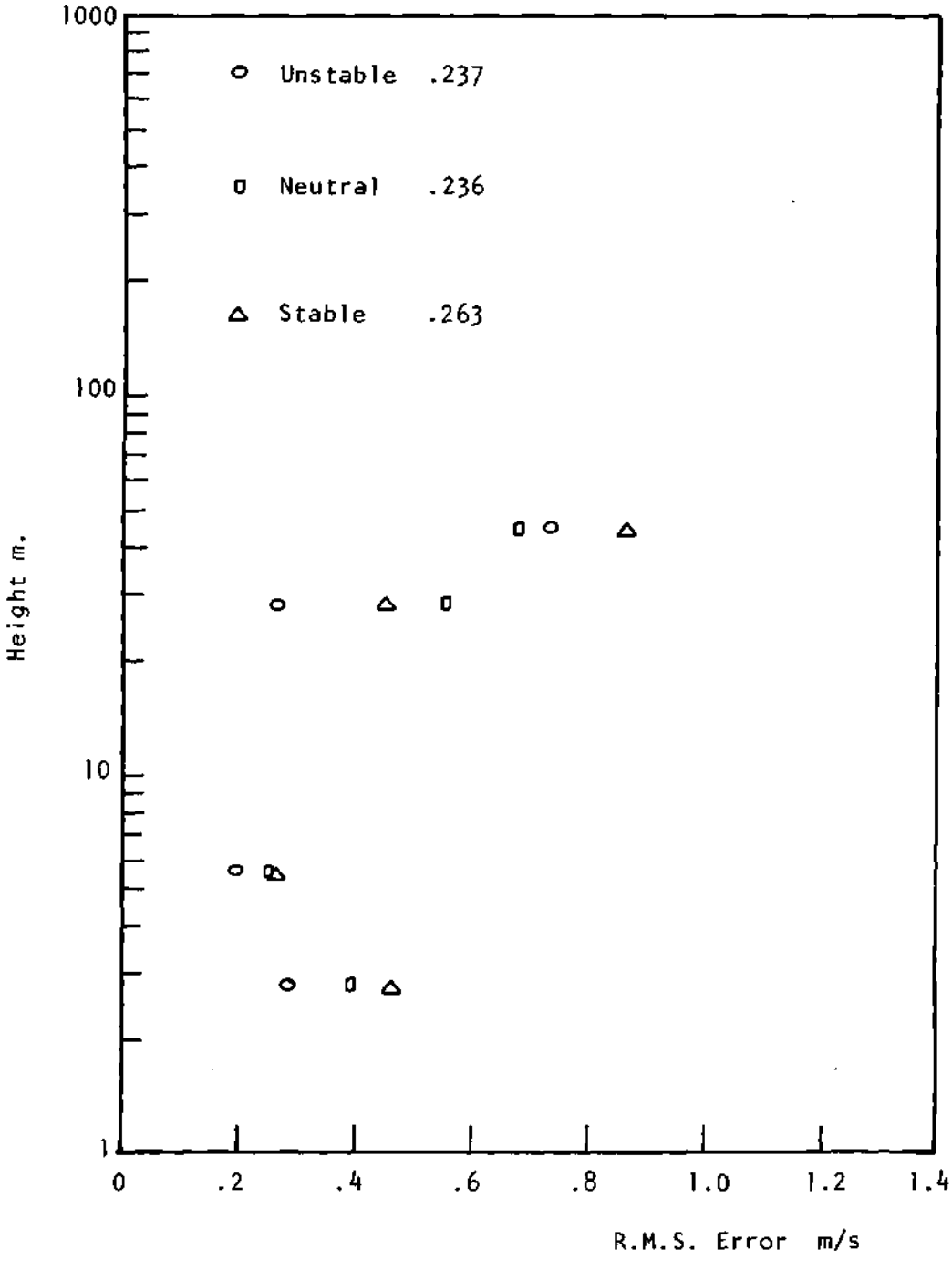

Figure 44. R.M.S. Error for Wind Speed Prediction of Argonne Data, Direction 5.

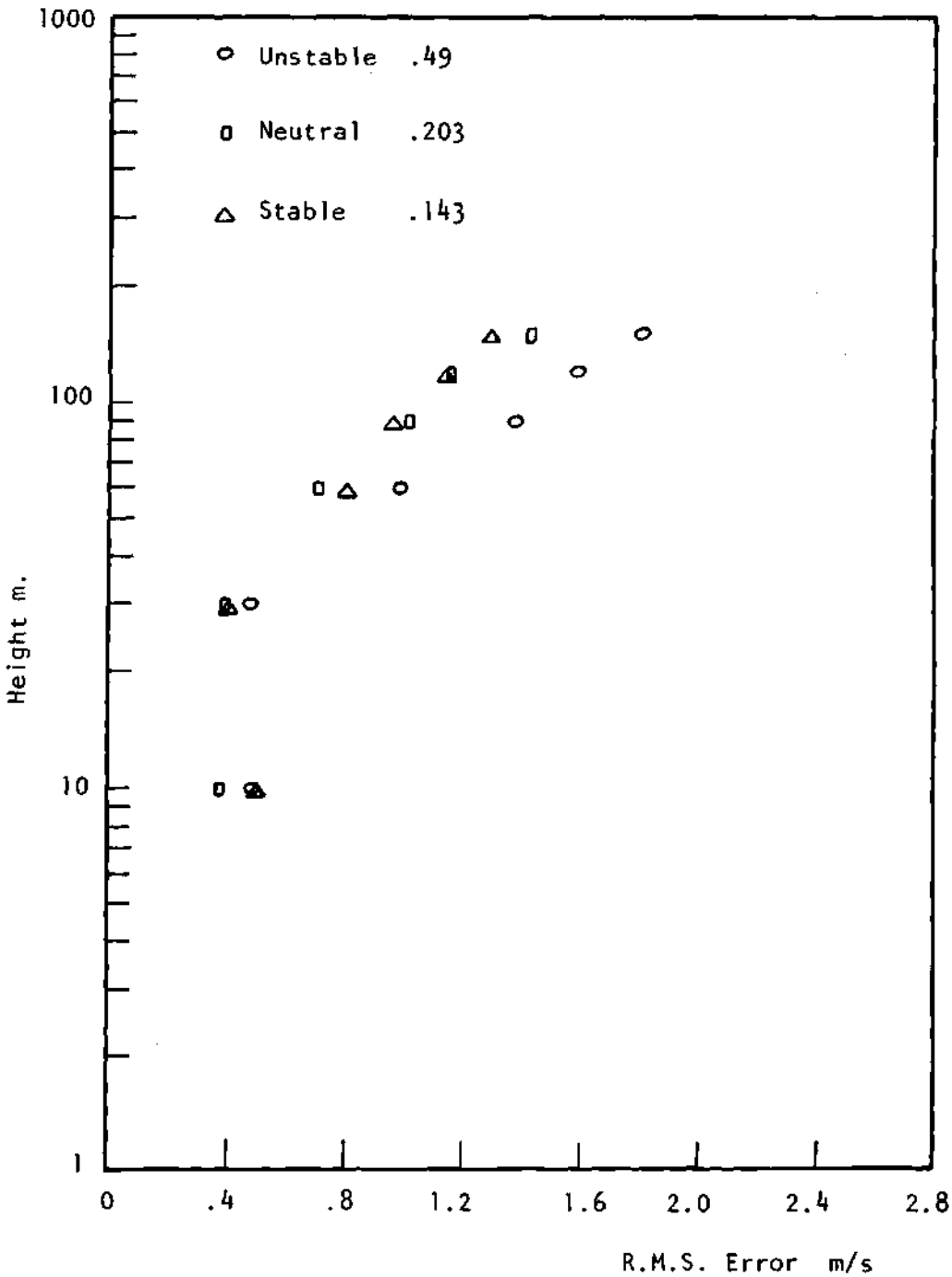

Figure 45. R.M.S. Error for Wind Speed Prediction of Kennedy Data, Direction 1.

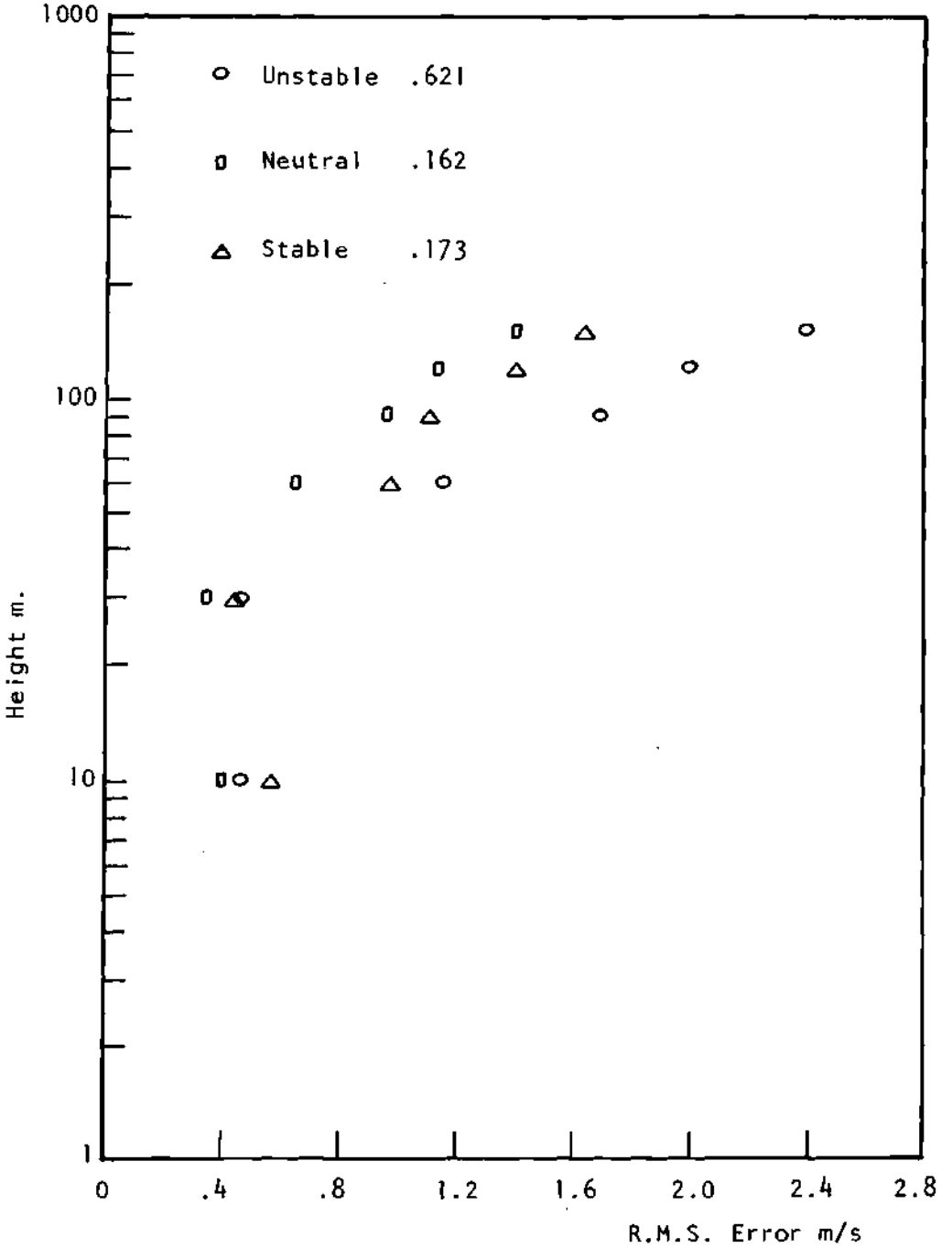

Figure 46. R.M.S. Error for Wind Speed Prediction of Kennedy Data, Direction 2.

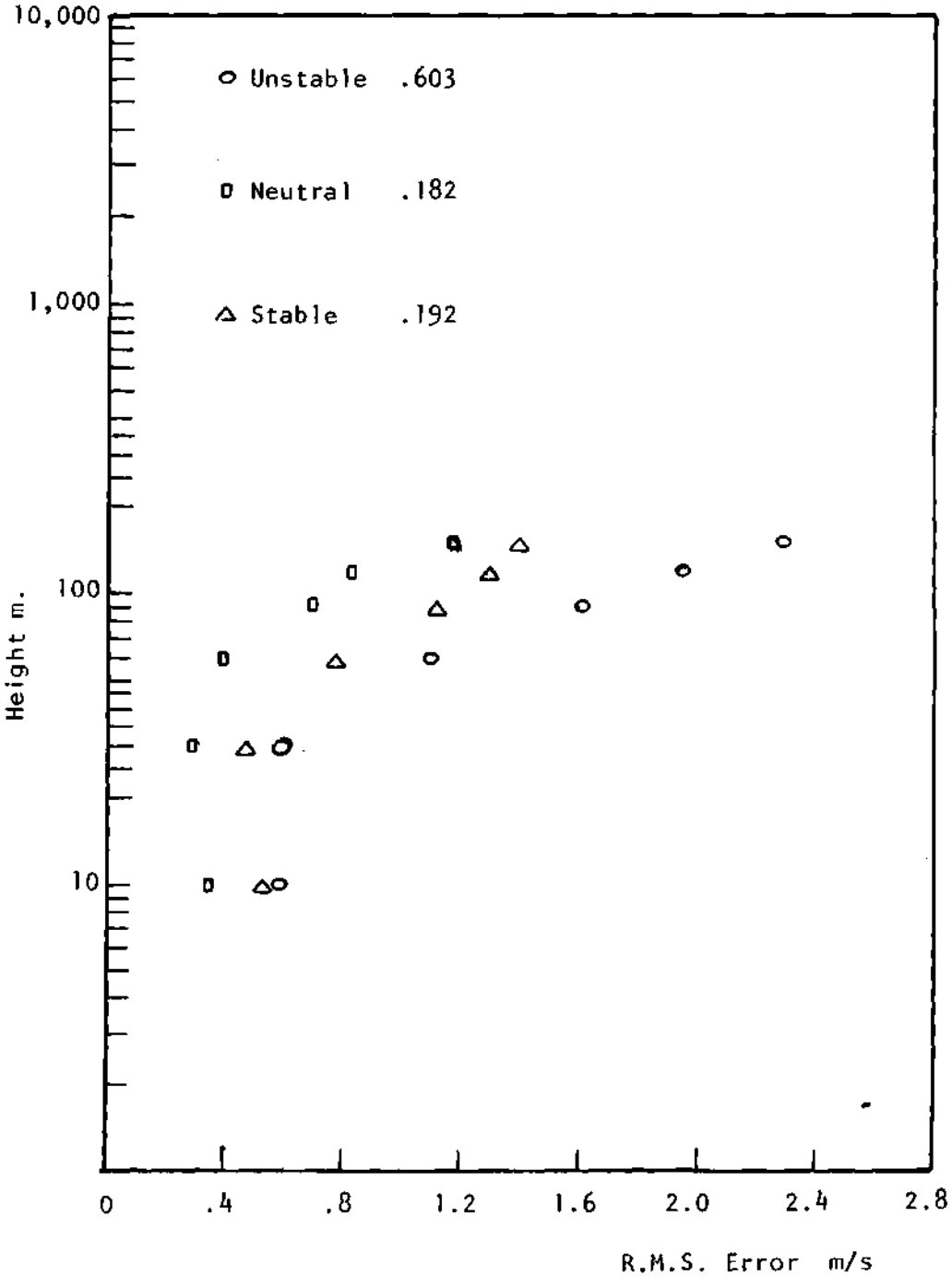

Figure 47. R.M.S. Error for Wind Speed Prediction of Kennedy Data, Direction 4.

stabilities averaged over direction is 1.1 m/s.

If the errors for the unstable region are included then the maximum r.m.s. error would be 1.6 m/s.

The average wind speed for the 45 m. level in Argonne is 6.7 m/s and for the 90 m. level in Kennedy is 8.36 m/s. Hence the errors associated with the prediction of an instantaneous wind speed using the given methodology for the 45 m. level in Argonne tower is 10% and for Kennedy tower is 13% and including the errors for the unstable region is 19%. These error percentages are maximum errors.

For the accuracy of the prediction of mean wind speed the following table gives the mean observed and predicted wind speed averaged over direction, for five years of data for Argonne and two years of data for Kennedy. The mean wind speeds are given for these different stabilities and for the 45 m. level for Argonne and 90, 120, 150 m. levels for Kennedy.

Table 18. The Accuracy of Prediction of Mean Wind Speed for Kennedy and Argonne Data

	Argonne 45 m. Level Mean Wind Speed			Kennedy 90 m. Level Mean Wind Speed		
Stability	Mean Observed	Mean Predicted	Error Percentage	Mean Observed	Mean Predicted	Error Percentage
Unstable	6.23	5.7	9%	8.66	7.54	13%
Neutral	7.62	7.2	6%	10.1	9.86	2%
Stable	6.28	6.22	1%	6.68	6.32	5%

(Continued)

Table 18. (Continued)

Stability	Kennedy 120 m. Level Mean Wind Speed			Kennedy 150 m. Level Mean Wind Speed		
	Mean Observed	Mean Predicted	Error Percentage	Mean Observed	Mean Predicted	Error Percentage
Unstable	9.18	7.78	12%	9.8	8.02	18%
Neutral	10.7	10.36	3%	11.3	11.0	3%
Stable	7.22	7.02	1%	7.76	7.6	2%

The maximum error of the mean wind speed prediction for Argonne is 9% and for Kennedy up to 120 m. is 13%.

3.8 The Relationship between the Monin-Obukov Length Based Stability and Pasquill-Gifford Stability Classes

For the average Argonne roughness the values of net radiation classes were related to Pasquill-Gifford radiation index and the wind speed intervals, adjusted to Pasquill-Gifford wind speed intervals such that the minimum value of $|1/L|$ would fall in Pasquill-Gifford class D which is the neutral stability. Hence the bounds of 1/L associated with each stability class were established for the average Argonne roughness. Then equation (41) was used to determine these bounds for different roughness lengths.

Figure 48 shows the relationship between (1/L) and Pasquill Gifford stability classes for different roughness lengths.

Golder (1972) related the Pasquill-Gifford stability classes to stability parameter (1/L) for different roughnesses by analyzing different tower data with roughness lengths varying between .002 to .4,

Figure 48. The two figures compare fairly well which could also be used as a verification for equation (41).

Table 19 gives Pasquill-Gifford stability categories as a function of 10 m. level wind speed, insolation given in three categories (strong, moderate, slight), and cloud cover information.

Table 19. Pasquill-Gifford Stability Classes

Surface Wind Speed at 10 m. m/s	Insolation			Night	
	Strong	Moderate	Slight	Thinly Overcast or $\geq$ 4/8 Low Cloud	$\leq$ 3/8 Cloud
< 2	A	A-B	B	-	-
2-3	A-B	B	C	E	F
3-5	B	B-C	C	D	E
5-6	C	C-D	D	D	D
> 6	C	D	D	D	D

The neutral category, D, should be assumed for overcast conditions during day or night.

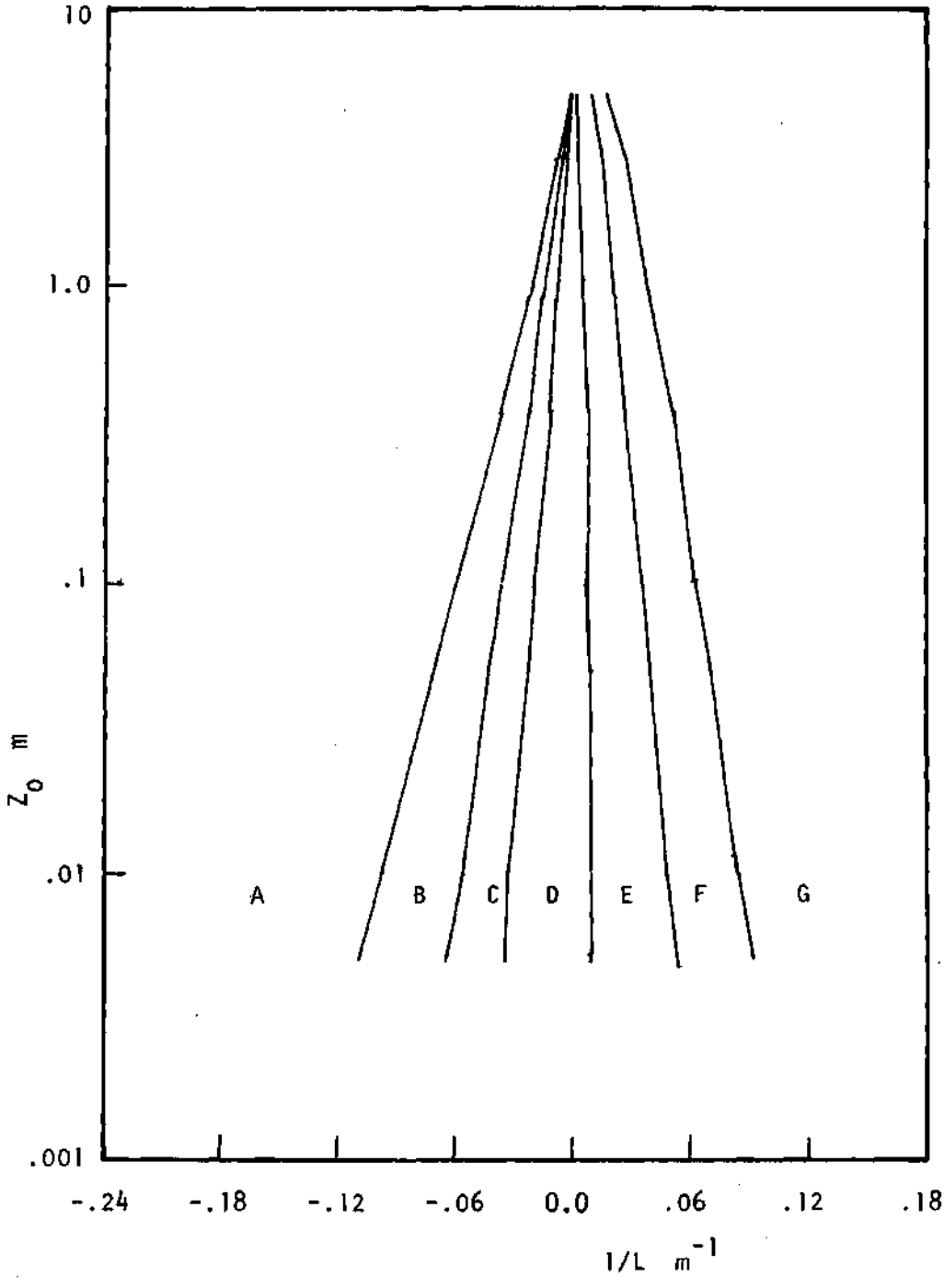

Figure 48. Relationship Between (1/L) and Pasquill-Gifford Stability Classes.

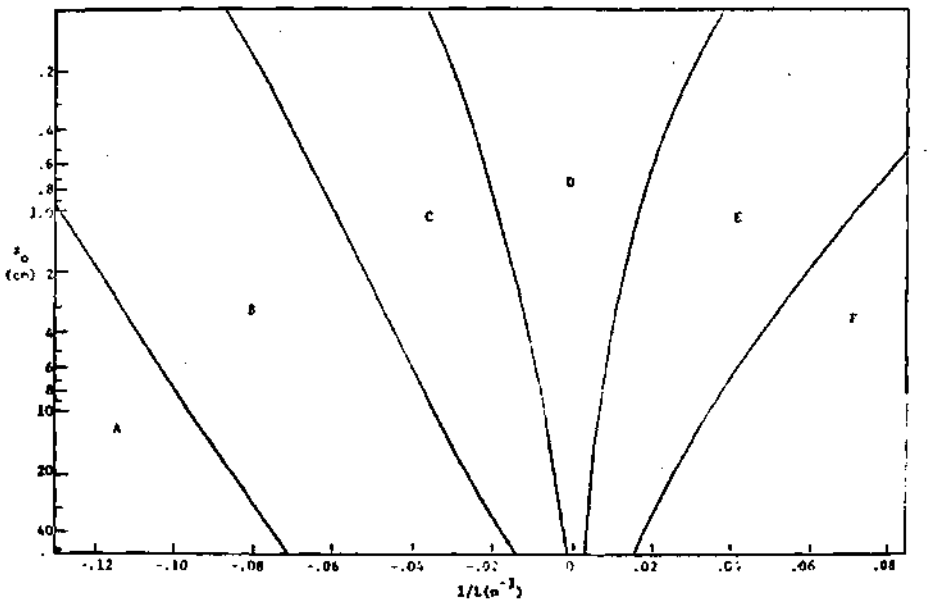

Figure 49. 1/L as a Function of Pasquill Classes and Z_o (Golder 1972).

CHAPTER IV

RECOMMENDATIONS

The model suggested requires a uniform or a gradual change of roughness with direction. The effect of sudden changes of topography and roughness on the atmospheric boundary layer needs to be investigated.

The effect of unsteady conditions on the accuracy of the model need to be examined. The inaccuracy of some of the results of Kennedy tower data might be traced to the unsteady conditions associated with ocean effect. Also the effect of the moving weather patterns on the accuracy of the model and the averaging periods for the different parameters should be examined.

The accuracy of the model needs to be further checked using different towers from the ones used in this thesis.

APPENDIX A

NOAA SOLAR MODEL

NOAA has prepared a set of linear regression equations to predict global (direct plus diffuse) solar radiation based largely on cloudiness and sunshine information. The approach involves two steps: first, prediction of clear sky solar radiation as a function of zenith angle of the sun (dependent on station latitude, time of day, and day of year), and second, a correction factor applied to the clear sky radiation for cloudiness and for less than maximum possible duration of sunshine.

The coefficients are derived from an approximately 25-year record of data at each of the 26-stations from which solar radiation data have been rehabilitated for pyranometer calibration degradation. The regression coefficients were estimated in the following fashion. The SOLMET data tapes consist of hourly records and contain among other observed weather data, the integrated hourly solar radiation, the number of minutes of sunshine, the tenths of opaque and total cloudiness. Five regression equations were developed for stations with sunshine records, three equations for the remaining stations. These include: 1) clear sky, 2) sunshine or opaque cloud, 3) opaque cloud only, 4) sunshine only, and 5) sky cover conditions. The description of the variables in the various equations are as follows:

1) Clear Sky: The hourly solar radiation value is the dependent variable. The independent variable is the cosine of the solar zenith

angle which is computed at the half hour of the given solar hour, there are zero tenths of total cloudiness encoded for this hour. The form of the equation is:

$$SRC = A_o + A_1 \cos ZA + A_2 \cos^2 ZA + A_3 \cos^3 ZA \qquad (A\text{-}1)$$

where

SRC is the clear sky hourly integral solar radiation (K. Joules/m.). The A_o terms were determined separately for the mornings and afternoons for each month of the year. The A_1, A_2, and A_3 terms were estimated for mornings and afternoons, hopefully to account for diurnal and seasonal variations of such factors as turbidity and water vapour. As might be expected, there seems to be strong similarities between stations in the same type of climatic regime, viz., eastern coastal stations or southwestern semi arid stations.

2) Sunshine-opaque cloud: The hourly solar radiation value is related to the function of possible sunshine, the tenths of opaque cloudiness and a precipitation variable. The equation form is

$$SF = SRC*[B_o + B_1 SS + B_2 OPQ + B_3 OPQ^2 + B_4 OPQ^3 + B_5 RN] \qquad (A\text{-}2)$$

where:

SR is the hourly solar radiation (K-Joules/m^2)

SRC is the clear sky solar radiation from (A-1)

SS is the number of minutes of sunshine/60.

OPQ is the tenths of opaque cloudiness/10.

RN is precipitation value which is zero for no precipitation and 1 if precipitation of some form is reported.

3) Opaque cloud only: This is the same as (A-2) except there is no sunshine term.

$$SR = SRC*[C_0 + C_2OPQ + C_3OPQ^2 + C_4OPQ^3 + C_5RN] \quad (A-3)$$

4) Sunshine only: This is the converse of (A-3) and is used when there is no opaque cloudiness information.

$$SR = SRC*[D_0 + D_1SS + D_5RN] \quad (A-4)$$

5) Sky Condition: This equation which is the least preferred of the regression equations, utilizes the sky cover information, the form of the equation is:

$$SR = SRC*[E_o + \sum_{i=1}^{7} E_iSC_i + E_8RN] \quad (A-5)$$

where:

SRC, SR and RN are as before

SC_i is 0 or 1 depending on whether the sky cover variable is present or absent at any of the four levels

SC_1 is thin scattered; 0.1 - 0.5 cover

SC_2 is opaque scattered; 0.1 - 0.5 cover

SC_3 is thin broken; 0.6 - 0.9 cover

SC_4 is opaque broken; 0.6 - 0.9 cover

SC_5 is thin overcast; 1.0 cover

SC_6 is opaque overcast; 1.0 cover

SC_7 is partial or total obscuration.

APPENDIX B

WIND POWER ESTIMATION ERROR ASSOCIATED WITH WIND SPEED PREDICTION ERROR

For a wind speed V the theoretically available power P_{th} in Watts is computed by

$$P_{th} = 8\rho V^3 A/27 \tag{B-1}$$

where the air density ρ is taken to be the sea level value 1.255 Kg/m^3, A is the rotor swept area in m^2 and the factor is (8/27) 1/2 the Betz coefficient of an ideal rotor. Hence the error in theoretical power output due to 15% error in wind speed prediction is given approximately by

$$\frac{\delta P_{th}}{P_{th}} = \frac{3\delta V}{V} = 3(15\%) = 45\% \tag{B-2}$$

The mean extractable power output $\overline{P}$ versus mean wind speed $\overline{V}$ was given by Justus et al. (1976) as

$$\frac{\overline{P}}{P_r} = a + b\frac{\overline{V}}{V_r} \tag{B-3}$$

where V_r is wind turbine rated wind speed and P_r is rated power. Hence

$$\frac{\delta\overline{P}}{\overline{P}} = \frac{b}{\left(a\frac{V_r}{\overline{V}} + b\right)}\frac{\delta\overline{V}}{\overline{V}} \tag{B-4}$$

substituting empirically observed values -0.3 for a and 1.0 for b, and assuming $V_r/\overline{V}$ to be approximately 1.3 (appropriate for optimally designed wind turbines) we obtain

$$\frac{\delta\overline{P}}{\overline{P}} = (1.6)\ \frac{\delta\overline{V}}{\overline{V}} \qquad \text{(B-5)}$$

for a maximum wind speed error prediction of 15% the corresponding mean power output error is 24%.

The above analysis shows that the mean power output error is of the same order of the wind speed prediction error. While the theoretical power output error is three times the wind speed error prediction.

REFERENCES

ASHRAE Handbook of Fundamentals, 1967.

Boeing Company Report, 1964, "Summary of Solar Radiation Observation," D2-90 577-1.

Bussinger, A. J., et al., 1966, "Transfer of Momentum and Heat in the Planetary Boundary Layer," Proc. Symp. Arctic Budget and Atmospheric Circulation, the RAND Corporation, 305-331.

Bussinger, A. J. et al., 1971, "Flux Profiles Relationships in the Atmospheric Surface Layer," work performed at Air Force Cambridge Research Labs., Common Wealth Scientific and Industrial Research Organization.

Calder, K. L., 1949, "Eddy Diffusion and Evaporation in Flow Over Aerodynamically Smooth and Rough Surfaces: a Treatment Based on Lab. Laws of Turbulent Flow with Special Reference to Conditions in the Lower Atmosphere," Quart. J. Mech. Appl. Math., 2:153-176.

Chamberlain, A. C., 1966, "Transport of Gases to and from Grass and Grass-like Surfaces," Proc. Roy Soc. (London), Ser. A, 290:236-265.

Ciono, R. M., 1965, "A Mathematical Model for Air Flow in a Vegetation Canopy," J. Appl. Met. 4:515-522.

Davenport, A. C., 1965, "A Relation of Wind Structure and Wind Loading," National Physics Lab. Symp. No. 16, Wind Effects on Buildings and Structure," pp. 54-102, Her Majesty's Stationary Office in London.

Ellison, H. T., 1957, "Turbulent Transfer of Heat and Momentum from an Infinite Rough Plane," J. of Fluid Mech., 2, p. 456.

Ernest, W. P., 1975, "The Riso Profiles, a Study of Wind and Temperature Data from the 123 m. Tower at Riso, Denmark," Quart. J. R. Met. Soc., 101, pp. 107-117.

Fichtl, G. E., 1969, "Characteristics of Turbulence Observed at NASA 150 Met. Tower," J. Appl. Met. Vol. 7, pp. 838.

Fichtl, G. E., and McVeil, G. E., 1970, "Longitudinal and Lateral Spectra of Turbulence in the Atmospheric Boundary Layer at the Kennedy Space Centre," J. Appl. Met., 9, 51-63.

Golder, Donald, 1972, "Relations Among Stability Parameters in the Surface Layer," B. L. Met., 3, 1972, 47-58.

Hanna, R. S., 1969, "The Thickness of the Planetary Boundary Layer," Atmospheric Environment Program Press, Vol. 3, pp. 519-536.

Justus, G. C. and Mikhail, S. A., 1976, "Height Variation of Wind Speed and Wind Distribution Statistics," Geophysical Research Letters, Vol. 3, No. 5.

Kimura, K. and Stephenson, D. G., 1969, "Solar Radiation on Cloudy Days," presented in ASHRAE semiannual meeting, Chicago, Illinois.

Monin, A. S. and Obukov, M. A., 1954, "Dimensionless Characteristics of Turbulence in the Surface Layer," Akad. Nauk. SSSR, Geofiz., Inst. Tr. No. 24, 163-187.

Paeschke, W., 1937, "Experimentalle Untersuchungen Zum Ranhigkeits-und Stabilitaets-Problem in der Freien Atmosphaere," Beitr. Phys. Atmos., 24:163-189.

Panofsky, H. A., 1961, "An Alternative Derivation of the Diabatic Wind Profile," Quart. J. Roy. Met. Soc., 87, p. 109.

Panofsky, H. A., 1962, "Similarity Theory and Temperature Structure in the Low Atmosphere," Quart. J. Roy. Met. Soc., 87, p. 109.

Panofsky, H. A. and Blackadar, K. A., 1973, "Investigation of the Turbulent Wind Below 150 m. Altitude at the Eastern Test Range," Final Report, Central NAS. 8-21140, The Pennsylvania State Univ.

Panofsky, H. A. and Peterson, E. L., 1972, "Wind Profiles and Change of Terrain Roughness at Riso.," Quart. J. Royal. Met. Soc. 98, 845-854.

Panofsky, H. A. et al., 1973, "Profiles of Wind and Temperature from Towers over Homogeneous Terrain," J. of Atm. Sci., Vol. 30, pp. 788-794.

Paulson, C. A., 1970, "The Mathematical Representation of Wind Speed and Temperature Profiles in Unstable Atmospheric Surface Layer," Quart. J. Roy. Met. Soc., 97, pp. 168-180.

Peterson, E. W., 1975, "The Riso Profiles: Study of Wind and Temperature Data from the 123 m. Tower at Riso, Denmark," Quart. J. R. Met. Soc., pp. 107-117.

Plate, E. and Quraishi, A., 1965, "Modeling of the Velocity Distribution Inside and Above Tall Crops," J. Appl. Met., 4, pp. 400-408.

Plate, J. E., 1971, "Aerodynamic Characteristics of Atmospheric Boundary Layers," Atomic Energy Commission, Division of Technical Information Extension, Oak Ridge, Tennessee.

Proudman, J., 1953, "Dynamical Oceanography," Methuen, London.

Reed, J. W., 1974, "Wind Power Climatology," Weatherwise, 27, 237-242.

Reed, J. W., 1975, "Wind Power Climatology of the United States," Saudia Laboratories, SAND74-0348.

Simin, Emil, 1973, "Logarithmic Profiles and Design Wind Speeds," Proc. Amer. Soc. Civil Engrs. (Engr. Mech. Div.), 99, EM5, 1073-1083.

Smith, M. E., 1968, "Recommended Guide for the Prediction of the Dispersion of the Airborne Effluents," Amer. Soc. Mech. Engrs., New York.

Smith, B. F., 1973, "A Scheme for Estimating the Vertical Dispersion of Neutral Plume from a Source Near Ground Level," 1973, T.D.N. No. 40.

Swinbank, W. C., 1964, "The Exponential Wind Profile," Quart. J. R. Met. Soc., 90, pp. 119-135.

Tennekes, H. and Lumley, J. L., 1972, "A First Course in Turbulence."

Webb, E. K., 1970, "Profile Relationships in the Log-Linear and Extension to Strong Stability," Quart. J. Roy. Met. Soc., 96, pp. 67-90.

Wyngaard, C. J., Coté, O. R., 1974, "The Evolution of the Convective Planetary Boundary Layer, a Higher Order Closure Model Study," B. L. Met. 7, p. 289-308.

Wyngaard, C. J., 1975, :Modeling of the Planetary Boundary Layer-Extension to the Stable Case," B. L. Met., 9, 441-460.

Yamamato, G., 1959, J. Met. Soc. Japan, II, 37, p. 60.

VITA

Amir Samaan Mikhail was born on July 22, 1948, in Minia, Egypt.

He attended the public schools in Egypt and was graduated from Minia Secondary School in June 1965. In September, 1965, Mr. Mikhail entered Cairo University and received the degree of Bachelor of Aeronautical Engineering in June, 1970. In September, 1970, he enrolled in the Department of Mathematics, at the same university, and received the degree of Bachelor of Science in Mathematics in June 1972. He worked as an assistant teacher at Cairo University from September 1970 to August 1973.

In the fall of 1973 he joined Georgia Institute of Technology as a graduate student and research assistant. He received his Master's degree in Aerospace Engineering in September 1974.